5-2006

A Generalized Instantaneous Nonactive Power Theory for Parallel Nonactive Power Compensation

Yan Xu
University of Tennessee - Knoxville

To the Graduate Council:

I am submitting herewith a dissertation written by Yan Xu entitled "A Generalized Instantaneous Nonactive Power Theory for Parallel Nonactive Power Compensation." I have examined the final electronic copy of this dissertation for form and content and recommend that it be accepted in partial fulfillment of the requirements for the degree of Doctor of Philosophy, with a major in Electrical Engineering.

John N. Chiasson, Major Professor

We have read this dissertation and recommend its acceptance:

Jack S. Lawler, Suzanne M. Lenhart, Seddik M. Djouadi

Accepted for the Council:

Carolyn R. Hodges

Vice Provost and Dean of the Graduate School

(Original signatures are on file with official student records.)

To the Graduate Council:

I am submitting herewith a dissertation written by Yan Xu entitled “A Generalized Instantaneous Nonactive Power Theory for Parallel Nonactive Power Compensation.” I have examined the final electronics copy of this dissertation for form and content and recommend that it be accepted in partial fulfillment of the requirements for the degree of Doctor of Philosophy, with a major in Electrical Engineering.

John N. Chiasson

Major Professor

We have read this dissertation
and recommend its acceptance:

Jack S. Lawler

Suzanne M. Lenhart

Seddik M. Djouadi

Accepted for the Council:

Anne Mayhew

Vice Chancellor and Dean of
Graduate Studies

(Original signatures are on file with official student records.)

A Generalized Instantaneous Nonactive Power Theory for Parallel Nonactive Power Compensation

A Dissertation

Presented for the

Doctor of Philosophy Degree

The University of Tennessee

Yan Xu

May 2006

Acknowledgments

I would like to thank many people for their kind help with my study and research so that I could finish my dissertation. I sincerely appreciate my advisor, Dr. John N. Chiasson, for his instruction, his supervision, and his selfless support.

I am very thankful to my committee members, Dr. Jack S. Lawler, Dr. Suzanne M. Lenhart, and Dr. Seddik M. Djouadi, for being on my committee and for their support and encouragement.

Special thanks go to Dr. Fang Z. Peng and Dr. Leon M. Tolbert, for their inspirational instruction and valuable directions.

I would like to thank all the people in the Power Engineering Laboratory at the University of Tennessee, especially Dr. Zhong Du, Dr. Kaiyu Wang, and Surin Khomfoi. I am also very thankful to Jeremy B. Campbell at Oak Ridge National Laboratory who has worked together with me on the experiments. I also thank Dr. Burak Ozpineci and Madhu Sudhan Chinthavali at Oak Ridge National Laboratory for their advice and help.

Finally I would like to express my appreciation and love to my parents and sisters. They have always loved me, supported me, and encouraged me unconditionally.

Abstract

Although the definitions of active power and nonactive power in a three-phase sinusoidal power system have been accepted as a standard, it has been an issue on how to define instantaneous nonactive power in power systems with non-sinusoidal or even non-periodic voltage and/or current.

This dissertation summarizes these nonactive power theories, and a generalized instantaneous nonactive power theory is presented. By changing the parameters in the instantaneous active current and nonactive current definitions, this theory is valid for power systems with different characteristics. Furthermore, other nonactive power theories can be derived from this generalized theory by changing parameters.

This generalized nonactive power theory is implemented in a shunt nonactive power compensation system. A three-phase four-wire nonactive compensation system configuration is presented, and a control scheme is developed. The compensator provides the nonactive current component, which is determined by the generalized nonactive power theory. Unity power factor, and/or fundamental sinusoidal utility source current can be achieved despite the characteristics of the nonlinear load. Both the simulation and experiment results verify the validity of the theory to different systems and the capability in a shunt nonactive compensation system.

Contents

List of Tables

List of Figures

CHAPTER 1

Introduction

Alternating current, three-phase electric power systems were developed in the late 1800s and have been adopted as the standard for more than 100 years. A typical power system consists of generation, transmission, and distribution. In today's power systems, most of the active power is generated by synchronous generators, and then transmitted to load centers by long distance transmission lines. In an ideal power system, the voltage and current are sinusoidal at a constant frequency (50 Hz or 60 Hz), and balanced (the same magnitude for each of the three phases, and the phase angle between consecutive phases being $2\pi/3$ radians). A system is considered ideal if the generation is ideal (a sinusoidal waveform with constant magnitude and constant fundamental frequency), and all the loads are linear, i.e., the loads only consist of resistance R, inductance L, and/or capacitance C. There are single-phase loads (two-wire), three-phase three-wire loads (three-phase without neutral), and three-phase four-wire loads (three-phase with neutral) in ac power systems.

1.1 Standard Definitions in Power Systems

A power network $\mathcal{N}$ has two ports as shown in Figure 1.1. The voltage between the two ports is $v(t)$, and the current is $i(t)$ with the direction flowing into the network $\mathcal{N}$.

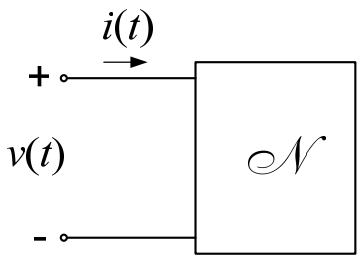

Figure 1.1. A two-port power network.

The network can be an individual device, such as a generator, or a load. It also can be a network which consists of multiple devices. For an ideal electric power system as defined above, both the voltage and the current are sinusoidal waveforms. For a single-phase system, let the voltage $v(t)$ and the current $i(t)$ be, respectively,

$$v(t) = \sqrt{2}V\cos(\omega t)\,, \tag{1.1}$$

and

$$i(t) = \sqrt{2}I\cos(\omega t + \theta)\,. \tag{1.2}$$

where $\omega \triangleq 2\pi f$ is the frequency in radians/second, and f if the frequency in Hz. $T \triangleq 1/f$ is the period in second. θ is the phase angle between $v(t)$ and $i(t)$, and $\theta \in (-\pi, \pi]$. V and I are the root mean square (rms) values of the voltage $v(t)$ and the current $i(t)$ over the period T, respectively,

$$V = \sqrt{\frac{1}{T}\int_0^T v^2(t)dt}\,, \tag{1.3}$$

and

$$I = \sqrt{\frac{1}{T}\int_0^T i^2(t)dt}\,. \tag{1.4}$$

The instantaneous power $p(t)$ is defined by

$$p(t) \triangleq v(t)i(t). \tag{1.5}$$

In this dissertation, the term "instantaneous" means that the voltage/current/power is defined for each time t rather than as an average value or an rms value. The instantaneous power $p(t)$ is the rate of change at which the electric energy is being transmitted into or out of the network $\mathcal{N}$ [1]. In the case of a sinusoidal voltage and current as given in (1.1) and (1.2), the instantaneous power is

$$p(t) = VI[\cos(2\omega t + \theta) + \cos\theta]. \tag{1.6}$$

The instantaneous power has a constant term, $VI\cos\theta$, and a sinusoidal term, $VI\cos(2\omega t+\theta)$, with a frequency which is twice of the fundamental frequency.

The average active power P over the time period T is the average value of the instantaneous power over one period of the waveform; that is,

$$P \triangleq \frac{1}{T}\int_0^T p(t)dt\,. \tag{1.7}$$

In the case of a sinusoidal voltage and current as given in (1.1) and (1.2), respectively, it follows that

$$P = \frac{1}{T}\int_0^T p(t)dt = VI\cos\theta\,. \tag{1.8}$$

The average power is equal to the constant term in the expression for instantaneous power given in (1.6). P is positive if $\theta \in (-\pi/2, \pi/2)$, which indicates that the network consumes active power; P is negative if $\theta \in (-\pi, -\pi/2)$ or $\theta \in (\pi/2, \pi)$, which shows that the network generates active power; and P is zero if $\theta = \pi/2$ or $\theta = -\pi/2$, which means that the network does not consume or generate any active power.

The apparent power is defined by

$$S \triangleq VI \,. \tag{1.9}$$

S is the capacity that a device or a network to generate, to consume, or to transmit power, including both active power and nonactive power. Therefore, S is often used to indicate the power rating of a device.

The average nonactive power is defined by

$$Q \triangleq \pm\sqrt{S^2 - P^2} \,. \tag{1.10}$$

In the case of a sinusoidal voltage and current as given in (1.1) and (1.2), respectively, it follows that

$$Q = VI \sin\theta \tag{1.12}$$

Q is positive if $\theta \in (0, \pi)$, that is, the current $i(t)$ is leading the voltage $v(t)$, and it indicates that the network generates nonactive power; Q is negative if $\theta \in (-\pi, 0)$, i.e., the current is lagging the voltage, and it indicates that the network consumes nonactive power. Q is zero if $\theta = 0$, and in this situation, the current is in phase with the voltage and no nonactive power is generated or consumed by the network.

The power factor pf is defined by

$$pf \triangleq \frac{P}{S} \,. \tag{1.13}$$

If the voltage and current are as given in (1.1) and (1.2), respectively, $pf = \cos\theta$.

For a multi-phase system with the phase number m, define the voltage vector $\boldsymbol{v}(t)$ by

$$\boldsymbol{v}(t) = [v_1(t), v_2(t), ..., v_m(t)]^T \,. \tag{1.14}$$

The current vector $\boldsymbol{i}(t)$ is defined by

$$\boldsymbol{i}(t) = [i_1(t), i_2(t), ..., i_m(t)]^T \,. \tag{1.15}$$

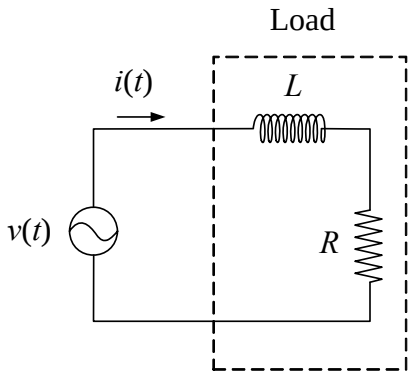

Figure 1.2. Single-phase *RL* load in an ac system.

The instantaneous power $p(t)$ is defined by

$$p(t) \triangleq \boldsymbol{v}(t)^T \boldsymbol{i}(t) = \sum_{k=1}^{m} v_k(t) i_k(t) . \tag{1.16}$$

These definitions of instantaneous power in (1.5) and (1.16) are also true for voltages and currents with arbitrary waveforms. However, other definitions are restricted to fundamental sinusoidal power systems. Many modifications have been made to these standard definitions to extend them to non-sinusoidal, non-periodic, and other cases. These power theories will be discussed in Chapter 2.

In the following two subsections, a single-phase *RL* load and a three-phase *RL* load will be used to illustrate the standard definitions in this subsection.

1.2 Single-Phase Fundamental Nonactive Power

Figure 1.2 shows a resistive and inductive load (*RL* load) connected to an ac power source. Let $v(t)$ denote the ac power source given by

$$v(t) = \sqrt{2}V \cos(\omega t) . \tag{1.17}$$

The impedance of the load is

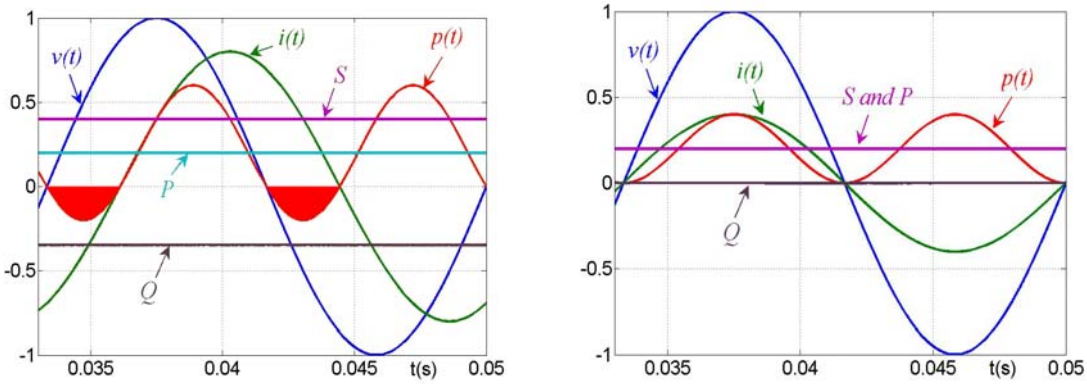

(a) $pf < 1$ (b) Unity power factor

Figure 1.3. Active power and nonactive power in a single-phase *RL* load.

$$Z = R + j\omega L = |Z| e^{j\theta}, \tag{1.18}$$

where

$$|Z| \triangleq \sqrt{R^2 + (\omega L)^2}, \tag{1.19}$$

and

$$\theta \triangleq \tan^{-1}\left(\frac{\omega L}{R}\right). \tag{1.20}$$

The instantaneous current $i(t)$ in this system is

$$i(t) = \sqrt{2} I \cos(\omega t - \theta) \tag{1.21}$$

where I is the rms value of $i(t)$ and may be written as

$$I = \frac{V}{|Z|}. \tag{1.22}$$

The waveforms of $v(t)$, $i(t)$, $p(t)$, as well as P, Q, and S are plotted in Figure 1.3. In Figure 1.3a, as $L \neq 0$, it follows that $\theta \neq 0$ and $i(t)$ is lagging $v(t)$ by θ. When $p(t) > 0$, $v(t)$ and $i(t)$ have the same polarity, which indicates that the power is flowing (on average) from the power source to the load; when $p(t) < 0$ (the red areas in Figure 1.3a), the

polarity of $i(t)$ is opposite to the polarity of $v(t)$, which indicates that the power is flowing (on average) from the load to the power source. The power that flows back and forth between the power source and the load is referred to as the **nonactive power**. This nonactive power has zero average value (over one period), but is actual power flowing in the power network. The average nonactive power Q indicates the amount of nonactive power that flows in this network.

In Figure 1.3b, the load has only resistance ($L = 0$), so that $\theta = 0$ and $i(t)$ is in phase with $v(t)$. The instantaneous power $p(t)$ is greater than or equal to zero at all times, which indicates that power is delivered from the source to the load at all times and no power is flowing back and forth. In both cases, the same amount of power is delivered to the load (average power P over one period), but the magnitude of $i(t)$ in Figure 1.3b is smaller than the current in Figure 1.3a. If $i(t)$ is in phase with $v(t)$ (i.e., unity power factor), $i(t)$ is the **minimum** current required to transmit any given amount of power. The average nonactive power Q is zero, which indicates that there is no nonactive power flowing in this network, so that the apparent power S is equal to the average power P.

1.3 Three-Phase Fundamental Nonactive Power

A three-phase RL load in an ac system is shown in Figure 1.4. The voltage vector $\boldsymbol{v}(t)$ and current vector $\boldsymbol{i}(t)$ are shown in Figures 1.5a and 1.5b.

$$\boldsymbol{v}(t) = \sqrt{2}V[\cos(\omega t), \cos(\omega t - 2\pi/3), \cos(\omega t + 2\pi/3)]^T , \tag{1.23}$$

$$\boldsymbol{i}(t) = \sqrt{2}I[\cos(\omega t + \theta), \cos(\omega t - 2\pi/3 + \theta), \cos(\omega t + 2\pi/3 + \theta)]^T \tag{1.24}$$

The instantaneous power $p(t)$ is

$$p(t) = 3VI\cos\theta . \tag{1.25}$$

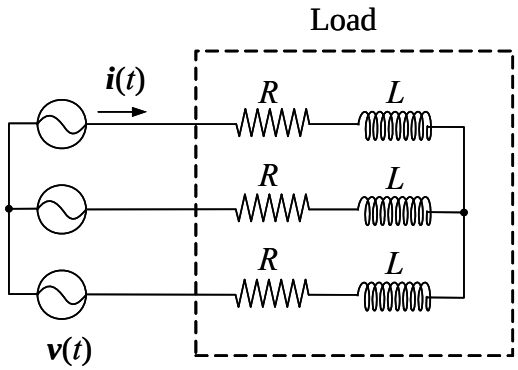

Figure 1.4. Three-phase *RL* load in an ac system.

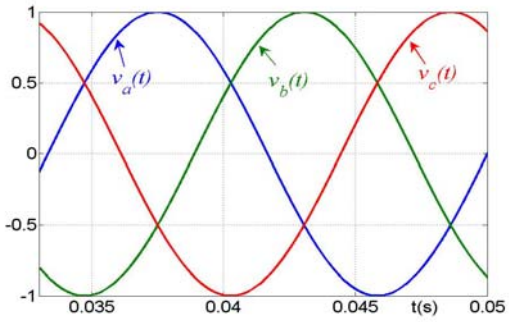

(a) Voltage ***v***(*t*)

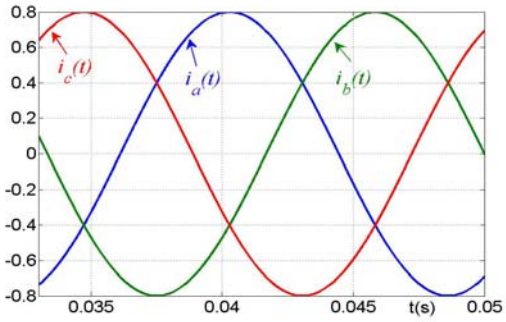

(b) Current ***i***(*t*)

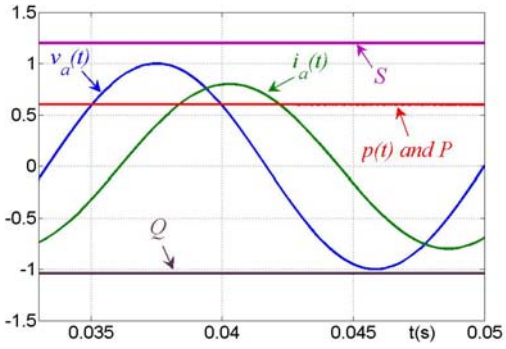

(c) *pf* < 1

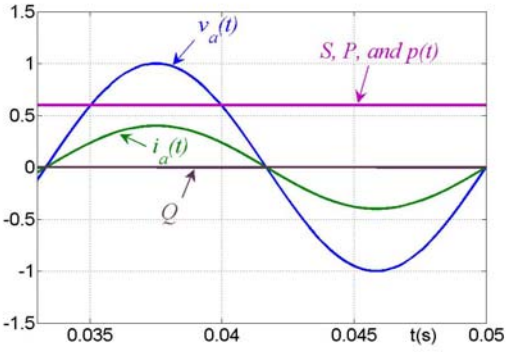

(d) Unity power factor

Figure 1.5. Active power and reactive power in a three-phase *RL* load.

The average active power P is

$$P = 3VI\cos\theta . \tag{1.26}$$

The apparent power S is

$$S = 3VI . \tag{1.27}$$

The average nonactive power Q is

$$Q = 3VI\sin\theta . \tag{1.28}$$

The phase angle θ between the voltage and the current is negative in a *RL* load system, i.e., the current is lagging the voltage. Figure 1.5c shows the phase angle between the voltage and the current in phase *a*. The instantaneous power $p(t)$, the average active power P, the average nonactive power Q, and the apparent power S are also plotted in Figure 1.5c. The instantaneous power, which is the sum of the instantaneous powers of three phases, is equal to the average active power at all times, although the instantaneous power of each phase is a sinusoidal waveform similar to the instantaneous power in the single-phase *RL* load case which was discussed in the previous subsection. Q is negative, which indicates that the load consumes nonactive power.

In Figure 1.5d, the same amount of average active power, which is also equal to the instantaneous power, is consumed by the load. However, the current is in phase with the voltage and the amplitude of the current is smaller than the one in Figure 1.5c. The apparent power is equal to the average active power and the average nonactive power is zero. If the current is in phase with the voltage, the required amount of current to carry a given amount of active power is minimum. Moreover, the average nonactive power is zero and the apparent is also the minimum value, which is equal to the average active power.

Loads of unity power factor are desired from the system point of view. If loads draw a large amount of nonactive power from the synchronous generators in a power system, the active power generation capability of the generators will be weakened. Furthermore, the current to carry the nonactive power increases system losses and demands higher current ratings of the transmission lines.

In a power system, the generation and consumption of active power must essentially be equal at any time as there is very little energy storage in a power system. In today's power systems, most active power is generated by synchronous generators and transmitted to loads. Furthermore, the generation and consumption of nonactive power must also be equal. The transmission lines and most loads consume nonactive power (inductive). The shortage of nonactive power can cause voltage instability and even voltage collapse which may lead to a blackout at a weak end of the system which is far away from the generator. The nonactive power could be generated by synchronous generators; however, it is not an optimal choice. One reason is because the generation of nonactive power by synchronous generators is at the cost of less active power generation, and it is usually at a higher price; and the other reason is the transmission of the nonactive power generated by synchronous generators to loads results in increased losses. Therefore, nonactive power should be compensated and balanced locally for the reason of reducing transmission losses and providing voltage support as well.

1.4 Nonlinear Loads and Distortion in Power Systems

Due to the nonlinear loads in a power system, there is distortion in the voltage and/or current waveforms, which deteriorates the quality of the electric power. For example, the

harmonics generated in the system may be amplified because of parallel and series resonance in the system. The existence of harmonics reduces the energy efficiency of a power system at the generation, transmission, and consumption points of the system. Harmonics can cause extra heating of the core of transformers and electrical machines. Furthermore, the harmonics may expedite the aging of the insulation of the components in the system and shorten their useful lifetime.

A nonactive compensator based on power electronics devices can be installed locally to compensate the nonlinear components. Specifically, a nonactive power compensator installed in the distribution level is an effective method to provide the fundamental nonactive component of load current so that it does not need to be transmitted all the way from the generator to the load. This reduces the losses of the transmission lines, and compensates the distortion in the system due to nonlinear loads.

In a system with distortion in the current and voltage waveforms, the standard definitions given in subsection 1.1 for nonactive power and nonactive current are no longer applicable to defining, measuring, or describing the power quality, which is a precondition to improve the power quality as well as to eliminate the distortion in the system. Different nonactive power theories have been proposed in the literature [2]-[37], and different nonactive power compensation methods have been implemented to compensate the nonactive power component in a power system [38]-[46]. In this dissertation, a new approach is presented on instantaneous nonactive power definitions, which can be used in a nonactive power compensation system for fundamental nonactive power and other nonactive power as well.

The following is a brief summary of the chapters in this dissertation. In Chapter 2, a literature survey is made of nonactive power theories and nonactive power compensation. In Chapter 3, a generalized instantaneous nonactive power theory is proposed. In Chapter 4, an implementation of the nonactive power theory in a shunt nonactive power compensator is presented and simulated. Chapter 5 presents an experimental study of the proposed method. In the last chapter, the main results of this generalized instantaneous nonactive power theory are summarized, and further research is proposed.

CHAPTER 2

Literature Survey

In this chapter, instantaneous nonactive power theories that have been proposed in the literature are reviewed, and their advantages as well as disadvantages are summarized. Also, various nonactive power compensation topologies are introduced and their shunt compensation is then discussed.

2.1 Nonactive Power Theories

As early as in the 1920s and 1930s, Fryze [2] and Budeanu [3] proposed instantaneous nonactive theories for periodic (but non-sinusoidal) waveforms in the time domain and the frequency domain, respectively. Different theories have been formulated in the last 30 years to describe the increasingly complex phenomena in power systems. Due to the existence of nonlinear loads, currents as well as voltages are distorted so that they are no longer pure sinusoids and sometimes not even periodic. They can be divided into the following categories:

1. Single-phase or multi-phase.
2. Periodic or non-periodic.

3. Balanced or unbalanced. For multi-phase voltages or currents, if the magnitude of each phase is equal and the phase angles between consecutive phases are also equal, then it is balanced, otherwise; it is unbalanced.

2.1.1 Instantaneous Nonactive Power Theories in Time Domain

Various nonactive power theories in the time domain have been discussed [4], and most of them can be divided into two categories. The first category is Fryze's theory [2] and its extensions, and the other is *p*-*q* theory [11]-[12] and its extensions.

Fryze's Theory In 1931, Fryze introduced his definition of nonactive power in [2] for sinusoidal power systems with harmonics by decomposing the source current $i(t)$ into an active component $i_a(t)$, which had the same waveform shape as (i.e., in phase with) the source voltage $v(t)$, and a nonactive component $i_n(t)$ by the following definitions:

$$i_a(t) \triangleq \frac{P}{\|v\|^2} v(t), \qquad i_n(t) \triangleq i(t) - i_a(t) \tag{2.1}$$

where $\|v\|$ is the root mean square (rms) value of $v(t)$ given by

$$\|v\| \triangleq \sqrt{\frac{1}{T}\int_0^T v^2(t)dt} \tag{2.2}$$

and P is the average value of $p(t) = v(t)i(t)$ over one period. If the source voltage is a pure sinusoid as in (1.1) (without harmonics), then $\|v\| = V$ as in (1.3). The currents $i_a(t)$ and $i_n(t)$ are mutually orthogonal; that is,

$$\int_0^T i_a(t) i_n(t) dt = 0 \tag{2.3}$$

The rms values $\|i_a\|$ and $\|i_n\|$ satisfy

$$\|i\|^2 = \|i_a\|^2 + \|i_n\|^2 . \tag{2.4}$$

By multiplying (2.4) by $\|v\|^2$, Fryze defined nonactive power Q_F as

$$Q_F \triangleq \|v\|\|i_n\| \tag{2.5}$$

Q_F is the same as the standard definition of Q in Chapter 1 if the voltage and current are steady-state fundamental sinusoidal waveforms.

The apparent power S is defined as

$$S^2 \triangleq \|v\|^2 \|i\|^2 . \tag{2.6}$$

The apparent power, active power, and nonactive power satisfy

$$S^2 = P^2 + Q_F^2 . \tag{2.7}$$

In an ideal system with fundamental sinusoidal voltage and current, Fryze's theory is consistent with the standard definitions in Chapter 1. This theory is valid for systems with harmonics. Based on average and rms values, the nonactive power Q_F is an average value, while the active current $i_a(t)$ and nonactive current $i_n(t)$ are instantaneous. Fryze's definition is the first definition of instantaneous nonactive power in the time domain given in the literature. It has been extended to multiple phases, and some contemporary definitions of active current are modifications of his idea. The theories discussed below are based on Fryze's theory.

Inductive and Capacitive Power In 1979, Kusters and Moore presented a theory for periodic non-sinusoidal waveforms in [5]-[6]. The active current i_a is defined the same as Fryze's theory in [2], but the nonactive current is subdivided into two components – the inductive (capacitive) reactive current and a residual current. The inductive (capacitive)

current can be completely eliminated by adding a capacitor (inductor) in parallel with the load. Their theory is applicable to passive compensation in single-phase systems.

Instantaneous Multi-Phase Currents Willems' [7] instantaneous multi-phase current theory, Rosssetto and Tenti's [8] instantaneous orthogonal current, Peng and Lai's [9] generalized instantaneous reactive power theory for three-phase system, and the instantaneous reactive quantity for multi-phase systems by Dai et al. [10] are essentially the same. They are an extension of Fryze's theory to multi-phase systems and use instantaneous values instead of average values. The voltage and the current are vectors in a multi-phase system, i.e.,

$$\boldsymbol{v}(t) \triangleq [v_1, v_2, ..., v_m]^T \tag{2.8}$$

$$\boldsymbol{i}(t) \triangleq [i_1, i_2, ..., i_m]^T \tag{2.9}$$

where m is the number of phases. The instantaneous active current is defined by

$$\boldsymbol{i}_p(t) \triangleq \frac{\boldsymbol{v}^T \boldsymbol{i}}{\boldsymbol{v}^T \boldsymbol{v}} \boldsymbol{v} \tag{2.10}$$

The instantaneous nonactive current is then defined as

$$\boldsymbol{i}_q(t) \triangleq \boldsymbol{i}(t) - \boldsymbol{i}_p(t) \tag{2.11}$$

$\boldsymbol{i}_p(t)$ and $\boldsymbol{i}_q(t)$ are orthogonal. The difference between the theory in [9] and [10] from that given in [7] and [8] is the definition of instantaneous nonactive power, which in [9] and [10] is the cross-product of the voltage vector and the current vector. The theory in [9] is only applicable to three-phase systems with or without neutral line. These theories assume that the voltage is purely sinusoidal and balanced. The current is instantaneous and not limited to periodic waveforms. However, if $\boldsymbol{i}(t)$ has harmonics, this theory generates harmonics with frequencies different from the harmonics in $\boldsymbol{i}(t)$ due to the

multiplication between the fundamental component and a harmonic or two harmonics with different frequencies.

***p-q* Theory** In 1984, Akagi et al. proposed an instantaneous reactive power theory known as *p-q* theory for three-phase systems [11]-[12]. Park's transformation is applied to transform the a-b-c quantities of the three-phase system to the α-β two-phase equivalent quantities according to

$$\begin{bmatrix} v_\alpha \\ v_\beta \end{bmatrix} \triangleq \sqrt{\frac{2}{3}} \begin{bmatrix} 1 & -1/2 & -1/2 \\ 0 & \sqrt{3}/2 & -\sqrt{3}/2 \end{bmatrix} \begin{bmatrix} v_a \\ v_b \\ v_c \end{bmatrix} \tag{2.12}$$

and

$$\begin{bmatrix} i_\alpha \\ i_\beta \end{bmatrix} \triangleq \sqrt{\frac{2}{3}} \begin{bmatrix} 1 & -1/2 & -1/2 \\ 0 & \sqrt{3}/2 & -\sqrt{3}/2 \end{bmatrix} \begin{bmatrix} i_a \\ i_b \\ i_c \end{bmatrix}. \tag{2.13}$$

The instantaneous active power *p* and reactive power *q* are then defined as

$$\begin{bmatrix} p \\ q \end{bmatrix} \triangleq \begin{bmatrix} v_\alpha & v_\beta \\ -v_\beta & v_\alpha \end{bmatrix} \begin{bmatrix} i_\alpha \\ i_\beta \end{bmatrix}. \tag{2.14}$$

A Fourier series expansion of *p* consists of a DC component $\bar{p}$, which is referred to as the fundamental component, and the higher order harmonic remaining terms denoted by $\tilde{p}$; that is,

$$p = \bar{p} + \tilde{p} \tag{2.15}$$

Similarly, *q* may be written as

$$q = \bar{q} + \tilde{q}\,. \tag{2.16}$$

The currents i_α and i_β are divided into two components. The α-axis component of the instantaneous active current is defined by

$$i_{\alpha p} = \frac{v_\alpha}{v_\alpha^2 + v_\beta^2} p = \frac{v_\alpha}{v_\alpha^2 + v_\beta^2} \bar{p} + \frac{v_\alpha}{v_\alpha^2 + v_\beta^2} \tilde{p} . \tag{2.17}$$

The α-axis component of the reactive current is defined by

$$i_{\alpha q} = \frac{-v_\beta}{v_\alpha^2 + v_\beta^2} q = \frac{-v_\beta}{v_\alpha^2 + v_\beta^2} \bar{q} + \frac{-v_\beta}{v_\alpha^2 + v_\beta^2} \tilde{q} . \tag{2.18}$$

Similarly, the β-axis component of the active current is defined by

$$i_{\beta p} = \frac{v_\beta}{v_\alpha^2 + v_\beta^2} p = \frac{v_\beta}{v_\alpha^2 + v_\beta^2} \bar{p} + \frac{v_\beta}{v_\alpha^2 + v_\beta^2} \tilde{p} \tag{2.19}$$

and the β-axis component of the reactive current is defined by

$$i_{\beta q} = \frac{v_\alpha}{v_\alpha^2 + v_\beta^2} q = \frac{v_\alpha}{v_\alpha^2 + v_\beta^2} \bar{q} + \frac{v_\alpha}{v_\alpha^2 + v_\beta^2} \tilde{q} . \tag{2.20}$$

Let the reactive current be defined by

$$i_{c\alpha} = \frac{v_\alpha}{v_\alpha^2 + v_\beta^2} \tilde{p} - \frac{v_\beta}{v_\alpha^2 + v_\beta^2} (\bar{q} + \tilde{q}) , \tag{2.21}$$

$$i_{c\beta} = \frac{v_\beta}{v_\alpha^2 + v_\beta^2} \tilde{p} + \frac{v_\alpha}{v_\alpha^2 + v_\beta^2} (\bar{q} + \tilde{q}) . \tag{2.22}$$

If $i_{c\alpha}$ and $i_{c\beta}$ can be supplied by a compensator, then the power utility only needs to provide the following active currents

$$i_{s\alpha} = \frac{v_\alpha}{v_\alpha^2 + v_\beta^2} \bar{p} \tag{2.23}$$

$$i_{s\beta} = \frac{v_\beta}{v_\alpha^2 + v_\beta^2} \bar{p} \tag{2.24}$$

and therefore only the active power $v_\alpha i_{s\alpha} + v_\beta i_{s\beta} = \bar{p}$.

The *p-q* theory has the following limitations:

1. The original *p-q* theory was developed for three-phase, three-wire systems, and later was used in three-phase, four-wire systems by introducing the zero-phase sequence components. However, it cannot be used in single-phase systems.
2. The assumption of this theory is that the voltage is purely sinusoidal and the three phases are balanced. However, in real power systems, there is distortion in the voltage, and the *p-q* theory will introduce errors if it is applied to a nonactive power compensation system [13].
3. Average values are still used ($\bar{p}$, $\bar{q}$, $\tilde{p}$, and $\tilde{q}$) in the theory, so it is not an actual instantaneous definition of real and reactive components, i.e., data from at least half of a cycle of the fundamental period are needed to calculate the average values.

***p-q-r* Theory** Kim et al. [14]-[15] proposed a theory based on two sets of transformations. The voltages and currents are transformed first from Cartesian *a-b-c* coordinates to Cartesian 0-α-β coordinates, and then from Cartesian 0-α-β coordinates to Cartesian *p-q-r* coordinates. It is valid in three-phase four-wire systems and completely eliminates the neutral current even if the system voltage is unbalanced or distorted by harmonics.

In addition to these theories, the Fryze-Buchholz-Depenbrock (FBD) method by Depenbrock [16] is valid in multi-phase periodic systems. The definitions of the active current and the nonactive current are an extension of Fryze's idea to multi-phase systems.

Because average values are used, complete compensation of nonactive current is only possible under steady-state conditions. Enslin and Van Wyk [17]-[20] modified Fryze's theory to single-phase non-periodic systems. They introduced a time interval ΔT for a non-periodic system and the active current and the nonactive current are defined based on this time interval. Therefore, the definitions depend on the interval ΔT and the time at which the interval starts.

Ferrero and Superti-Furga's Park power theory [21]-[22] is the same as *p-q* theory [11]-[12], except the definition of Park imaginary power (instantaneous nonactive power). In addition, they also extended Fryze's theory [2] to three-phase three-wire systems. Nabae and Tanaka [23] defined the voltage and current space vectors in polar coordinates. It is restricted to three-phase systems. All the definitions of currents and powers are originated from fundamental frequency and balanced systems. Systems with harmonics or unbalanced are not discussed in the papers. Table 2.1 summarizes the nonactive power theories in the time domain.

2.1.2 Instantaneous Nonactive Power Theories in Frequency Domain

Instantaneous nonactive power theories developed in the frequency domain share a key idea that the voltage and the current are decomposed into a fundamental component and harmonics by using the Fourier series decomposition. Of course, this is applicable to periodic systems only. Furthermore, it requires at least one half cycle of the fundamental period to compute the average values and thus is not instantaneous. Because of the cross multiplication between harmonics, the definition of power is more complex than in the time domain. To meet the standard definitions in [1], some theories have to define several

Table 2.1. Comparison of nonactive power theories in the time domain.

Theory [Reference]	Phases			Time Period		Voltage[1]	Current Waveforms		
	1	3	*m*	Ave-rage	Instan-taneous		Funda-mental	Harm-onics	Non-Periodic
Fryze's Theory [2]	√			√		a	√	√	
Inductive and Capacitive Power [5]-[6]	√			√		a	√	√	
Instantaneous Multi-Phase Currents [7]-[10]		√	√		√	b	√	√	
p-q Theory [11]-[12]		√			√	b	√	√	
p-q-r Theory [14]-[15]		√			√	c	√	√	
FBD Method [16]		√	√	√		b	√	√	
Single-Phase Non-Periodic [17]-[20]	√			√		d	√	√	√
Park Power [21]-[22]		√			√	b	√	√	
Nabae and Tanaka [23]		√			√	b	√		

Notes: 1. The assumptions of the system voltage, which are

a. Fundamental sine wave

b. Fundamental sine wave and balanced

c. Periodic, but non-sinusoidal

d. No assumption

nonactive power components, which do not have explicit physical meanings or provide a good foundation for nonactive power compensation.

Budeanu's Approach The first definition of nonactive power in the frequency domain was proposed in 1929 by Budeanu [3]. He extended the notion of nonactive power from systems with sinusoidal voltage and current to those with periodic non-sinusoidal waveforms using the Fourier series decomposition. The voltage $v(t)$ and current $i(t)$ are decomposed as

$$v(t) \triangleq \sum_{n=1}^{\infty} \sqrt{2} V_n \cos(n\omega t + \alpha_n), \tag{2.25}$$

$$i(t) \triangleq \sum_{n=1}^{\infty} \sqrt{2} I_n \cos(n\omega t + \beta_n). \tag{2.26}$$

The active power P is given by

$$P = \frac{1}{T}\int_0^T v(t)i(t)dt = \sum_{n=1}^{\infty} V_n I_n \cos(\alpha_n - \beta_n). \tag{2.27}$$

The rms values of $v(t)$ and $i(t)$ are, respectively,

$$V = \sqrt{\sum_{n=1}^{\infty} V_n^2} \tag{2.28}$$

and

$$I = \sqrt{\sum_{n=1}^{\infty} I_n^2}. \tag{2.29}$$

The apparent power S is given by

$$S = VI. \tag{2.30}$$

The total reactive power Q_B is defined as

$$Q_B = \sum_{n=1}^{\infty} V_n I_n \sin(\alpha_n - \beta_n)\,. \tag{2.31}$$

However, $S^2 \neq P^2 + Q_B^2$, which is not consistent with the standard definitions in [1]. Therefore, the distortion power D_B is introduced so that

$$S^2 \triangleq P^2 + Q_B^2 + D_B^2 \tag{2.32}$$

They do not have physical meanings and the minimization of Q_B does not necessarily improve the power factor [24].

Hilbert Space Techniques [25] An *n*-phase system is considered, in which the time-domain vector waveforms $\boldsymbol{v}(t)$ and $\boldsymbol{i}(t)$ are periodic with a fundamental period T. Such waveforms can be represented by a summable Fourier series, i.e.,

$$v(t) = \sum_{l=-\infty}^{\infty} V_l e^{jl\omega t} \tag{2.33}$$

and

$$i(t) = \sum_{n=-\infty}^{\infty} I_l e^{jl\omega t}\,. \tag{2.34}$$

V_l and I_l are defined as the Fourier coefficients, that is,

$$V_l = \frac{1}{T}\int_T v(t) e^{-jl\omega t} dt \triangleq \langle v(t) \rangle_l\,, \text{ where } l = -\infty, ..., \infty \tag{2.35}$$

and

$$I_l = \frac{1}{T}\int_T i(t) e^{-jl\omega t} dt \triangleq \langle i(t) \rangle_l\,, \text{ where } l = -\infty, ..., \infty\,. \tag{2.36}$$

The instantaneous active current $\boldsymbol{i}_{\boldsymbol{a}}(t)$ and the instantaneous inactive current $\boldsymbol{i}_{\boldsymbol{x}}(t)$ are defined by

$$\boldsymbol{i}_a(t) \triangleq \frac{\boldsymbol{i}(t)^T \boldsymbol{v}(t)}{\boldsymbol{v}(t)^T \boldsymbol{v}(t)} \boldsymbol{v}(t) = \frac{p(t)}{\boldsymbol{v}(t)^T \boldsymbol{v}(t)} \boldsymbol{v}(t) \tag{2.37}$$

$$\boldsymbol{i}_x(t) \triangleq \boldsymbol{i}(t) - \boldsymbol{i}_a(t) \tag{2.38}$$

The definitions of active current and nonactive current in this theory are the same as the theories in [7]-[10], and their problems are:

1. The active current $\boldsymbol{i}_a(t)$ may have harmonic components with frequencies different from the harmonics in $\boldsymbol{i}(t)$. As shown in (2.37), the new harmonic components are generated due to the multiplication between the fundamental component and a harmonic or two harmonics with different frequencies. The goal of nonactive power compensation is to provide the nonactive component in the current, including fundamental nonactive power, harmonics, and other nonactive components. Although the aim of this definition is to minimize the source current (in rms) that supplies the same power as the original load current, this definition increases the harmonic content in the current instead of improving it.
2. If $n = 1$ (a single-phase system), $i_a(t) \equiv i(t)$, and $i_x(t) \equiv 0$. This theory is not able to separate the active power and nonactive power in a single-phase system.

In addition to the theories which have been discussed in the frequency domain, references [26]-[36] decompose the nonactive power or nonactive current into several components. Some of the definitions of active power in these papers are consistent with the physical meaning of active power, while others are not. The definitions of nonactive power in some theories have active power components. All the theories in the frequency domain assume that the Fourier series of the voltage and current are known, which is not practically useful for nonactive power compensation applications.

2.2 Nonactive Power Compensation

Linear loads which do not have unity power factor draw fundamental nonactive power. Nonlinear loads cause problems such as harmonics, unbalance, and distortion in power systems, in addition to the problem of fundamental nonactive power. Some nonlinear loads draw irregular currents, which are neither sinusoidal nor periodic. Variable-speed motor drives, arc furnaces [37], computer power supplies, and single-phase loads (unbalanced in a three-phase system) are the most common nonlinear loads in power systems. Both linear and nonlinear loads cause "pollution" in power systems, i.e., low power factor, excess transmission losses, voltage sags, voltage surges, and electromagnetic interference (EMI), which deteriorate the power quality, and utility or consumer equipment is damaged in some extreme cases.

Nonactive power compensation is an effective method to clean up the pollution in power systems. Synchronous generators, capacitor banks, and parallel- or series-connected reactors can compensate the fundamental reactive power and improve the power factor, and passive *L*-*C* filters can reduce harmonics. However, these are all steady-state devices and have little instantaneous capability. With the development of power electronics technology, solid-state switching devices such as thyristors, gate turn-off thyristors (GTOs) and insulated gate bipolar transistors (IGBTs), new approaches are possible for nonactive power compensation [38]-[40].

2.2.1 Series-Connected Compensators

Depending on the characteristics of a nonlinear load, it can be represented as a voltage-source load or as a current-source load. For a voltage-source load, a compensator

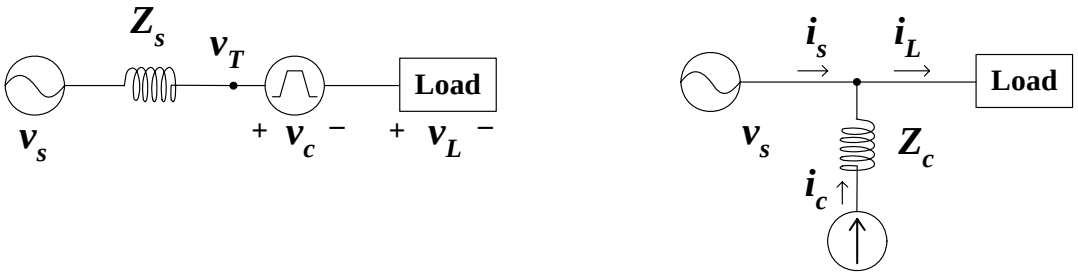

(a) Series-Connected Compensator (b) Parallel-Connected Compensator

Figure 2.1. Topologies of series and parallel compensators.

is connected in series with the load (Figure 2.1a). Most loads are represented as current-source loads [39], and the compensator acts as a nonactive power source in parallel (shunt) with the utility and injects a certain amount of current (the nonactive component of the load current) to the system so that the utility only provides the active component to the load.

2.2.2 Parallel-Connected Compensators

As mentioned above, most loads can be represented as current sources. To compensate the nonactive component in the load current, a parallel compensator is needed which injects the same amount of nonactive current (i_c in Figure 2.1b) as the nonactive component in the load current so that the utility provides active current only (i_s in Figure 2.1b).

2.2.3 Static Synchronous Compensator (STATCOM)

There are different topologies of nonactive power compensators, such as the thyristor controlled reactor (TCR), the thyristor switched capacitor (TSC), and the static synchronous compensator (STATCOM). Among them, STATCOM is a shunt-connected

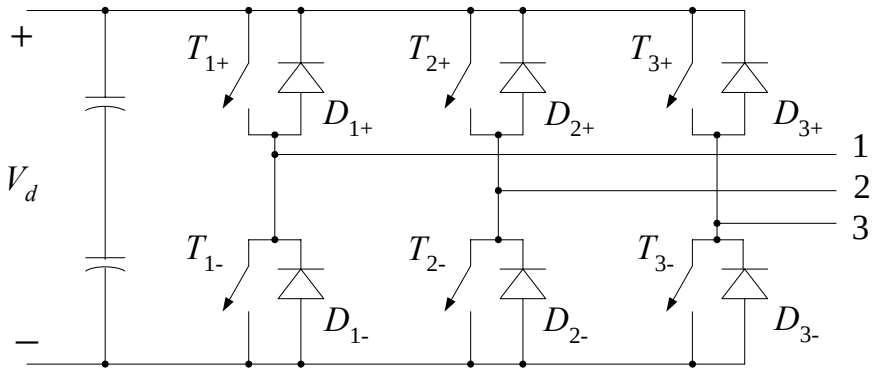

Figure 2.2. A three-phase inverter.

static var compensator whose output current can be controlled independent of the ac system voltage. A STATCOM uses IGBTs or GTOs, which have turn-on and turn-off capabilities; it does not require an energy source, and requires only very limited energy storage if it performs nonactive power compensation only. Also referred to as an active filter, the STATCOM has lent itself to real-time nonactive power/current compensation applications which is independent of the system voltage because of its flexibility in the control of switches.

Figure 2.2 shows a typical topology of a three-phase inverter, which is widely used in STATCOMs. This is a voltage-source inverter which has capacitors on the dc side as it provides nonactive current only so that no energy source is needed. The ac side is connected to the system in parallel with the utility to provide demanded current to the load. The system configuration of a STATCOM will be discussed in more detail in Chapter 4. Nonactive power theories are implemented for a shunt nonactive compensation, and the control strategies and practical issues are discussed in [41]-[46].

2.3 Summary

A survey on the nonactive power/current theories in both the time domain and the frequency domain was provided. As explained, the theories in the time domain are divided into two categories, Fryze's approach and the *p*-*q* approach. Both approaches were characterized according to the number of phases they are applicable to, the time period which is used to define the quantities (instantaneous or average), and their ability to handle current waveforms (fundamental, distorted with harmonics, or non-periodic). Their advantages and disadvantages were discussed as well as their applicability to the compensation of nonactive power.

The nonactive power/current theories developed in the frequency domain were also briefly discussed. It was stated that they are restricted to periodic systems and result in the definitions of two or more nonactive power components which do not have any physical meanings. Some of the proposed definitions of active power were not consistent with the real (physics-based) meaning of active power. It is assumed that both the voltage and the current are in steady state so that they can be presented by the Fourier series, so the ability of these theories to handle a transient state is poor. Furthermore, at least one cycle of the fundamental period is needed to perform the Fourier decomposition. Therefore, these theories cannot be applied to instantaneous nonactive power compensation.

CHAPTER 3

Generalized Nonactive Power Theory

Many definitions of nonactive power/current have been discussed in the previous chapter. There is little debate about the definitions of active power or nonactive power in sinusoidal cases, but the theories differ in the case of non-sinusoidal and non-periodic waveforms. Some definitions work well in three-phase, three-wire systems, but are not able to handle the single-phase case, while others can only be applied to periodic waveforms. Furthermore, some definitions are related to physical quantities, while other do not have any physical meaning.

The theory proposed by Peng and Lai [9] is a generalized theory of instantaneous active power/current and instantaneous nonactive power/current for a three-phase system. Active power is the time rate of energy generation, transmission, or consumption. The current that carries active power is the active current, which is the component of current in phase with the voltage. Nonactive power is the time rate of the energy that circulates back and forth between the source and load. In a multi-phase circuit, it also includes the power that circulates among phases.

3.1 Generalized Nonactive Power Theory

The generalized nonactive power theory proposed in this dissertation is based on Fryze's idea of nonactive power/current discussed in section 2.1.1 and is an extension of the theory proposed in [47].

Let a voltage vector $\boldsymbol{v}(t)$ and a current vector $\boldsymbol{i}(t)$ be given by

$$\boldsymbol{v}(t) = [v_1(t), v_2(t), ..., v_m(t)]^T , \tag{3.1}$$

and

$$\boldsymbol{i}(t) = [i_1(t), i_2(t), ..., i_m(t)]^T , \tag{3.2}$$

respectively, where m is the number of phases.

The **instantaneous power** $p(t)$ is defined by

$$p(t) \triangleq \boldsymbol{v}^T(t)\boldsymbol{i}(t) = \sum_{k=1}^{m} v_k(t) i_k(t) . \tag{3.3}$$

The **average power** $P(t)$ is defined as the average value of the instantaneous power $p(t)$ over the averaging interval $[t\text{-}T_c, t]$, i.e.,

$$P(t) \triangleq \frac{1}{T_c} \int_{t-T_c}^{t} p(\tau) d\tau . \tag{3.4}$$

The **instantaneous active current** $\boldsymbol{i_a(t)} = [i_{a1}(t), i_{a2}(t), \ldots, i_{am}(t)]^T$ and **instantaneous nonactive current** $\boldsymbol{i_n(t)} = [i_{n1}(t), i_{n2}(t), \ldots, i_{nm}(t)]^T$ are, respectively,

$$\boldsymbol{i_a}(t) \triangleq \frac{P(t)}{V_p^2(t)} \boldsymbol{v_p}(t) , \tag{3.5}$$

and

$$\boldsymbol{i_n}(t) \triangleq \boldsymbol{i}(t) - \boldsymbol{i_a}(t) . \tag{3.6}$$

The rms value $V(t)$ of a voltage vector $\boldsymbol{v}(t)$ is defined by

$$V(t) \triangleq \sqrt{\frac{1}{T_c}\int_{t-T_c}^{t} \boldsymbol{v}^T(\tau)\boldsymbol{v}(\tau)d\tau}\,. \tag{3.7}$$

In (3.5), the voltage $v_p(t)$ is the reference voltage, which is chosen based on the characteristics of the system and the desired compensation results. It will be elaborated in subsection 3.1.2. $V_p(t)$ is the corresponding rms value of the reference voltage $\boldsymbol{v_p}(t)$, i.e.,

$$V_p(t) \triangleq \sqrt{\frac{1}{T_c}\int_{t-T_c}^{t} \boldsymbol{v_p^T}(\tau)\boldsymbol{v_p}(\tau)d\tau}\,. \tag{3.8}$$

Based on the above definitions for $\boldsymbol{i_a}(t)$ and $\boldsymbol{i_n}(t)$, the **instantaneous active power** $p_a(t)$ and **instantaneous nonactive power** $p_n(t)$ are defined as

$$p_a(t) \triangleq \boldsymbol{v}^T(t)\boldsymbol{i_a}(t) = \sum_{k=1}^{m} v_k(t)i_{ak}(t)\,, \tag{3.9}$$

and

$$p_n(t) \triangleq \boldsymbol{v}^T(t)\boldsymbol{i_n}(t) = \sum_{k=1}^{m} v_k(t)i_{nk}(t)\,. \tag{3.10}$$

The rms values of the active current $\boldsymbol{i_a}(t)$, nonactive current $\boldsymbol{i_n}(t)$, and current $\boldsymbol{i}(t)$ are, respectively,

$$I_a(t) \triangleq \sqrt{\frac{1}{T_c}\int_{t-T_c}^{t} \boldsymbol{i_a^T}(\tau)\boldsymbol{i_a}(\tau)d\tau}\,, \tag{3.11}$$

$$I_n(t) \triangleq \sqrt{\frac{1}{T_c}\int_{t-T_c}^{t} \boldsymbol{i_n^T}(\tau)\boldsymbol{i_n}(\tau)d\tau}\,, \tag{3.12}$$

and

$$I(t) \triangleq \sqrt{\frac{1}{T_c}\int_{t-T_c}^{t} \boldsymbol{i}^T(\tau)\boldsymbol{i}(\tau)d\tau}\,. \tag{3.13}$$

The **average active power** $P_a(t)$ is defined as the average value of the instantaneous active power $p_a(t)$ over the averaging interval $[t\text{-}T_c, t]$, i.e.,

$$P_a(t) \triangleq \frac{1}{T_c} \int_{t-T_c}^{t} p_a(\tau) d\tau \,. \tag{3.14}$$

The **average nonactive power** $P_n(t)$ is defined as the average value of the instantaneous nonactive power $p_n(t)$ over the averaging interval $[t\text{-}T_c, t]$, i.e.,

$$P_n(t) \triangleq \frac{1}{T_c} \int_{t-T_c}^{t} p_n(\tau) d\tau \,. \tag{3.15}$$

Based on the rms values defined above, the **apparent power** $S(t)$ is defined by

$$S(t) = V(t) I(t) \,. \tag{3.16}$$

The **apparent active power** $P_p(t)$ is defined by

$$P_p(t) = V(t) I_a(t) \,. \tag{3.17}$$

The **apparent nonactive power** $Q(t)$ is defined by

$$Q(t) = V(t) I_n(t) \,. \tag{3.18}$$

3.1.1 Averaging Interval T_c

The standard definitions for an ideal three-phase, sinusoidal power system use the fundamental period T to define the rms values and average active power and nonactive power. In the generalized nonactive power theory, the averaging time interval T_c can be chosen arbitrarily from zero to infinity, and for different T_c, the resulting active current and nonactive current will have different characteristics. The flexibility of choosing different T_c as well as the reference voltage results in this theory being applicable for defining nonactive power for a larger class of systems than in the current literature. For

each case, a specific value of T_c can be chosen to fit the application or to achieve an optimal result. The choice of T_c will be discussed in the following subsections.

3.1.1.1 $T_c = 0$

In this case, the definitions of average powers are the same as the instantaneous powers, and the rms definitions have different forms, i.e.,

$$V(t) = \boldsymbol{v}^T(t)\boldsymbol{v}(t), \tag{3.19}$$

$$I(t) = \boldsymbol{i}^T(t)\boldsymbol{i}(t), \tag{3.20}$$

and

$$V_p(t) = \boldsymbol{v}_{\boldsymbol{p}}^{\boldsymbol{T}}(t)\boldsymbol{v}_{\boldsymbol{p}}(t). \tag{3.21}$$

Further, the definitions of instantaneous active current $\boldsymbol{i}_{\boldsymbol{a}}(t)$ and instantaneous nonactive current $\boldsymbol{i}_{\boldsymbol{n}}(t)$ are, respectively,

$$\boldsymbol{i}_{\boldsymbol{a}}(t) = \frac{p(t)}{V_p^2(t)}\boldsymbol{v}_{\boldsymbol{p}}(t), \tag{3.22}$$

and

$$\boldsymbol{i}_{\boldsymbol{n}}(t) = \boldsymbol{i}(t) - \boldsymbol{i}_{\boldsymbol{a}}(t). \tag{3.23}$$

If $\boldsymbol{v}_{\boldsymbol{p}}(t) = \boldsymbol{v}(t)$, the instantaneous active power $p_a(t)$ is equal to the instantaneous power $p(t)$, and the instantaneous nonactive power $p_n(t)$ is identically zero, that is,

$$p_a(t) = \boldsymbol{v}^T(t)\boldsymbol{i}_{\boldsymbol{a}}(t) \equiv p(t), \tag{3.24}$$

$$p_n(t) = \boldsymbol{v}^T(t)\boldsymbol{i}_{\boldsymbol{n}}(t) \equiv 0. \tag{3.25}$$

More specifically, in a single-phase system, the instantaneous active current $i_a(t)$ is always equal to the current $i(t)$, and the instantaneous nonactive current $i_n(t)$ is always

zero, therefore, T_c = 0 is not suitable for nonactive power/current definitions in single-phase systems.

3.1.1.2 T_c is a finite value

For most applications, T_c will be chosen as a finite value. For a periodic system with fundamental period T, T_c is chosen as $T_c = T/2$. If $\boldsymbol{v_p}$(t) is chosen as a periodic waveform with period T, then the average power $P(t)$ and the rms value $V_p(t)$ are both constant numbers, i.e., $P(t) = P$, and $V_p(t) = V_p$.

$$\boldsymbol{i}_a(t) = \frac{P}{V_p^2}\boldsymbol{v}_p(t)\,. \tag{3.26}$$

The instantaneous active current is proportional to and has the same shape as the reference voltage. Therefore, by choosing different reference voltages, the instantaneous active current can have different waveforms.

The generalized nonactive power theory does not specify the characteristics of the voltage $\boldsymbol{v}(t)$ and current $\boldsymbol{i}(t)$, i.e., they can theoretically be any waveforms. However in a power system, the voltage is usually sinusoidal with/without harmonic distortion, and the distortion of the voltage is usually lower than that of the currents (the total harmonic distortion (THD) of the voltage is usually less than 5%.). Therefore in this dissertation, the voltage is assumed to be periodic for all cases. A non-periodic system is referred to as a system with periodic voltage and a non-periodic current. In a non-periodic system, the instantaneous current varies with different averaging interval T_c, which is different from the periodic cases. In applications such as nonactive power compensation, T_c is usually chosen to be 1-10 times that of the fundamental period based on the tradeoff between

acceptable compensation results and reasonable capital costs. This will be illustrated in Chapter 4.

3.1.1.3 $T_c \to \infty$

This is a theoretical analysis of a non-periodic system, in which a finite T_c can not completely account for the entire nonactive component in the current. It will be elaborated in Subsection 3.2.2. However, $T_c \to \infty$ is not practical in an actual power system application, and a finite T_c will be used instead.

3.1.2 Reference Voltage $\boldsymbol{v_p(t)}$

If $P(t)$ and $V_p(t)$ are constant, which can be achieved with $T_c = T/2$ for a periodic system, or with $T_c \to \infty$ for a non-periodic system, the active current $\boldsymbol{i_a}(t)$ is in phase with $\boldsymbol{v_p}(t)$ (as shown in (3.26)), and the waveforms of $\boldsymbol{i_a}(t)$ and $\boldsymbol{v_p}(t)$ have the same shape and they differ only by a scale factor. Theoretically, $\boldsymbol{v_p}(t)$ can be arbitrarily chosen, but in practice, it is chosen based on the voltage $\boldsymbol{v}(t)$, the current $\boldsymbol{i}(t)$, and the desired active current $\boldsymbol{i_a}(t)$. Choices for $\boldsymbol{v_p}(t)$ include

1. $\boldsymbol{v_p}(t) = \boldsymbol{v}(t)$. If $\boldsymbol{v}(t)$ is a pure sinusoid; or the active current $\boldsymbol{i_a}(t)$ is preferred to have the same waveform as $\boldsymbol{v}(t)$.
2. $\boldsymbol{v_p}(t) = \boldsymbol{v_f}(t)$, where $\boldsymbol{v_f}(t)$ is the fundamental positive sequence component of $\boldsymbol{v}(t)$. In power systems, if $\boldsymbol{v}(t)$ is distorted or even unbalanced, and a purely sinusoidal $\boldsymbol{i_a}(t)$ is desired, then $\boldsymbol{v_p}(t)$ is chosen as the fundamental positive sequence component of $\boldsymbol{v}(t)$. This ensures that $\boldsymbol{i_a}(t)$ is balanced and does not contain any harmonics.
3. Other references to eliminate certain components in current $\boldsymbol{i}(t)$. For example, in a hybrid nonactive power compensation system with a STATCOM and a passive

LC filter, the lower order harmonics in the current are compensated by the STATCOM, and the higher order harmonics will be filtered by the passive filter due to the limit of the switching frequency of the STATCOM. In this case, a reference voltage with the higher order harmonics is chosen so that the resulting nonactive current which will be compensated by the STATCOM does not contain these harmonics.

By choosing different reference voltages, $\boldsymbol{i}_a(t)$ can have various desired waveforms and the unwanted components in $\boldsymbol{i}(t)$ can be eliminated. Furthermore, the elimination of each component is independent of each other.

The definitions of the generalized nonactive power theory are consistent with the standard definitions for ideal sinusoidal cases. The theory also extends the definitions to other situations. Table 3.1 summarizes the definitions of the generalized nonactive power theory. All the definitions are functions of time. Column 1 contains the definitions of the instantaneous voltage, currents, and powers. The voltage and currents are vectors, while the powers are scalars. Column 2 contains the rms values of the instantaneous voltages and currents in column 1. They are the root mean square values of the corresponding instantaneous definitions from column 4 over the time interval $[t\text{-}T_c,\ t]$. Column 3 contains the average values of the instantaneous powers in column 1 over the time interval $[t\text{-}T_c,\ t]$. Finally, column 4 gives the definitions of apparent powers, which are derived from the rms values of the voltages and currents. The characteristics and the physical meaning of the definitions and the relationship of these definitions will be discussed in more detail in the following subsection.

Table 3.1. Definitions of the generalized nonactive power theory.

Instantaneous Definitions	**Root Mean Square (rms) Definitions**	**Average Powers**	**Apparent Powers**
$\boldsymbol{v}(t) = [v_1(t), \ldots, v_m(t)]^T$	$V(t) = \sqrt{\frac{1}{T_c}\int_{t-T_c}^{t} \boldsymbol{v}^T(\tau)\boldsymbol{v}(\tau)d\tau}$		
$\boldsymbol{i}(t) = [i_1(t), \ldots, i_m(t)]^T$	$I(t) = \sqrt{\frac{1}{T_c}\int_{t-T_c}^{t} \boldsymbol{i}^T(\tau)\boldsymbol{i}(\tau)d\tau}$		
$\boldsymbol{i}_a(t) = \frac{P(t)}{V_p^2(t)}\boldsymbol{v}_p(t)$	$I_a(t) = \sqrt{\frac{1}{T_c}\int_{t-T_c}^{t} \boldsymbol{i}_a^T(\tau)\boldsymbol{i}_a(\tau)d\tau}$		
$\boldsymbol{i}_n(t) = \boldsymbol{i}(t) - \boldsymbol{i}_a(t)$	$I_n(t) = \sqrt{\frac{1}{T_c}\int_{t-T_c}^{t} \boldsymbol{i}_n^T(\tau)\boldsymbol{i}_n(\tau)d\tau}$		
$p(t) = \boldsymbol{v}^T(t)\boldsymbol{i}(t)$		$P(t) = \frac{1}{T_c}\int_{t-T_c}^{t} p(\tau)d\tau$	
$p_a(t) = \boldsymbol{v}^T(t)\boldsymbol{i}_a(t)$		$P_a(t) = \frac{1}{T_c}\int_{t-T_c}^{t} p_a(\tau)d\tau$	
$p_n(t) = \boldsymbol{v}^T(t)\boldsymbol{i}_n(t)$		$P_n(t) = \frac{1}{T_c}\int_{t-T_c}^{t} p_n(\tau)d\tau$	
			$S(t) = V(t)I(t)$
			$P_p(t) = V(t)I_a(t)$
			$Q(t) = V(t)I_n(t)$

3.2 Characteristics of the Generalized Nonactive Power Theory

In general, the nonactive power theory has the following characteristics.

1. $\boldsymbol{i_a}(t)$ and $\boldsymbol{i_n}(t)$ are orthogonal.

The instantaneous active current $\boldsymbol{i_a}(t)$ and the instantaneous nonactive current $\boldsymbol{i_n}(t)$ are orthogonal, that is,

$$\int_{t-T_c}^{t} \boldsymbol{i}_{\boldsymbol{a}}^{\boldsymbol{T}}(\tau)\boldsymbol{i}_{\boldsymbol{n}}(\tau)d\tau = 0, \tag{3.27}$$

so that

$$I^2(t) = I_a^2(t) + I_n^2(t). \tag{3.28}$$

The instantaneous active current is in phase with the voltage $\boldsymbol{v}(t)$, while the instantaneous nonactive current is 90° out of phase with $\boldsymbol{v}(t)$. The physical meaning of this characteristic is that the active current carries active power and the nonactive current carries nonactive power.

2. The instantaneous active power $p_a(t)$ and nonactive power $p_n(t)$.

The instantaneous power $p(t)$ is decomposed into two components, the instantaneous active power $p_a(t)$ and the instantaneous nonactive power $p_n(t)$, which satisfy

$$p(t) = p_a(t) + p_n(t). \tag{3.29}$$

Similar to the instantaneous active current and nonactive current, at any moment, the power flowing in the system has two components, i.e., the active power component and the nonactive power component.

3. The apparent powers.

If $\boldsymbol{v_p}(t) = \boldsymbol{v}(t)$, the apparent powers $S(t)$, $P_p(t)$, and $P_n(t)$ satisfy

$$S^2(t) = P_p^2(t) + Q^2(t). \tag{3.30}$$

The generalized theory has different characteristics when it is applied to different systems. Three-phase systems will be first discussed in subsection 3.2.1; periodic and non-periodic systems will be discussed in subsections 3.2.2 and 3.2.3. The unbalanced system will be discussed in subsection 3.2.4.

3.2.1 Three-Phase Fundamental Systems

In particular, a three-phase fundamental system will be discussed in this subsection since most of the power systems are three-phase. The voltage $\boldsymbol{v}(t)$ and current $\boldsymbol{i}(t)$ are, respectively

$$\boldsymbol{v}(t) = \begin{bmatrix} v_1(t) & v_2(t) & v_3(t) \end{bmatrix}^T, \tag{3.31}$$

and

$$\boldsymbol{i}(t) = \begin{bmatrix} i_1(t) & i_2(t) & i_3(t) \end{bmatrix}^T. \tag{3.32}$$

The instantaneous active current and the instantaneous nonactive current are, respectively,

$$\boldsymbol{i_a}(t) = \begin{bmatrix} i_{a1}(t) \\ i_{a2}(t) \\ i_{a3}(t) \end{bmatrix} = \frac{P(t)}{V_p^2(t)} \begin{bmatrix} v_{p1}(t) \\ v_{p2}(t) \\ v_{p3}(t) \end{bmatrix}, \tag{3.33}$$

and

$$\boldsymbol{i_n}(t) = \begin{bmatrix} i_{n1}(t) \\ i_{n2}(t) \\ i_{n3}(t) \end{bmatrix} = \begin{bmatrix} i_1(t) \\ i_2(t) \\ i_3(t) \end{bmatrix} - \begin{bmatrix} i_{a1}(t) \\ i_{a2}(t) \\ i_{a3}(t) \end{bmatrix}. \tag{3.34}$$

where

$$P(t) = \frac{1}{T_c} \int_{t-T_c}^{t} \left[v_1(\tau) i_1(\tau) + v_2(\tau) i_2(\tau) + v_3(\tau) i_3(\tau) \right] d\tau \,, \tag{3.35}$$

and

$$V_p(t) = \sqrt{\frac{1}{T_c} \int_{t-T_c}^{t} \left[v_{p1}^2(\tau) + v_{p2}^2(\tau) + v_{p3}^2(\tau) \right] d\tau} \,. \tag{3.36}$$

For a three-phase four-wire system, the neutral current i_0(t) is the sum of the other three phases, i.e.,

$$i_0(t) \triangleq i_1(t) + i_2(t) + i_3(t) \,. \tag{3.37}$$

The instantaneous active power $p_a(t)$ and the instantaneous nonactive power $p_n(t)$ are, respectively,

$$p_a(t) = \begin{bmatrix} v_1(t) & v_2(t) & v_3(t) \end{bmatrix} \begin{bmatrix} i_{a1}(t) \\ i_{a2}(t) \\ i_{a3}(t) \end{bmatrix} = v_1(t) i_{a1}(t) + v_2(t) i_{a2}(t) + v_3(t) i_{a3}(t) \,, \tag{3.38}$$

and

$$p_n(t) = \begin{bmatrix} v_1(t) & v_2(t) & v_3(t) \end{bmatrix} \begin{bmatrix} i_{n1}(t) \\ i_{n2}(t) \\ i_{n3}(t) \end{bmatrix} = v_1(t) i_{n1}(t) + v_2(t) i_{n2}(t) + v_3(t) i_{n3}(t) \,. \tag{3.39}$$

In a three-phase balanced sinusoidal system, both the voltage and the current are sinusoidal and have the same frequency. The voltage and current vectors are represented as

$$\boldsymbol{v}(t) \triangleq \left[\sqrt{2} V \cos(\omega t + \alpha) \quad \sqrt{2} V \cos(\omega t - 2\pi/3 + \alpha) \quad \sqrt{2} V \cos(\omega t + 2\pi/3 + \alpha) \right]^T, \tag{3.40}$$

and

$$\boldsymbol{i}(t) \triangleq \left[\sqrt{2} I \cos(\omega t + \beta) \quad \sqrt{2} I \cos(\omega t - 2\pi/3 + \beta) \quad \sqrt{2} I \cos(\omega t + 2\pi/3 + \beta) \right]^T. \tag{3.41}$$

The phase angle between the voltage and the current is given by α-β. Let the averaging interval T_c be half of the system period, i.e.,

$$T_c = \frac{T}{2} = \frac{\pi}{\omega}. \tag{3.42}$$

The instantaneous power $p(t)$ and average power $P(t)$ are

$$p(t) = \boldsymbol{v}^T(t)\boldsymbol{i}(t) = 3VI\cos(\alpha - \beta), \tag{3.43}$$

and

$$P(t) = \frac{1}{T_c}\int_{t-T_c}^{t} \boldsymbol{v}^T(\tau)\boldsymbol{i}(\tau)d\tau = 3VI\cos(\alpha - \beta). \tag{3.44}$$

$P(t)$ and $p(t)$ are equal in this three-phase system. Furthermore, $P(t)$ is equal to $p(t)$ in any multi-phase balanced sinusoidal system.

Let the reference voltage be the system voltage $\boldsymbol{v}(t)$, that is,

$$\boldsymbol{v}_p(t) = \boldsymbol{v}(t). \tag{3.45}$$

The instantaneous active current $\boldsymbol{i}_a(t)$ and the instantaneous nonactive current $\boldsymbol{i}_n(t)$ are, respectively, given by

$$\boldsymbol{i}_a(t) = \frac{P(t)}{V_p^2(t)}\boldsymbol{v}_p(t) = \begin{bmatrix} \sqrt{2}I\cos(\alpha-\beta)\cos(\omega t+\alpha) \\ \sqrt{2}I\cos(\alpha-\beta)\cos(\omega t-2\pi/3+\alpha) \\ \sqrt{2}I\cos(\alpha-\beta)\cos(\omega t+2\pi/3+\alpha) \end{bmatrix}, \tag{3.46}$$

and

$$\boldsymbol{i}_n(t) = \boldsymbol{i}(t) - \boldsymbol{i}_a(t) = \begin{bmatrix} \sqrt{2}I\sin(\alpha-\beta)\sin(\omega t+\alpha) \\ \sqrt{2}I\sin(\alpha-\beta)\sin(\omega t-2\pi/3+\alpha) \\ \sqrt{2}I\sin(\alpha-\beta)\sin(\omega t+2\pi/3+\alpha) \end{bmatrix}. \tag{3.47}$$

The active current vector $\boldsymbol{i_a}(t)$ is in phase with the system voltage vector $\boldsymbol{v}(t)$ and is the active component of $\boldsymbol{i}(t)$, and $\boldsymbol{i_n}(t)$ is the nonactive component. The two currents $\boldsymbol{i_a}(t)$ and $\boldsymbol{i_n}(t)$ are orthogonal, that is,

$$\frac{1}{T_c}\int_{t-T_c}^{t} \boldsymbol{i_a}^T(\tau)\boldsymbol{i_n}(\tau)d\tau = 0\,. \tag{3.48}$$

The instantaneous active power $p_a(t)$ and instantaneous nonactive power $p_n(t)$ are, respectively,

$$p_a(t) = \boldsymbol{v}^T(t)\boldsymbol{i_a}(t) = 3VI\cos(\alpha-\beta) = p(t)\,, \tag{3.49}$$

and

$$p_n(t) = \boldsymbol{v}^T(t)\boldsymbol{i_n}(t) = 0\,. \tag{3.50}$$

The average active power $P_a(t)$ and the average nonactive power $P_n(t)$ are, respectively,

$$P_a(t) = \frac{1}{T_c}\int_{t-T_c}^{t} \boldsymbol{v}^T(\tau)\boldsymbol{i_a}(\tau)d\tau = 3VI\cos(\alpha-\beta) = P(t)\,, \tag{3.51}$$

and

$$P_n(t) = \frac{1}{T_c}\int_{t-T_c}^{t} \boldsymbol{v}^T(\tau)\boldsymbol{i_n}(\tau)d\tau = 0\,. \tag{3.52}$$

The apparent power $S(t)$, apparent active power $P_p(t)$, and the apparent nonactive power $Q(t)$ are, respectively

$$S(t) = 3VI\,, \tag{3.53}$$

$$P_p(t) = 3VI\cos(\alpha-\beta)\,, \tag{3.54}$$

and

$$Q(t) = 3VI\sin(\alpha - \beta). \tag{3.55}$$

The sum of the instantaneous active power of the three phases is equal to the sum of the instantaneous power (3.49), and the sum of the nonactive power is zero (3.50). This indicates that there is no nonactive power at any time for all three phases, but there is nonactive power/current flowing in each phase, as shown in (3.47). The amplitude of the current in each phase of $\boldsymbol{i}(t)$ is $\sqrt{2}I$, in which only the active component (the amplitude of the current in each phase of $\boldsymbol{i_a}(t)$, which is given by $\sqrt{2}I\cos(\alpha - \beta)$) is the effective part to carry active power, and the rest of it (the amplitude of the current in each phase of $\boldsymbol{i_n}(t)$, which is $\sqrt{2}I\sin(\alpha - \beta)$) is the current flowing back and forth between the source and the load which carries nonactive power.

The average powers $P(t)$, $P_a(t)$, and $P_n(t)$ indicate the energy utilization in the system. $P(t)$ is always equal to $P_a(t)$, and $P_n(t)$ is equal to zero. The apparent powers $S(t)$, $P_p(t)$, and $Q(t)$ indicate the power flow in the system, which includes the nonactive power flowing back and forth between the source and the load or among the phases.

3.2.2 Periodic Systems

The three-phase, sinusoidal case discussed in the previous subsection is generalized to a periodic system with m phases. For a periodic system with periodic T, if $T_c = kT/2$, $k = 1, 2,\ldots$, and $v_p(t) = v(t)$, $P(t)$ and $V_p(t)$ are constant values, i.e., $P(t) = P$, and $V_p(t) = V(t) = V$. Specifically,

$$P_a(t) = \frac{1}{T_c}\int_{t-T_c}^{t} v(\tau)\frac{P}{V^2}v_p(\tau)d\tau = \frac{P}{V^2}\frac{1}{T_c}\int_{t-T_c}^{t} v^2(\tau)d\tau = P, \tag{3.56}$$

$$P_n(t) = \frac{1}{T_c}\int_{t-T_c}^{t} v(\tau)\left[i(\tau) - \frac{P}{V^2} v_p(\tau) \right] d\tau = P(t) - \frac{P}{V^2}\frac{1}{T_c}\int_{t-T_c}^{t} v^2(\tau) d\tau = 0 . \quad (3.57)$$

That is, $P_a(t) = P$ and $P_n(t) = 0$. Over the time interval $[t\text{-}T_c, t]$, $P_a(t)$, the average value of $p_a(t)$, is equal to $P(t)$ (the average value of $p(t)$); and $P_n(t)$, the average value of $p_n(t)$, is zero. It indicates that instantaneously $p(t)$ has both active and nonactive components, but on average, $P(t)$ has only the active power, which is equal to $P_a(t)$. The average value of $p_n(t)$ is zero, which indicates that the nonactive power $p_n(t)$ flows back and forth, and over the time interval T_c, there is no net energy utilization. This is consistent with the conventional definition of active power and nonactive power.

For a periodic system, the apparent power $S(t)$, apparent active power $P_p(t)$, apparent nonactive power $Q(t)$ satisfy

$$S^2(t) = P_p^2(t) + Q^2(t) . \quad (3.58)$$

A periodic function $f(t)$ of fundamental period T satisfies

$$f(t) = f(t + kT) . \quad (3.59)$$

$f(t)$ can be expressed as a Fourier series given by

$$f(t) = A_0 + \sum_{k=1}^{\infty} A_k \cos(k\omega_1 t + \theta_k), \text{ where } \omega_1 = \frac{2\pi}{T} . \quad (3.60)$$

As to periodic waveforms in a power system, if the frequencies are all integral multiples of the system fundamental frequency, it is said to have only harmonics (Subsection 3.2.2.1.); if the waveform is pure sine wave with the fundamental frequency, it is a sinusoidal case (Subsection 3.2.2.2.); and if the frequency content of the waveforms contains frequencies which are not integral multiples of the system fundamental frequency (50/60 Hz), then it is said to contain sub-harmonics (Subsection 3.2.2.3.).

3.2.2.1 Sinusoidal Systems

A sinusoidal system with voltage vector $\boldsymbol{v}(t)$ and current vector $\boldsymbol{i}(t)$ and period T,

$$\boldsymbol{v}(t) = [v_1(t), v_2(t), ..., v_m(t)]^T, \tag{3.61}$$

where $v_k(t) = \sqrt{2}V\cos(\omega t - 2k\pi/m + \alpha), \qquad k = 0,1,...,m-1,$

and $\omega = 2\pi/T$.

$$\boldsymbol{i}(t) = [i_1(t), i_2(t), ..., i_m(t)]^T, \tag{3.62}$$

where $i_k(t) = \sqrt{2}I\cos(\omega t - 2k\pi/m + \beta), \qquad k = 0,1,...,m-1.$

For both the voltage and current, the magnitude of each phase is equal, and the phase angle between each two contiguous phases is also equal, i.e., the system is balanced.

The average power $P(t)$ is

$$P(t) = \frac{1}{T_c}\int_{t-T_c}^{t} p(\tau)d\tau = mVI\cos(\alpha - \beta) = P. \tag{3.63}$$

Let $\boldsymbol{v_p}(t) = \boldsymbol{v}(t)$, the rms value of $\boldsymbol{v_p}(t)$ is

$$V_p(t) = \sqrt{m}V = V_p. \tag{3.64}$$

Therefore, the instantaneous active current $\boldsymbol{i_a}(t)$ and the nonactive current $\boldsymbol{i_n}(t)$ are, respectively

$$\boldsymbol{i_a}(t) = \frac{P}{V_p^2}\boldsymbol{v}(t) = \sqrt{2}I\cos(\alpha - \beta)[\cos(\omega t), \cos(\omega t - \frac{2\pi}{m}), ..., \cos(\omega t - \frac{2(m-1)\pi}{m})]^T, \tag{3.65}$$

$$\boldsymbol{i_n}(t) = \sqrt{2}I\sin(\alpha - \beta)[\sin(\omega t), \sin(\omega t - \frac{2\pi}{m}), ..., \sin(\omega t - \frac{2(m-1)\pi}{m})]^T. \tag{3.66}$$

The instantaneous active power $p_a(t)$ and the instantaneous nonactive power $p_n(t)$ are, respectively

$$p_a(t) = mVI\cos(\alpha - \beta)\,, \tag{3.67}$$

and

$$p_n(t) = 0\,. \tag{3.68}$$

The rms values of $\boldsymbol{i}(t)$, $\boldsymbol{i_a}(t)$, and $\boldsymbol{i_n}(t)$ are, respectively

$$I(t) = \sqrt{m}I\,, \tag{3.69}$$

$$I_a(t) = \sqrt{m}I\cos(\alpha - \beta)\,, \tag{3.70}$$

and

$$I_n(t) = \sqrt{m}I\sin(\alpha - \beta)\,. \tag{3.71}$$

The apparent power $S(t)$, the apparent active power $P_p(t)$, and the apparent nonactive power $Q(t)$ are, respectively

$$S(t) = V(t)I(t) = mVI\,, \tag{3.72}$$

$$P_p(t) = V(t)I_a(t) = mVI\cos(\alpha - \beta)\,, \tag{3.73}$$

and

$$Q(t) = V(t)I_n(t) = mVI\sin(\alpha - \beta)\,. \tag{3.74}$$

The average active power $P_a(t)$, and the average nonactive power $P_n(t)$ are, respectively

$$P_a(t) = mVI\cos(\alpha - \beta) = P(t) = P_p(t)\,, \tag{3.75}$$

and

$$P_n(t) = 0\,. \tag{3.76}$$

The instantaneous active current is in phase with the voltage, and magnitude is reduced to $\sqrt{2}I\cos(\alpha - \beta)$. The instantaneous nonactive current is 90° out of phase with

the voltage, and the magnitude is $\sqrt{2}I\sin(\alpha-\beta)$. Both the instantaneous active current and the nonactive current are independent of the number of phases *m*.

Other definitions are listed in Table 3.2. There are some interesting characteristics for a balanced sinusoidal system.

1. The instantaneous active current is in phase with the voltage, and the instantaneous nonactive current is 90° out of phase with the voltage.

2. The instantaneous power, active power, and nonactive power are all constant, and the instantaneous active power is equal to the instantaneous power; the instantaneous nonactive power is zero.

3. All the rms values and the average powers are constant. The average powers are equal to their correspondent instantaneous powers.

4. The apparent active power is equal to the average active power, but the apparent nonactive power is not equal to the average nonactive power. The average powers indicate the power utilization in a system; therefore, the average active power is equal to the average power, while the nonactive power is zero. The apparent powers indicate the power carried by the currents, therefore, if there is nonactive current flowing in the system, there is apparent nonactive power, which is proportional to the rms value of the instantaneous nonactive current. The apparent powers satisfy

$$S^2 = P_p^2 + Q^2 . \tag{3.77}$$

5. The definitions are independent of the choice of T_c, as long as T_c is zero or $T_c = kT/2$, $k = 1, 2, \ldots$ Usually smaller T_c is preferred, which will be illustrated in the next

Table 3.2. Definitions of the generalized nonactive power theory in sinusoidal systems.

Instantaneous Definitions	**rms Definitions**	**Average Powers**	**Apparent Powers**
$\boldsymbol{v}(t)$	$V(t)=\sqrt{m}V$		
$\boldsymbol{i}(t)$	$I(t)=\sqrt{m}I$		
$\boldsymbol{i_a}(t)$	$I_a(t)=\sqrt{m}I\cos(\alpha-\beta)$		
$\boldsymbol{i_n}(t)$	$I_n(t)=\sqrt{m}I\sin(\alpha-\beta)$		
$p(t)=mVI\cos(\alpha-\beta)$		$P(t)=mVI\cos(\alpha-\beta)$	
$p_a(t)=mVI\cos(\alpha-\beta)$		$P_a(t)=mVI\cos(\alpha-\beta)$	
$p_n(t)=0$		$P_n(t)=0$	
			$S(t)=mVI$
			$P_p(t)=mVI\cos(\alpha-\beta)$
			$Q(t)=mVI\sin(\alpha-\beta)$

chapter when the theory is implemented in a shunt nonactive power system. In this case, T_c is chosen as $T/2$.

3.2.2.2 Periodic Systems with Harmonics

It is assumed that both the voltage and current are balanced, i.e., the magnitude of each frequency component is equal, and the phase angle between two contiguous phases is also equal. Therefore, the voltage $\boldsymbol{v}(t)$ and current $\boldsymbol{i}(t)$ can be expressed as

$$\boldsymbol{v}(t) = [v_1(t), v_2(t), ...v_m(t)]^T, \tag{3.78}$$

where $v_k(t) = \sqrt{2}V_1 \cos(\omega_1 t - \frac{2k\pi}{m} + \alpha_1) + \sum_{h=2}^{\infty} \sqrt{2}V_h \cos(h\omega_1 t - \frac{2k\pi}{hm} + \alpha_h)$,

$k = 0, \ldots, m\text{-}1$.

$$\boldsymbol{i}(t) = [i_1(t), i_2(t), ...i_m(t)]^T, \tag{3.79}$$

where $i_k(t) = \sqrt{2}I_1 \cos(\omega_1 t - \frac{2k\pi}{m} + \beta_1) + \sum_{h=2}^{\infty} \sqrt{2}I_h \cos(h\omega_1 t - \frac{2k\pi}{hm} + \beta_h)$,

$k = 0, \ldots, m\text{-}1$.

The averaging interval T_c is chosen to be half of the fundamental period, i.e.,

$$T_c = \frac{T}{2} = \frac{\pi}{\omega_1}. \tag{3.80}$$

The average power $P(t)$ is

$$P(t) = \frac{1}{T_c} \int_{t-T_c}^{t} \boldsymbol{v}^T(\tau)\boldsymbol{i}(\tau)d\tau = mV_1I_1 \cos(\alpha_1 - \beta_1) + m\sum_{h=2}^{\infty} V_hI_h \cos(\alpha_h - \beta_h). \tag{3.81}$$

The first term in (3.81) is the power contributed by the fundamental component, and the rest is the contribution from the higher-order harmonics. A harmonic component contributes to average real power only when both the voltage and the current have the

same frequency component. This is because sinusoids of different frequencies are orthogonal to each other.

The rms value of $v(t)$ and $i(t)$ are, respectively,

$$V(t) = \sqrt{m(V_1^2 + \sum_{h=2}^{\infty} V_h^2)} \ , \tag{3.82}$$

and

$$I(t) = \sqrt{m(I_1^2 + \sum_{h=2}^{\infty} I_h^2)} \ . \tag{3.83}$$

In this case, $P(t)$, $V(t)$, and $I(t)$ are all constant if T_c is a multiple of half of the fundamental period.

When the voltage is not sinusoidal, it is very important to choose the reference voltage. For a voltage with harmonics, the reference can be chosen as the voltage itself or the fundamental component of the voltage.

First, let $\boldsymbol{v}(t)$ itself be the reference voltage, i.e.,

$$\boldsymbol{v}_{\boldsymbol{p}}(t) = \boldsymbol{v}(t) \ . \tag{3.84}$$

Then the instantaneous active current and the nonactive current are, respectively

$$\boldsymbol{i}_{\boldsymbol{a}}(t) = \frac{P(t)}{V_p^2(t)} \boldsymbol{v}_{\boldsymbol{p}}(t) = \frac{V_1 I_1 \cos(\alpha_1 - \beta_1) + \sum_{h=2}^{\infty} V_h I_h \cos(\alpha_h - \beta_h)}{V_1^2 + \sum_{h=2}^{\infty} V_h^2} \boldsymbol{v}(t) \ , \tag{3.85}$$

and

$$\boldsymbol{i}_{\boldsymbol{n}}(t) = \boldsymbol{i}(t) - \boldsymbol{i}_{\boldsymbol{a}}(t) \ . \tag{3.86}$$

Both $P(t)$ and $V_p(t)$ are constant, therefore the instantaneous active current $\boldsymbol{i_a}(t)$ has the same shape as the voltage $\boldsymbol{v}(t)$ and is in phase with it. The rms values of the components of $\boldsymbol{i_a}(t)$ are

$$I_{ak} = \frac{V_1 I_1 \cos(\alpha_1 - \beta_1) + \sum_{h=2}^{\infty} V_h I_h \cos(\alpha_h - \beta_h)}{V_1^2 + \sum_{h=2}^{\infty} V_h^2} V_k, \text{ where } k = 1, 2, \ldots, \infty. \tag{3.87}$$

Let $\boldsymbol{i_a}(t)$ be

$$\boldsymbol{i_a}(t) = [i_{a1}(t), i_{a2}(t), \ldots, i_{am}(t)]^T, \tag{3.88}$$

where $i_{ak}(t) = \sqrt{2} I_{a1} \cos(\omega_1 t - \frac{2k\pi}{m} + \alpha_1) + \sum_{h=2}^{\infty} \sqrt{2} I_{ah} \cos(h\omega_1 t - \frac{2k\pi}{hm} + \alpha_h)$, $k = 0, \ldots, m\text{-}1$.

The rms values of $\boldsymbol{i_a}(t)$ and $\boldsymbol{i_n}(t)$ are, respectively,

$$I_a(t) = \sqrt{m(I_{a1}^2 + \sum_{h=2}^{\infty} I_{ah}^2)} = \frac{V_1 I_1 \cos(\alpha_1 - \beta_1) + \sum_{h=2}^{\infty} V_h I_h \cos(\alpha_h - \beta_h)}{V_1^2 + \sum_{h=2}^{\infty} V_h^2} V(t), \tag{3.89}$$

and

$$I_n(t) = \sqrt{m(I_{n1}^2 + \sum_{h=2}^{\infty} I_{nh}^2)}. \tag{3.90}$$

The apparent power $S(t)$ is

$$S(t) = V(t) I(t) = m \sqrt{(V_1^2 + \sum_{h=2}^{\infty} V_h^2)(I_1^2 + \sum_{h=2}^{\infty} I_h^2)}. \tag{3.91}$$

The apparent active power $P_p(t)$ is

$$P_p(t) = V(t) I_a(t) = m \sqrt{(V_1^2 + \sum_{h=2}^{\infty} V_h^2)(I_{a1}^2 + \sum_{h=2}^{\infty} I_{ah}^2)}. \tag{3.92}$$

The apparent nonactive power $Q(t)$ is

$$Q(t) = V(t) I_n(t) = m\sqrt{(V_1^2 + \sum_{h=2}^{\infty} V_h^2)(I_{n1}^2 + \sum_{h=2}^{\infty} I_{nh}^2)} \,. \tag{3.93}$$

The average active power $P_a(t)$ and the nonactive power $P_n(t)$ are, respectively

$$P_a(t) = \frac{1}{T_c} \int_{t-T_c}^{t} p_a(\tau) d\tau = \frac{1}{T_c} \int_{t-T_c}^{t} \boldsymbol{v}^T(\tau) \boldsymbol{i_a}(\tau) d\tau = \frac{1}{T_c} \frac{P(t)}{V^2(t)} \int_{t-T_c}^{t} \boldsymbol{v}^T(\tau) \boldsymbol{v}(\tau) d\tau = P(t) \,, \tag{3.94}$$

and

$$P_n(t) = \frac{1}{T_c} \int_{t-T_c}^{t} p_n(\tau) d\tau = 0 \,. \tag{3.95}$$

If a sinusoidal waveform is preferred for $\boldsymbol{i_a}(t)$, the reference voltage can be chosen as the fundamental component of $\boldsymbol{v}(t)$, i.e.,

$$\boldsymbol{v_p}(t) = [v_{p1}(t), v_{p2}(t), ..., v_{pm}(t)]^T \,, \tag{3.96}$$

where $v_{pk}(t) = \sqrt{2} V_1 \cos(\omega_1 t - \frac{2k\pi}{m} + \alpha_1)$, $k = 0, \ldots, m\text{-}1$.

The instantaneous active current $\boldsymbol{i_a}(t)$ is

$$\begin{aligned} \boldsymbol{i_a}(t) &= \frac{P(t)}{V_p^2(t)} \boldsymbol{v_p}(t) \\ &= \left[\sqrt{2} I_1 \cos(\alpha_1 - \beta_1) + \sum_{h=2}^{\infty} \sqrt{2} \frac{V_h}{V_1} I_h \cos(\alpha_h - \beta_h) \right] [\cos(\omega_1 t + \alpha_1), ..., \cos(\omega_1 t - \frac{2(m-1)\pi}{m} + \alpha_1)]^T \end{aligned} \tag{3.97}$$

$\boldsymbol{i_a}(t)$ carries the active power from both the active current of the fundamental component and the active currents of the harmonics.

In (3.97), the first component of $\boldsymbol{i_a}(t)$ represents the active power of the fundamental component, and the remaining components represent the active power in each of the harmonic components. Now the active current $\boldsymbol{i_a}(t)$ is a pure sinusoid and in phase with the reference voltage. The active current $\boldsymbol{i_a}(t)$ carries all the active power in current $\boldsymbol{i}(t)$, and all the nonactive power is carried by the nonactive current $\boldsymbol{i_n}(t) = \boldsymbol{i}(t) - \boldsymbol{i_a}(t)$, specifically,

$$\boldsymbol{i_n}(t) = [i_{n1}(t), i_{n2}(t), ..., i_{nm}(t)]^T, \tag{3.98}$$

where

$$\begin{aligned} i_{nk}(t) = {} & \sqrt{2} I_1 \sin(\alpha_1 - \beta_1) \sin(\omega_1 t - \frac{2k\pi}{m} + \alpha_1) \\ & - \sum_{h=2}^{\infty} \frac{V_h}{V_1} I_h \cos(\alpha_h - \beta_h) \cos(\omega_1 t - \frac{2k\pi}{m} + \alpha_1) \\ & + \sum_{h=2}^{\infty} \sqrt{2} I_h \cos(h\omega_1 t - \frac{2k\pi}{hm} + \beta_h) \end{aligned}$$

$k = 0, 1, \ldots, m\text{-}1.$ (3.99)

The first term in $i_{nk}(t)$ is the fundamental nonactive component in the load current; the second and the third terms are the nonactive components in the harmonics.

The rms value of $\boldsymbol{i_a}(t)$ is

$$I_a(t) = \sqrt{m} (I_1 \cos(\alpha_1 - \beta_1) + \sum_{h=2}^{\infty} \frac{V_h}{V_1} I_h \cos(\alpha_h - \beta_h)). \tag{3.100}$$

The average active power $P_a(t)$ is

$$P_a(t) = \frac{1}{T_c} \int_{t-T_c}^{t} v(\tau) i_a(\tau) d\tau = V_1 I_1 \cos(\alpha_1 - \beta_1) + \sum_{h=2}^{\infty} V_h I_h \cos(\alpha_h - \beta_h) = P(t). \tag{3.101}$$

The average nonactive power over T_c is zero as

$$P_n(t) = \frac{1}{T_c}\int_{t-T_c}^{t} v(\tau) i_n(\tau) d\tau = \frac{1}{T_c}\int_{t-T_c}^{t} v(\tau)(i(\tau) - i_a(\tau)) d\tau = 0 . \quad (3.102)$$

3.2.2.3 Periodic Systems with Sub-Harmonics

Sub-harmonics are the components in a waveform whose frequencies are not an integral multiple of the fundamental frequency. For simplicity of exposition, let there be only one sub-harmonic in a single-phase system with the voltage $v(t)$ and the current $i(t)$.

$$v(t) = \sqrt{2}V_1 \cos(\omega_1 t + \alpha_1) + \sqrt{2}V_s \cos(\omega_{s1} t + \alpha_s) , \quad (3.103)$$

and

$$i(t) = \sqrt{2}I_1 \cos(\omega_1 t + \beta_1) + \sqrt{2}I_s \cos(\omega_{s2} t + \beta_s) , \quad (3.104)$$

where

$\omega_1 = 2\pi f_1$, $\omega_{s1} = 2\pi f_{s1}$, and $\omega_{s2} = 2\pi f_{s2}$.

The instantaneous power $p(t)$ is

$$\begin{aligned} p(t) = v(t)i(t) = {} & V_1 I_1 \cos(\alpha_1 - \beta_1) + V_1 I_1 \cos(2\omega_1 t + \alpha_1 + \beta_1) \\ & + V_1 I_s \cos[(\omega_1 - \omega_{s2})t + \alpha_1 - \beta_s] + V_1 I_s \cos[(\omega_1 + \omega_{s2})t + \alpha_1 + \beta_s] \\ & + V_s I_1 \cos[(\omega_1 - \omega_{s1})t - \alpha_s + \beta_1] + V_s I_1 \cos[(\omega_1 + \omega_{s1})t + \alpha_s + \beta_1] \\ & + V_s I_s \cos[(\omega_{s1} - \omega_{s2})t + \alpha_s - \beta_s] + V_s I_s \cos[(\omega_{s1} + \omega_{s2})t + \alpha_s + \beta_s] \end{aligned} \quad (3.105)$$

The instantaneous power $p(t)$ contains seven frequencies due to the modulation (multiplication) between the fundamental and the sub-harmonics, which are $2f_1$, $f_1 + f_{s1}$, $f_1 - f_{s1}$, $f_1 + f_{s2}$, $f_1 - f_{s2}$, $f_{s1} + f_{s2}$, and $f_{s1} - f_{s2}$.

Let v_p(t) be chosen as the fundamental component of $v(t)$, i.e.,

$$v_p(t) = \sqrt{2}V_1 \cos(\omega_1 t + \alpha_1) . \quad (3.106)$$

The rms value $V_p(t)$ is then

$$V_p(t) = \sqrt{\frac{1}{T_c}\int_{t-T_c}^{t} v_p^2(\tau)d\tau} = V_1, \tag{3.107}$$

and the active current $i_a(t)$ is

$$i_a(t) = \frac{P(t)}{V_1^2}\sqrt{2}V_1\cos(\omega_1 t + \alpha_1). \tag{3.108}$$

If T_c is chosen as an integral multiple of the periods of all the frequencies in $p(t)$, the average value $P(t)$ is a constant. Therefore, $i_a(t)$ is purely sinusoidal and in phase with the fundamental component of $v(t)$. T_c is the common multiple of the periods of all these frequencies.

Now let v_p(t) be chosen as $v(t)$ itself, i.e.,

$$v_p(t) = \sqrt{2}V_1\cos(\omega_1 t + \alpha_1) + \sqrt{2}V_s\cos(\omega_{s1} t + \alpha_s). \tag{3.109}$$

There are three new frequencies $2f_{s1}$, f_1+f_{s1}, and $|f_1-f_{s1}|$ in $v_p^2(t)$. If T_c is chosen as an integral multiple of the periods of all the harmonics in $p(t)$ and $v_p^2(t)$, both the average value $P(t)$ and rms value of the reference voltage V_p(t) are constants. Therefore, the waveform of $i_a(t)$ has the same shape as the waveform of $v(t)$.

In the periodic system with harmonics case described in subsection 3.2.2.2, where all frequencies were integral multiples of the fundamental frequency, choosing T_c as an integral multiple of a half cycle of the fundamental frequency will guarantee that T_c is the common multiple of the periods of all the frequencies in $p(t)$ and $v_p^2(t)$, i.e., $i_a(t)$ is proportional to v_p(t).

In the sub-harmonics case discussed in this subsection, if T_c is the common multiple of the periods of all the harmonics in $p(t)$ and $v_p^2(t)$ (with sub-harmonics present, T_c is larger than the fundamental period), then the waveform of $i_a(t)$ has the same shape as the waveform of $v_p(t)$. If T_c is not chosen this way, there are still sub-harmonic components in $i_a(t)$, i.e., the nonactive component is not completely eliminated.

3.2.3 Non-Periodic Systems

For a non-periodic system, choosing $T_c = t$, the average power $P(t)$, rms value of the reference voltage $\boldsymbol{v_p}(t)$, and the active current $\boldsymbol{i_a}(t)$ are defined by

$$P(t) = \frac{1}{T_c}\int_{t-T_c}^{t} \boldsymbol{v}^T(\tau)\boldsymbol{i}(\tau)d\tau = \frac{1}{t}\int_{0}^{t} \boldsymbol{v}^T(\tau)\boldsymbol{i}(\tau)d\tau\,, \tag{3.110}$$

$$V_p(t) = \sqrt{\frac{1}{T_c}\int_{t-T_c}^{t} \boldsymbol{v_p}^T(\tau)\boldsymbol{v_p}(\tau)d\tau} = \sqrt{\frac{1}{t}\int_{0}^{t} \boldsymbol{v_p}^T(\tau)\boldsymbol{v_p}(\tau)d\tau}\,, \tag{3.111}$$

and

$$\boldsymbol{i_a}(t) = \frac{P(t)}{V_p^2(t)}\boldsymbol{v_p}(t)\,. \tag{3.112}$$

In a power system, the voltage and the current are finite power waveforms, i.e.,

$$P(t) = \lim_{t\to\infty}\frac{1}{t}\int_{0}^{t} \boldsymbol{v}^T(\tau)\boldsymbol{i}(\tau)d\tau = P\,, \tag{3.113}$$

$$V_p(t) = \lim_{t\to\infty}\sqrt{\frac{1}{t}\int_{0}^{t} \boldsymbol{v_p}^T(\tau)\boldsymbol{v_p}(\tau)d\tau} = V_p\,, \tag{3.114}$$

and

$$\boldsymbol{i_a}(t) = \frac{P(t)}{V_p^2(t)}\boldsymbol{v_p}(t) \to \frac{P}{V_p^2}\boldsymbol{v_p}(t), \text{ as } t\to\infty\,. \tag{3.115}$$

The generalized nonactive power theory is valid for voltage and current of any waveform, and the nonactive current can only be completely eliminated when $T_c = t$ and $t \rightarrow \infty$ ($\boldsymbol{i}_a(t)$ has the shape as and is in phase with $\boldsymbol{v}_p(t)$ so that unity power factor is achieved). However, this is not practical in a power system, and T_c is chosen to have a finite value. The voltage in an ac power system usually is a sine wave with fundamental frequency *f,* and for a non-periodic voltage, it is usually a sum of the fundamental component and the non-periodic component. T_c is usually chosen as a few multiples of the fundamental period, and this finite T_c will mitigate the distortion. This will be discussed further in Chapter 4.

3.2.4 Unbalance

Let the voltage and current in an unbalanced sinusoidal system be, respectively,

$$\boldsymbol{v}(t) = \left[\sqrt{2}V_1 \cos(\omega t + \alpha_1) \quad \sqrt{2}V_2 \cos(\omega t + \alpha_2) \quad \sqrt{2}V_3 \cos(\omega t + \alpha_3) \right]^T, \tag{3.116}$$

and

$$\boldsymbol{i}(t) = \left[\sqrt{2}I_1 \cos(\omega t + \beta_1) \quad \sqrt{2}I_2 \cos(\omega t + \beta_2) \quad \sqrt{2}I_3 \cos(\omega t + \beta_3) \right]^T. \tag{3.117}$$

If the reference voltage is chosen as the voltage itself, then the definitions are similar to the definitions in subsection 3.2.2. In this case, the active current is still unbalanced because of the unbalanced voltage.

If a balanced active current is preferred, a balanced reference voltage is needed. Usually, the referenced voltage is chosen as the positive sequence component of the system voltage.

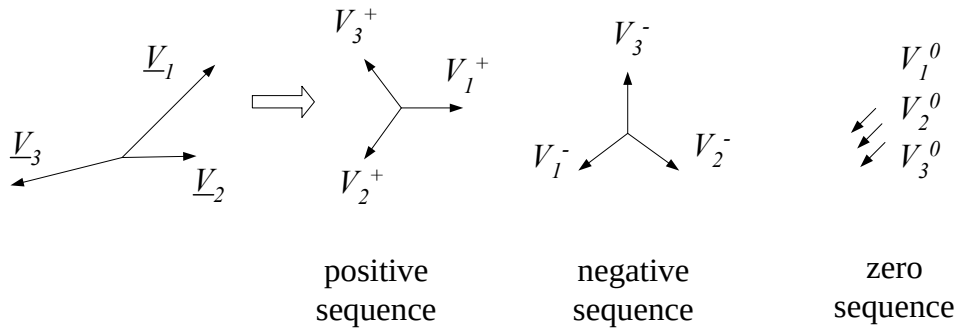

Figure 3.1. Sequence analysis of a three-phase waveform.

Using complex rotating vectors $\underline{V}_1(t)$, $\underline{V}_2(t)$, and $\underline{V}_3(t)$ to represent $v_1(t) = \mathrm{Re}\{\underline{V}_1(t)\}$, $v_2(t) = \mathrm{Re}\{\underline{V}_2(t)\}$, and $v_3(t) = \mathrm{Re}\{\underline{V}_3(t)\}$:

$$\underline{V}_1(t) = \sqrt{2}V_1 e^{j(\omega t+\alpha_1)},$$

$$\underline{V}_2(t) = \sqrt{2}V_2 e^{j(\omega t+\alpha_2)}, \tag{3.118}$$

$$\underline{V}_3(t) = \sqrt{2}V_3 e^{j(\omega t+\alpha_3)}.$$

The unbalanced voltages of the three phases are decomposed into three sequences: a positive sequence, a negative sequence, and a zero sequence (as shown in Figure 3.1). Specifically, let

$$\begin{bmatrix} \underline{V}^+(t) \\ \underline{V}^-(t) \\ \underline{V}^0(t) \end{bmatrix} \triangleq \frac{1}{3}\begin{bmatrix} 1 & a & a^2 \\ 1 & a^2 & a \\ 1 & 1 & 1 \end{bmatrix}\begin{bmatrix} \underline{V}_1(t) \\ \underline{V}_2(t) \\ \underline{V}_3(t) \end{bmatrix} = \begin{bmatrix} \sqrt{2}V^+ e^{j(\omega t+\theta^+)} \\ \sqrt{2}V^- e^{j(\omega t+\theta^-)} \\ \sqrt{2}V^0 e^{j(\omega t+\theta^0)} \end{bmatrix}, \tag{3.119}$$

where $a = e^{j\frac{2\pi}{3}}$.

$\sqrt{2}V^+$, $\sqrt{2}V^-$, and $\sqrt{2}V^0$ are the amplitudes of the positive sequence, negative sequence, and zero sequence components, respectively, and the angles θ^+, θ^-, and θ^0

are the phase angles of phase 1 of these three sequences. Therefore, the positive sequence component $\boldsymbol{v}^+(t)$ of $\boldsymbol{v}(t)$ is

$$\boldsymbol{v}^+(t) \triangleq \begin{bmatrix} v_1^+(t) \\ v_2^+(t) \\ v_3^+(t) \end{bmatrix} = \begin{bmatrix} \sqrt{2}V^+ \cos(\omega t + \theta^+) \\ \sqrt{2}V^+ \cos(\omega t + \theta^+ - 2\pi/3) \\ \sqrt{2}V^+ \cos(\omega t + \theta^+ + 2\pi/3) \end{bmatrix}. \tag{3.120}$$

The negative sequence component $\boldsymbol{v}^-(t)$ is

$$\boldsymbol{v}^-(t) \triangleq \begin{bmatrix} v_1^-(t) \\ v_2^-(t) \\ v_3^-(t) \end{bmatrix} = \begin{bmatrix} \sqrt{2}V^- \cos(\omega t + \theta^-) \\ \sqrt{2}V^- \cos(\omega t + \theta^- + 2\pi/3) \\ \sqrt{2}V^- \cos(\omega t + \theta^- - 2\pi/3) \end{bmatrix}. \tag{3.121}$$

The zero sequence component $\boldsymbol{v}^0(t)$ is

$$\boldsymbol{v}^0(t) \triangleq \begin{bmatrix} v_1^0(t) \\ v_2^0(t) \\ v_3^0(t) \end{bmatrix} = \begin{bmatrix} \sqrt{2}V^0 \cos(\omega t + \theta^0) \\ \sqrt{2}V^0 \cos(\omega t + \theta^0) \\ \sqrt{2}V^0 \cos(\omega t + \theta^0) \end{bmatrix}. \tag{3.122}$$

If the system is balanced, the voltage has only the positive sequence component, and both the negative sequence component and the zero sequence component are zero. In an unbalanced system, usually the positive sequence component $\boldsymbol{v}^+(t)$ is the dominant component, which is sinusoidal and balanced by design. Therefore, a sinusoidal and balanced active current can be achieved by choosing $\boldsymbol{v}^+(t)$ as the reference voltage.

3.3 Generalized Theory

Table 3.3 shows the different combinations of $\boldsymbol{v_p}$ and T_c for different loads, and the corresponding compensation results are shown in the last column. The choice of the

Table 3.3. Summary of the parameters $\boldsymbol{v}_p$ and T_c in the nonactive power theory.

Load Current $\boldsymbol{i}(t)$	$\boldsymbol{v}_p$	$\boldsymbol{T}_c$	**Active Current $\boldsymbol{i}_a(t)$**
Three-phase fundamental nonactive current	$\boldsymbol{v}$	0	Unity *pf* and pure fundamental sine wave
		$T/2$	
Single-phase or multi-phase fundamental nonactive current and harmonic current	$\boldsymbol{v}$	$T/2$	Unity *pf* and same shape of $\boldsymbol{v}$
	$\boldsymbol{v}_f$	$T/2$	Pure sine wave and in phase with $\boldsymbol{v}_{f+}$.
	$\boldsymbol{v}$	0	Instantaneous current
Sub-harmonic current	$\boldsymbol{v}_f$	nT	Pure fundamental sine wave or smoothed sine wave
Non-periodic current	$\boldsymbol{v}_f$	nT	Smoothed and near sine wave
Non-periodic current	$\boldsymbol{v}$	$T_c \rightarrow \infty$	In phase with $\boldsymbol{v}$ with unity *pf*
Unbalanced voltage	$\boldsymbol{v}_{f+}$	$T/2$	Balanced and sinusoidal current

Notes: Both $\boldsymbol{v}(t)$ and $\boldsymbol{i}(t)$ are distorted except in Case 1.

$\boldsymbol{v}_f$ is the fundamental component of $\boldsymbol{v}$.

$\boldsymbol{v}_{f+}$ is the positive sequence of the fundamental component of $\boldsymbol{v}$.

reference voltage influences the active current. A pure fundamental sinusoidal active current can be achieved by choosing the positive sequence component of the fundamental voltage. For a system with fundamental component and/or harmonics, the nonactive current component can be completely eliminated by choosing the averaging interval to be $T/2$.

The above discussion shows that this theory is valid in different situations, and for each situation, it is specified by the parameters $\boldsymbol{v}_p$ and T_c. This theory covers many of the other nonactive power theories presented in Chapter 2.

For *p-q* theory by Akagi et al. [11]-[12], choosing a three-phase system with $\boldsymbol{v}_p = \boldsymbol{v}$ (fundamental only and balanced using the method of *p-q* theory), and $T_c = T$, the theory proposed here will reduce to *p-q* theory. For complete compensation of the nonactive power, *p-q* theory requires the dc component of the instantaneous power, which requires at least half of the fundamental cycle to determine it. Therefore, it has the same result as this generalized theory when T_c is chosen to be $T/2$ or T.

For the Hilbert space technique based theory in the frequency domain [25], the definitions of active current $\boldsymbol{i}_a(t)$ and inactive current $\boldsymbol{i}_x(t)$ are exactly equal to the generalized theory of this dissertation if $T_c \to 0$. However, this is not recommended as the active current is neither sinusoidal nor in phase with the voltage.

3.4 Summary

In this chapter, a generalized nonactive power theory was presented. The instantaneous active current $\boldsymbol{i}_a(t)$, the instantaneous nonactive current $\boldsymbol{i}_n(t)$, the instantaneous active power $\boldsymbol{p}_a(t)$, and the instantaneous nonactive power $\boldsymbol{p}_n(t)$ were

defined in a system with a voltage $\boldsymbol{v}(t)$ and a current $\boldsymbol{i}(t)$. The average active power $P_a(t)$ and average nonactive power $P_n(t)$ are defined by averaging the instantaneous powers over time interval $[t\text{-}T_c, t]$. The apparent power $S(t)$, apparent active power $P_p(t)$, and the apparent nonactive power $Q(t)$ are also defined based on the rms values of the voltage and currents.

The generalized nonactive theory presented in this dissertation did not have any limitations such as the number of the phases; the voltage and the current were sinusoidal or non-sinusoidal, periodic or non-periodic. That is, the theory in this dissertation is valid for

1. Single-phase or multi-phase systems
2. Sinusoidal or non-sinusoidal systems
3. Periodic or non-periodic systems
4. Balanced or unbalanced systems

The reference voltage $\boldsymbol{v_p}(t)$ and the averaging interval T_c were two important factors. By changing $\boldsymbol{v_p}(t)$ and T_c, this theory had the flexibility to define nonactive current and nonactive power in different systems. Several cases were discussed in details combining the system characteristics and the choices of $\boldsymbol{v_p}(t)$ and T_c.

It was a generalized theory that other nonactive power theories discussed in Chapter 2 could be derived from this theory by changing the reference voltage and the averaging interval. The flexibility was illustrated by applying the theory to different cases such as a sinusoidal system, a periodic system with harmonics, a periodic system with sub-harmonics, and a system with non-periodic currents.

CHAPTER 4

Implementation in Shunt Compensation System

A STATCOM is a shunt nonactive power compensator, which utilizes a dc-ac inverter to compensate the nonactive current component in a load current without any energy sources. It provides power factor correction, harmonics elimination, peak current mitigation, and current regulation. The generalized nonactive power theory proposed in Chapter 3 is implemented in a STATCOM to determine the nonactive current that the STATCOM needs to compensate. A compensation system configuration for three-phase, four-wire system compensation is also proposed. Control schemes of regulating the DC link voltage and controlling the compensator current are discussed.

The compensation system is simulated, and results of several cases are analyzed. The averaging interval T_c and the reference voltage $\boldsymbol{v_p}(t)$ are discussed as well as some practical issues, such as the DC link capacitance, the DC link voltage, and the coupling inductance required for a STATCOM installation.

4.1 Configuration of Shunt Nonactive Power Compensation

In a shunt nonactive power compensation system, the compensator is connected to the utility at the point of common coupling (PCC) and in parallel with the load. It injects a certain amount of current, which is usually the nonactive component in the load current

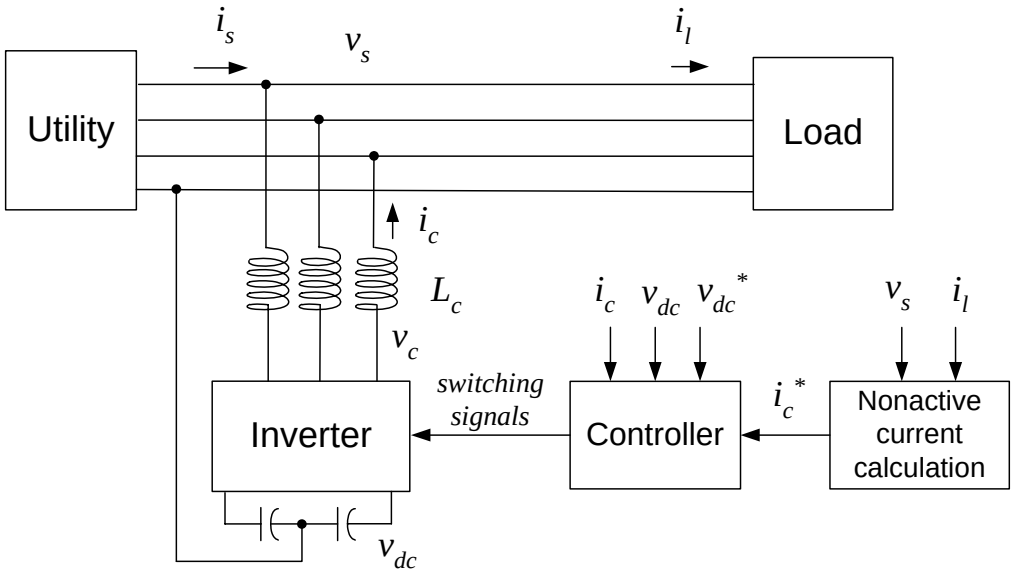

Figure 4.1. System configuration of shunt nonactive power compensation.

$\boldsymbol{i_n}(t)$, into the system so that the utility only needs to provide the active component of the load current $\boldsymbol{i_a}(t)$. In Figure 4.1, $\boldsymbol{i_l}$ is the load current, $\boldsymbol{i_s}$ is the source current, and $\boldsymbol{i_c}$ is the compensator current. Therefore, if the nonactive current is completely produced by the compensator, then $\boldsymbol{i_s} = \boldsymbol{i_a}(t)$, and $\boldsymbol{i_c} = \boldsymbol{i_n}(t)$. The theory can be implemented in a three-phase three-wire, three-phase four-wire, or a single-phase system. The system configuration shown in Figure 4.1 is a three-phase four-wire system.

The compensator consists of three parts, i.e., the nonactive power/current calculator, the controller, and the inverter. In the nonactive power/current calculator, the system voltage $\boldsymbol{v_s}$ and load current $\boldsymbol{i_l}$ are measured and used to calculate the nonactive component of $\boldsymbol{i_l}$ as explained in Chapter 3. This is the current the shunt compensator needs to inject to the power system ($\boldsymbol{i_c^*}$ in Figure 4.1). In the theory discussed in Chapter 3, the compensation system was assumed to be lossless; however in an actual power system,

losses exist in the switches, capacitors, and inductors. If the compensator does not have any energy source, the energy stored in the DC link capacitor is drawn to compensate these losses causing v_{dc} to drop. The active power required to replace the losses is drawn from the source by regulating the DC link voltage v_{dc} to the reference V_{dc}^{*} .

4.2 Control Scheme and Practical Issues

There are two components in the compensator current $\boldsymbol{i_c}$. The first is the nonactive component $\boldsymbol{i_{cn}}$ to compensate the nonactive component of the load current, and the second is the active component $\boldsymbol{i_{ca}}$ to meet the compensator's losses by regulating the DC link voltage v_{dc}, then

$$\boldsymbol{i_c} = \boldsymbol{i_{cn}} + \boldsymbol{i_{ca}} \tag{4.1}$$

4.2.1 DC Link Voltage Control

A PI controller is used to regulate the DC link voltage v_{dc}, as shown in Figure 4.2 [48]. The active current required to meet the losses is in phase with $\boldsymbol{v_s}$ (In Figure 4.2, $\boldsymbol{i_{ca}^{*}}$ has a minus sign because its direction is opposite to the convention of $\boldsymbol{i_c}$ in Figure 4.1). The amplitude of the active current is controlled by the difference between the reference voltage V_{dc}^{*} and the actual DC link voltage v_{dc}. $\boldsymbol{i_{ca}^{*}}$ is calculated by the amplitude modulation of $\boldsymbol{v_s}$ as follows

$$\boldsymbol{i_{ca}^{*}} = -\boldsymbol{v_s}\left[K_{P1}(V_{dc}^{*} - v_{dc}) + K_{I1}\int_{0}^{t}(V_{dc}^{*} - v_{dc})dt\right]. \tag{4.2}$$

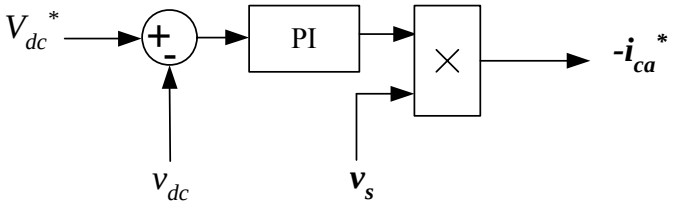

Figure 4.2. DC link voltage control diagram.

4.2.2 Nonactive Current Control

The equivalent circuit of the shunt compensation system is shown in Figure 4.3a, where $\boldsymbol{v_s}$ is the system voltage, $\boldsymbol{v_c}$ is the output voltage of the inverter, L_c is the coupling inductance, and $\boldsymbol{i_c}$ is the compensator current. The active current of the compensator $\boldsymbol{i_{ca}}$ is a small fraction of the whole compensator current $\boldsymbol{i_c}$, so the active component is neglected at present for simplicity. The relationship between the compensator's current $\boldsymbol{i_c}$ and the system voltage is

$$L_c \frac{d\boldsymbol{i_c}}{dt} = \boldsymbol{v_c} - \boldsymbol{v_s} . \tag{4.3}$$

The reference of the compensator nonactive current $\boldsymbol{i_c^*}$ and the reference of the compensator output voltage $\boldsymbol{v_c^*}$ satisfy

$$L_c \frac{d\boldsymbol{i_c^*}}{dt} = \boldsymbol{v_c^*} - \boldsymbol{v_s} \tag{4.4}$$

where $\boldsymbol{i_c^*}$ is the nonactive current calculated based on the nonactive power/current theory presented in Chapter 3. The reference compensator output voltage $\boldsymbol{v_c^*}$ is

$$\boldsymbol{v_c^*} = L_c \frac{d\boldsymbol{i_c^*}}{dt} + \boldsymbol{v_s} . \tag{4.5}$$

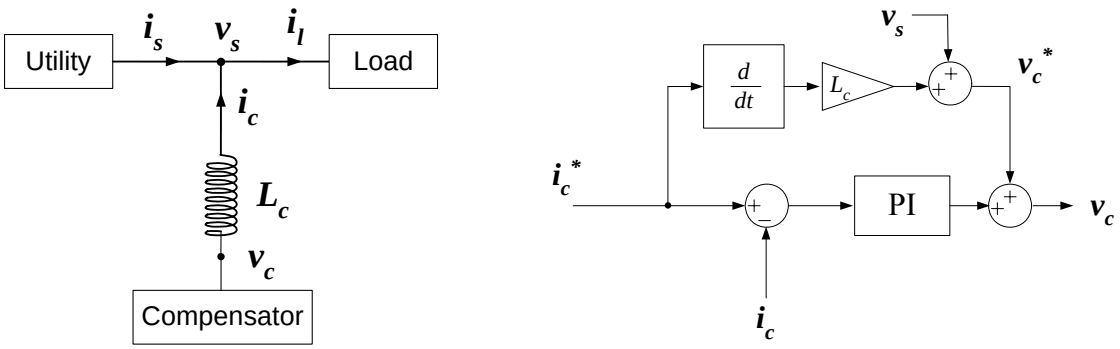

(a) Equivalent circuit (b) Feedforward controller

Figure 4.3. Nonactive current control diagram.

Subtract (4.3) from (4.4) to obtain

$$L_c \frac{d(\boldsymbol{i}_c^* - \boldsymbol{i}_c)}{dt} = \boldsymbol{v}_c^* - \boldsymbol{v}_c \,. \tag{4.6}$$

Using a PI controller and substituting (4.5) into (4.6), the output voltage of the compensator v_c is calculated by

$$\boldsymbol{v}_c = \boldsymbol{v}_s + L_c \frac{d\boldsymbol{i}_c^*}{dt} + K_{P2}(\boldsymbol{i}_c^* - \boldsymbol{i}_c) + K_{I2}\int_0^t (\boldsymbol{i}_c^* - \boldsymbol{i}_c)dt \tag{4.7}$$

A feedforward controller based on (4.7) is shown in Figure 4.3b.

Figure 4.4 is the complete control diagram of the shunt compensation system. The inner loop is the compensator current control which controls the output voltage of the compensator according the required nonactive current $\boldsymbol{i}_c^*$. The outer loop controls the active current drawn by the compensator by regulating the DC link voltage v_{dc}, and combines the active current $\boldsymbol{i}_{ca}^*$ together with the nonactive current $\boldsymbol{i}_{cn}^*$.

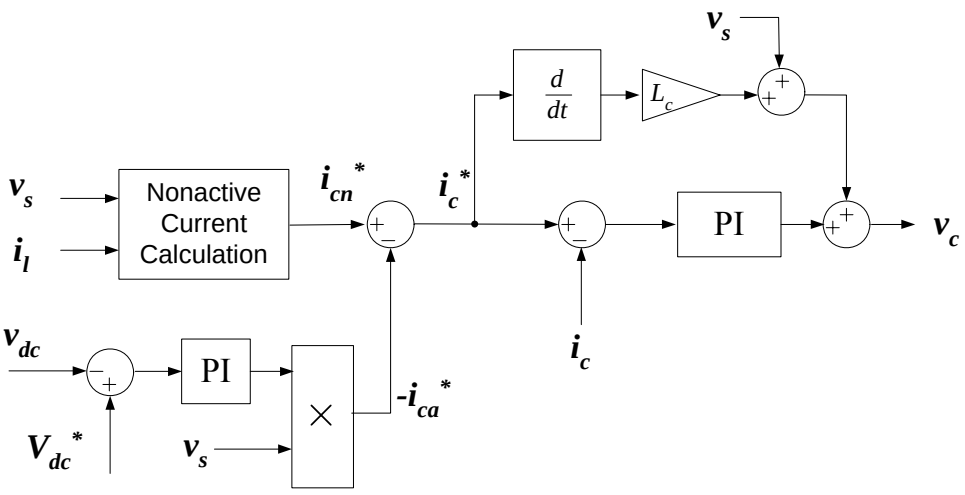

Figure 4.4. Control diagram of the shunt compensation system.

4.3. Simulations

The compensation system presented in subsection 4.1 is simulated in Matlab Simulink using the Power System Blockset. Figure 4.5 shows the main diagram of the simulation model. The power system and the controller are separated as shown in Figure 4.5a. The simulation in the "power" block is faster than the simulation in the "control" block. There are an inverter and a pulse width modulation (PWM) generator in the power block, which require a small simulation stepsize for accurate simulation, while the control block requires a larger simulation stepsize to simulate how the controller would execute in real time. Specifically, the simulation stepsize in the power block is 1 μs, while the simulation stepsize in the control block is 50 μs, except for the case of high-order harmonic compensation, which requires a smaller stepsize. The power block diagram is shown in Figure 4.5b. The utility, the load, and the inverter with a DC link capacitor are simulated. The system voltage, load current, compensator current, and the DC link

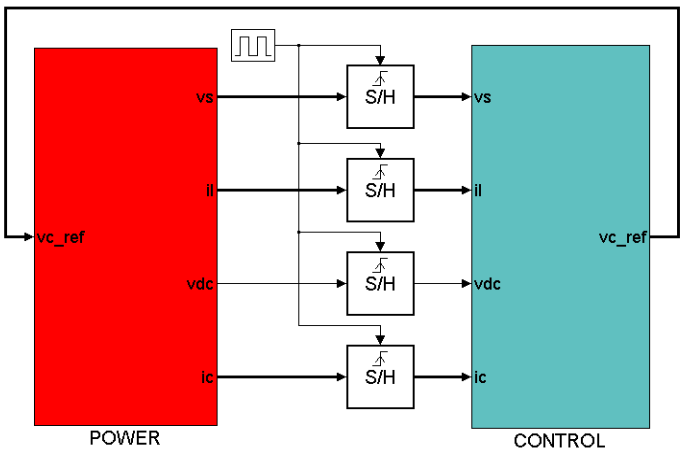

(a) Main diagram, the power block (fast) and the control block (slow)

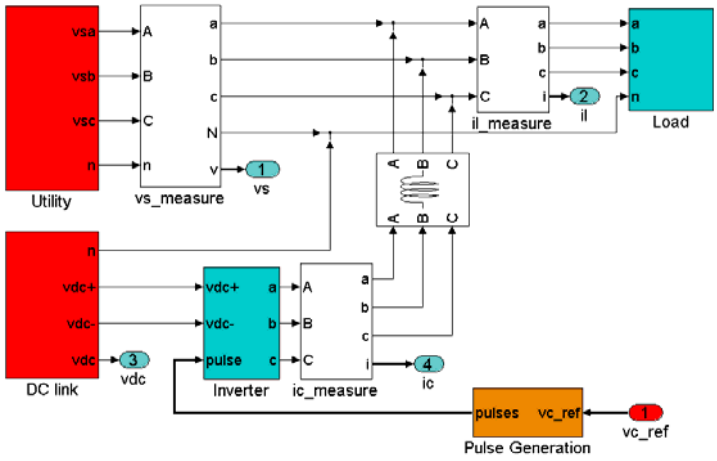

(b) Power block

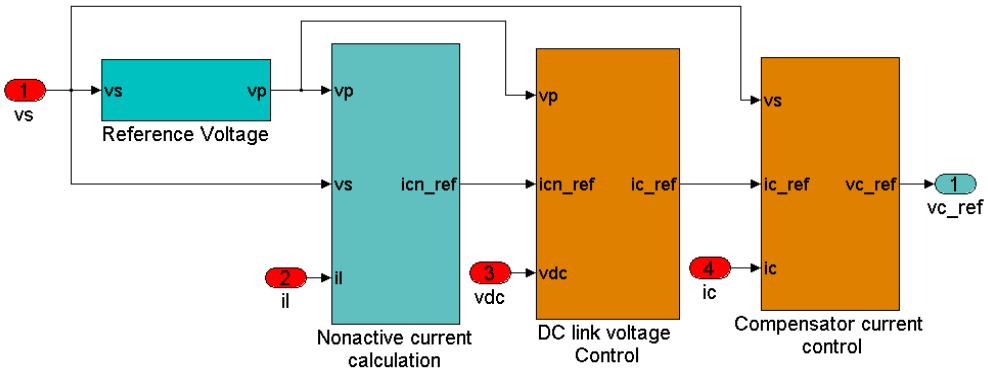

(c) Control block

Figure 4.5. Simulation model diagrams of the nonactive power compensation system.

voltage are measured and output to the control block; while the reference inverter output voltage is provided by the control block. The diagram in Figure 4.5c is the control block, which takes the measurements from the power block, calculates the nonactive current component of the load current, controls the DC link voltage by drawing a certain amount of active current from the utility, and generates a reference voltage for the inverter output. This reference voltage is compared to a triangle waveform with the frequency of the inverter switching frequency to generate PWM signals for the inverter.

4.3.1 Three-Phase Periodic System

The simulation starts with a common case, i.e., a three-phase *RL* load. Compensation of harmonics is simulated in three different conditions, harmonic current and fundamental sinusoidal voltage, and harmonics in both current and voltage where the reference voltage is chosen as the distorted system voltage itself or the fundamental component. The requirements of the DC link capacitance C, the DC link voltage v_{dc}, and the coupling inductance L_c are determined in the *RL* load case, and these requirements in other systems are analyzed based on the *RL* load system.

4.3.1.1 Three-Phase Balanced *RL* or *RC* Load

In this case, the load consists of resistors, and/or inductors, and/or capacitors, and the values of R, L, and C in each phase are equal. Moreover, the transmission lines and most loads in power systems are inductive, therefore, a three-phase balanced load with resistors and inductors are simulated. The load current is a fundamental sine wave, and the phase angle between the current and the voltage is lagging. As shown in Figure 4.6, the line-to-neutral voltage is 120V (rms) (Figure 4.6a), the load current is 20A (rms)

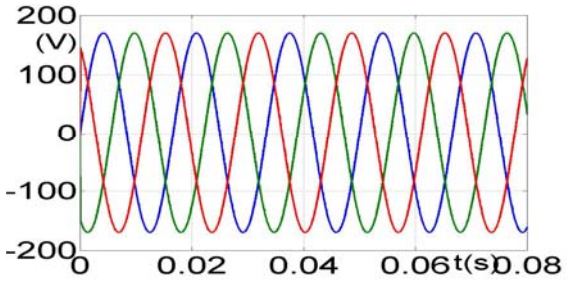

(a) System voltage $\boldsymbol{v_s}$ (V)

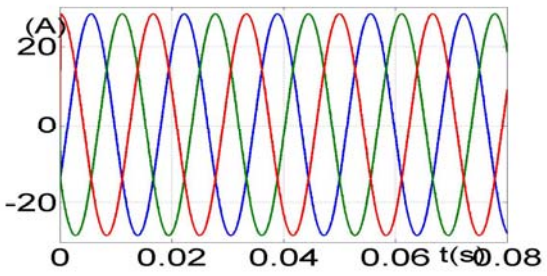

(b) Load current $\boldsymbol{i_l}$ (A)

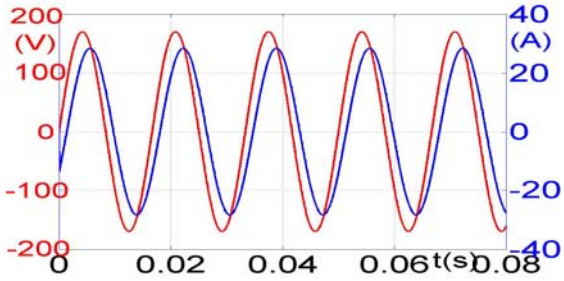

(c) Phase *a* voltage v_{sa} and load current i_{la}

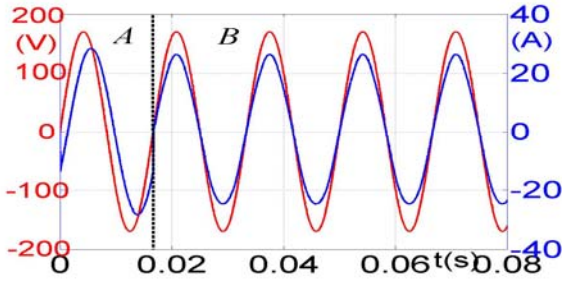

(d) Phase *a* voltage v_{sa} and source current i_{sa}

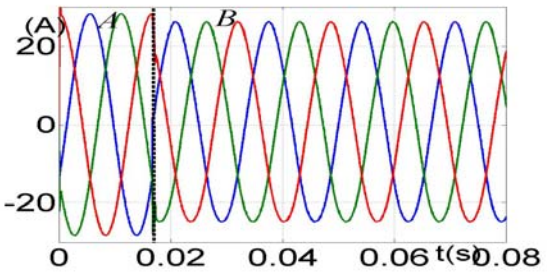

(e) Source current $\boldsymbol{i_s}$

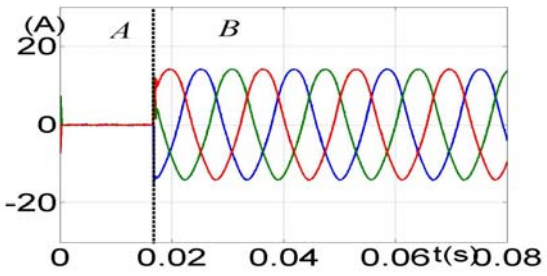

(f) Compensator current $\boldsymbol{i_c}$

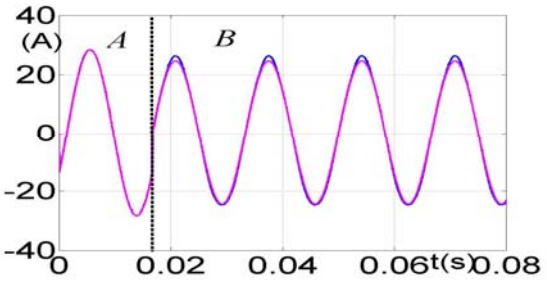

(g) Phase *a* calculated source current and real source current

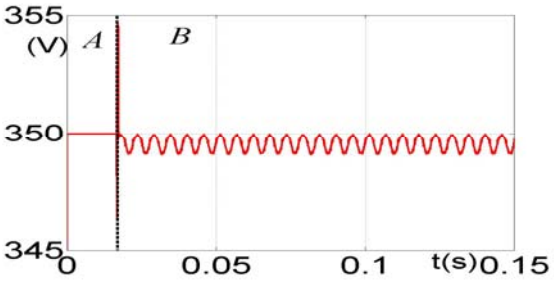

(h) DC link voltage v_{dc}

Figure 4.6. Three-phase *RL* load simulation.

Table 4.1. Parameters of the three-phase *RL* load compensation.

rms of the system voltage $\boldsymbol{v}_s$ (line-to-neutral) (V)	120
rms of the fundamental load current $\boldsymbol{i}_l$ (A)	20
Fundamental frequency (Hz)	60
DC link capacitance C (μF)	100
DC link voltage v_{dc} (V)	350
Coupling inductance L_c (mH)	1
Averaging interval T_c	$T/2$
Switching frequency (kHz)	20

(Figure 4.6b), and the phase angle of the current is π/6 radians lagging (Figure 4.6c). The parameters are shown in Table. 4.1.

The nonactive power and current are calculated according to the generalized nonactive power theory presented in Chapter 3. In each phase, the resistor R = 5.196Ω, and the inductor L = 7.96mH. The voltage and the load current are, respectively,

$$\boldsymbol{v}(t) = [120\sqrt{2}\cos(\omega t), 120\sqrt{2}\cos(\omega t - 2\pi/3), 120\sqrt{2}\cos(\omega t + 2\pi/3)]^T, \quad (4.8)$$

and

$$\boldsymbol{i}_l(t) = [20\sqrt{2}\cos(\omega t - \pi/6), 20\sqrt{2}\cos(\omega t - 5\pi/6), 20\sqrt{2}\cos(\omega t + \pi/2)]^T. \quad (4.9)$$

According to the generalized nonactive power theory presented in Chapter 3, this load current $\boldsymbol{i}_l(t)$ has the active current component $\boldsymbol{i}_a(t)$ and the nonactive current component $\boldsymbol{i}_n(t)$. The active current is provided by the source, and is denoted as $\boldsymbol{i}_s(t)$ and is calculated according to (3.5) (with $\boldsymbol{v}_p(t) = \boldsymbol{v}(t)$, $P(t) = 3VI$ = 6235.4W, and $V_p(t) = \sqrt{3}V$ = 207.8V),

$$\boldsymbol{i}_s(t) = [\sqrt{2}I_s\cos(\omega t), \sqrt{2}I_s\cos(\omega t - 2\pi/3), \sqrt{2}I_s\cos(\omega t + 2\pi/3)]^T, \quad (4.10)$$

where $I_s = 17.32$.

The nonactive current $\boldsymbol{i_n}(t)$, i.e., $\boldsymbol{i_c}(t)$ is calculated according to (3.6),

$$\boldsymbol{i_c}(t) = [\sqrt{2}I_c \sin(\omega t), \sqrt{2}I_c \sin(\omega t - 2\pi/3), \sqrt{2}I_c \sin(\omega t + 2\pi/3)]^T \text{ , where } I_c = 10. \tag{4.11}$$

The source current and compensator current before and after the compensator start to run are shown in Figures 4.6d - 4.6f, where the time interval *A* is before the compensator starts, and the time interval *B* is after it starts. The compensator starts to run at $t = 0.017$s, Figure 4.6d shows the phase *a* source current $i_{sa}(t)$ (blue waveform) is in phase with the phase *a* voltage and its amplitude is smaller than the amplitude before compensation. Figure 4.6e shows all the three source currents, which are sinusoidal and balanced. Figure 4.6f shows the compensator current, whose amplitude is equal to the value calculated from the generalized nonactive power theory in (4.11). After the compensator starts to run, the $\boldsymbol{i_c}(t)$ is the nonactive component of the load current, which is out of phase with the voltage.

As discussed in subsection 3.2.2, the average power $P(t)$ and the rms value of $\boldsymbol{v}(t)$ are constants, and they do not change whether the averaging interval T_c is chosen as 0 or integer multiples of $T/2$. Therefore, the instantaneous nonactive power compensation without average values (average power $P(t)$ and rms value of $\boldsymbol{v}(t)$) can be achieved in this case.

The following shows how to determine the requirements of the DC link voltage V_{dc} and the coupling inductance L_c.

DC link voltage V_{dc}

Based on the equivalent circuit of the nonactive power compensation system in Figure 4.3a, the compensator current $\boldsymbol{i_c}(t)$, the compensator output voltage $\boldsymbol{v_c}(t)$, and the system voltage $\boldsymbol{v_s}(t)$ satisfy

$$L_c \frac{d\boldsymbol{i_c}(t)}{dt} = \boldsymbol{v_c}(t) - \boldsymbol{v_s}(t) \tag{4.12}$$

The fundamental component of $\boldsymbol{v_c}(t)$ is in phase with $\boldsymbol{v_s}(t)$, and the amplitude is larger than $\boldsymbol{v_s}(t)$ when the compensator is providing nonactive power to the system. If the high frequency components in $\boldsymbol{v_c}(t)$ are neglected, $\boldsymbol{v_c}(t)$ can be written as

$$\boldsymbol{v_c}(t) = [\sqrt{2}V_c \cos(\omega t), \sqrt{2}V_c \cos(\omega t - 2\pi/3), \sqrt{2}V_c \cos(\omega t + 2\pi/3)]^T . \tag{4.13}$$

Solve $\boldsymbol{i_c}(t)$ from (4.12),

$$\boldsymbol{i_c}(t) = \sqrt{2}\frac{V_c - V_s}{L_c}\begin{bmatrix} \int_0^t \cos\omega t dt + i_{ca}(0) \\ \int_0^t \cos(\omega t - 2\pi/3)dt + i_{cb}(0) \\ \int_0^t \cos(\omega t + 2\pi/3)dt + i_{cc}(0) \end{bmatrix} = \sqrt{2}\frac{V_c - V_s}{\omega L_c}\begin{bmatrix} \sin\omega t + i_{ca}(0) \\ \sin(\omega t - 2\pi/3) + i_{cb}(0) \\ \sin(\omega t + 2\pi/3) + i_{cc}(0) \end{bmatrix} \tag{4.14}$$

The initial values $i_{ca}(0)$, $i_{cb}(0)$, and $i_{cc}(0)$ are zero because the currents flowing through the inductors cannot change instantaneously. Therefore, the nonactive current is

$$\boldsymbol{i_c}(t) = \sqrt{2}\frac{V_c - V_s}{\omega L_c}[\sin(\omega t), \sin(\omega t - 2\pi/3), \sin(\omega t + 2\pi/3)]^T . \tag{4.15}$$

The amplitude $\sqrt{2}I_c$ of the nonactive current is calculated in the generalized nonactive power theory. The rms value of the compensator output voltage V_c is

$$V_c = \omega L_c I_c + V_s . \tag{4.16}$$

This is the rms value of the compensator output voltage for fundamental nonactive current compensation. According to [49], the DC link voltage V_{dc} is

$$V_{dc} = 2\sqrt{2}V_c = 2\sqrt{2}(\omega L_c I_c + V_s) . \tag{4.17}$$

A smaller coupling inductor is preferred so that the compensator output voltage is lower; however, a certain amount of inductance is needed to filter the ripple in the nonactive compensator current $\boldsymbol{i_c}(t)$. For compensation of harmonic load current, V_{dc} should include the harmonics' voltage drop on the coupling inductor, which is proportional to the harmonics' frequencies.

Coupling inductance L_c

In (4.7), the differential of the reference current (the second term on the right) can be neglected, and the integral gain K_{I2} is much smaller than the proportional gain K_{P2}. Therefore, (4.7) can be approximately written as

$$\boldsymbol{v_c} = \boldsymbol{v_s} + K_{P2}(\boldsymbol{i_c^*} - \boldsymbol{i_c}) . \tag{4.18}$$

If rms values are used, it can be written as

$$V_c = V_s + K_{P2}(I_c^* - I_c) = V_s + K_{P2}\Delta I_c . \tag{4.19}$$

Combine (4.16) and (4.19),

$$\omega L_c I_c = K_{P2}\Delta I_c . \tag{4.20}$$

Therefore, the proportional gain K_{P2} can be determined by

$$K_{P2} = \omega L_c \frac{I_c}{\Delta I_c} = X_c \frac{I_c}{\Delta I_c} . \tag{4.21}$$

K_{P2} is proportional to the coupling impedance X_c, and inversely proportional to the compensator current error ΔI_c. A smaller error requires a larger gain; however in a real system, there is noise from the measurement, EMI from the switching and other interference, which may be amplified to an intolerable level if a large gain is used. This is another reason a smaller L_c is preferred.

The inductance L_c between the power system and the compensator could be the inductance of a step-up transformer or a coupling reactor. It also acts as a filter for the compensation current $\boldsymbol{i_c}$, which can have high ripple content if a PWM inverter is used. If L_c is too small, it cannot filter the ripple in the compensation current i_c; on the other hand, if L_c is too large, as mentioned above, a higher DC link voltage is required, especially for higher-order harmonics compensation.

If the compensator current is I_c, then the voltage drop on the coupling inductor L_c is

$$V_{L_c} = \omega L_c I_c . \tag{4.22}$$

This voltage drop V_{Lc} is usually chosen as 3% - 9% of the system voltage V_s for fundamental component. This number is chosen for two reasons. A smaller L_c is preferred from the point of decreasing the DC link voltage V_{dc} and the proportional gain K_{P2}. However, distortion will be introduced to the system voltage $\boldsymbol{v_s}$ if L_c is too small. The coupling inductance can be determined from (4.22),

$$L_c = (3\% - 9\%)\frac{V_s}{\omega I_c} . \tag{4.23}$$

The coupling inductance L_c is maintained small to reduce the DC link voltage, and accordingly the gains of the PI controller are kept small also, as long as the desired compensation results are obtained.

4.3.1.2 Three-Phase Harmonic Load and Sinusoidal Voltage

Harmonics are a common cause of distortion in power systems, existing in both voltage and current. Harmonics compensation is independent of the averaging interval T_c if T_c is an integer multiple of $T/2$. According to the definition of active current given in (3.5):

$$\boldsymbol{i}_a(t) \triangleq \frac{P(t)}{V_p^2(t)} \boldsymbol{v}_p(t). \tag{4.24}$$

For harmonics compensation, $P(t)$ and $V_p(t)$ are constant, i.e., $\boldsymbol{i}_a(t)$ is in phase with $\boldsymbol{v}_p(t)$ and has the same waveform shape as $\boldsymbol{v}_p(t)$ if T_c is an integer multiple of $T/2$. If the system voltage is not distorted, and the load current has harmonics, then the system voltage itself can be used as the reference voltage to achieve sinusoidal, balanced, and unity power factor source current after compensation. This case is simulated with the parameters in Table 4.2 (except as noted below), and the simulation results are illustrated in Figure 4.7.

The load current in Figure 4.7b contains harmonic components from the 5th order to the 23rd order. Because of the high order harmonics, the switching frequency is increased to 50 kHz (20 kHz in the previous case). The DC link voltage is increased to 420V, and other parameters are shown in Table 4.2. The fundamental system voltage and the distorted load current are shown in Figures 4.7a and 4.7b, respectively. Figure 4.7c shows the phase *a* load current is distorted and lags the voltage, while in Figure 4.7d, the source current is a fundamental sine wave and in phase with the voltage when the compensator is operating (after t = 0.017s in Figure 4.7). The source current in Figure 4.7e now contains the active component of the load current, and the compensator current in Figure

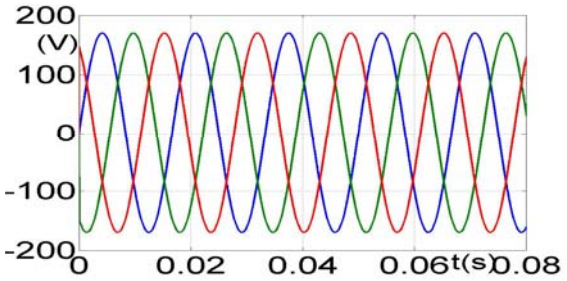

(a) System voltage $\boldsymbol{v_s}$ (V)

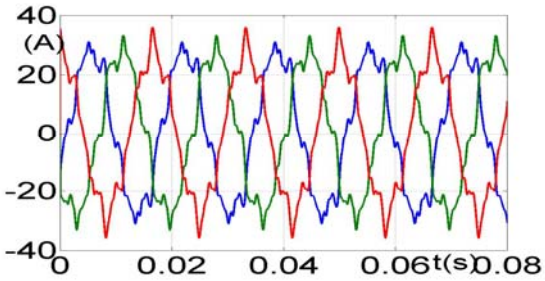

(b) Load current $\boldsymbol{i_l}$ (A)

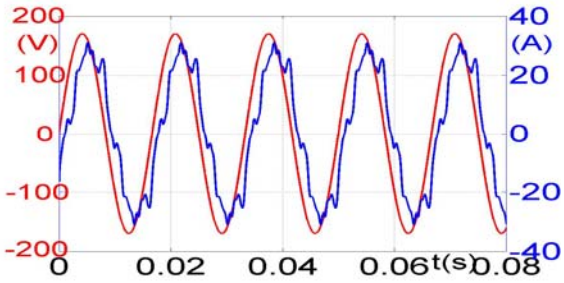

(c) Phase *a* voltage v_{sa} and load current i_{la}

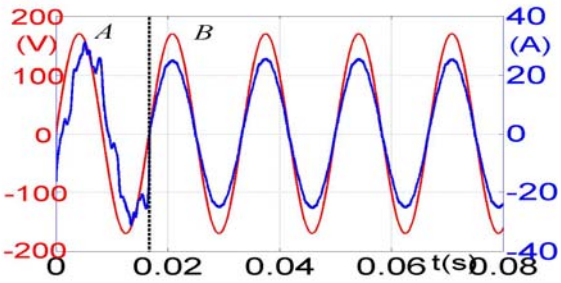

(d) Phase *a* voltage v_{sa} and source current i_{sa}

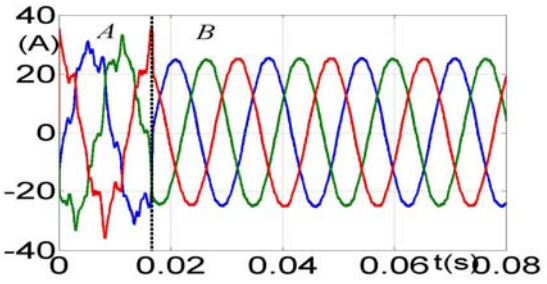

(e) Source current $\boldsymbol{i_s}$

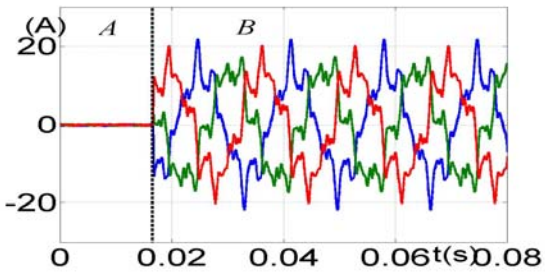

(f) Compensator current $\boldsymbol{i_c}$

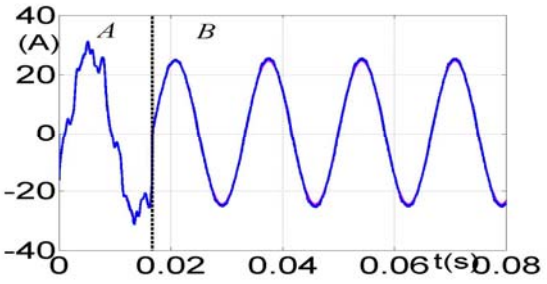

(g) Phase *a* calculated source current and real source current

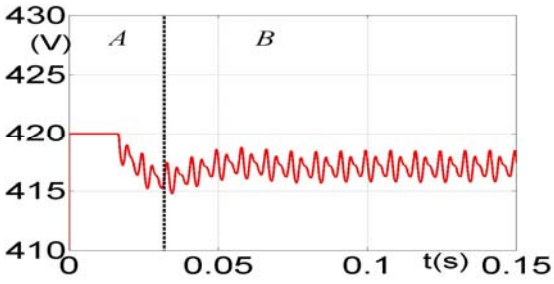

(h) DC link voltage v_{dc}

Figure 4.7. Three-phase harmonic load with fundamental $\boldsymbol{v_s}$.

Table 4.2. Parameters of the three-phase harmonics compensation with fundamental sinusoidal $\boldsymbol{v}_s(t)$.

rms of the system voltage $\boldsymbol{v}_s(t)$ (line-to-neutral) (V)	120
rms of the fundamental load current $\boldsymbol{i}_l(t)$ (A)	20
Fundamental frequency (Hz)	60
DC link capacitance C (μF)	1000
DC link voltage v_{dc} (V)	420
Coupling inductance L_c (mH)	1.5
Averaging interval T_c	$T/2$
Switching frequency (kHz)	50

4.7f has the nonactive component. In Figure 4.7g, the phase *a* calculated active load current (magenta) and the actual source current are compared. The actual source current is slightly larger than the calculated active load current, because of the active current drawn by the compensator to meet the losses. The DC link voltage $v_{dc}(t)$ is shown in Figure 4.7g. The variation of v_{dc} is inversely proportional to the DC link capacitance. The output voltage of the inverter satisfies

$$\boldsymbol{v}_c(t) = L_c \frac{d\boldsymbol{i}_c(t)}{dt} + \boldsymbol{v}_s(t) . \tag{4.25}$$

Phase *a* of the system voltage $\boldsymbol{v}_s(t)$ is

$$v_{sa}(t) = \sqrt{2} V_s \cos(\omega t) . \tag{4.26}$$

Phase *a* of the compensator current is

$$i_{ca}(t) = \sqrt{2} I_c \cos(\omega t \pm \frac{\pi}{2}) + \sum_{k=2}^{\infty} \sqrt{2} I_k \cos(k\omega t + \theta_k) . \tag{4.27}$$

The plus sign indicates that the compensator provides capacitive nonactive power, and the minus sign indicates that the compensator provides inductive nonactive power. Phase *a* of the compensator voltage is

$$v_{ca}(t) = \sqrt{2}(V_s \mp \omega L_c I_c)\cos(\omega t) + \sum_{k=2}^{\infty} \sqrt{2} k\omega L_c I_k \cos(k\omega t + \theta_k)\,. \tag{4.28}$$

For a compensator current with harmonics, the magnitudes of the harmonics in $\boldsymbol{v_c}(t)$ are *k* times of the harmonics in the current. For the worst case, in which the compensator is providing inductive fundamental nonactive current and all the harmonics reach the peak value at the same time, the DC link voltage v_{dc} should be twice the peak line-to-line voltage $\boldsymbol{v_c}(t)$ to be capable of completely compensating the nonactive components in the load current.

Compared to the fundamental nonactive power compensation, a larger inverter output voltage, i.e., a larger DC link voltage v_{dc} is required, and the magnitude is proportional to the frequency of the harmonics.

4.3.1.3 Three-Phase Harmonic Load and Distorted System Voltage

If the system voltage is also distorted, choosing a different reference voltage will result in a different source current. The compensation with the system voltage itself is discussed in this subsection, and the compensation by choosing the fundamental component of the system voltage as the reference voltage will be discussed in the next subsection. In both of these cases, the load current and the system voltage contain 5^{th} and 7^{th} harmonics. A compensator with a switching frequency of 20 kHz will be used in these two simulations. The parameters of the simulation are listed in Table 4.3. The DC link voltage is higher than for the *RL* load case, since there are harmonics in the compensator

Table 4.3. Parameters of the three-phase harmonics compensation with distorted $\boldsymbol{v}_s$.

rms of the system voltage $\boldsymbol{v}_s$ (line-to-neutral) (V)	120
rms of the fundamental load current $\boldsymbol{i}_l$ (A)	20
Fundamental frequency (Hz)	60
DC link capacitance C (μF)	500
DC link voltage v_{dc} (V)	370
Coupling inductance L_c (mH)	0.5
Averaging interval T_c	$T/2$
Switching frequency (kHz)	20

current. The DC link capacitance is larger than for the *RL* load case because the instantaneous power is not zero in this case which requires the DC link capacitor to provide and to consume power from time to time.

The system source voltage $\boldsymbol{v}_s(t)$, the load current $\boldsymbol{i}_l(t)$, the source current $\boldsymbol{i}_s(t)$, and the compensator current $\boldsymbol{i}_c(t)$ are shown in Figures 4.8a – 4.8d, respectively. The source current is still distorted after compensation. More specifically, the system voltage and the source current of each phase are compared in Figures 4.8e – 4.8g, which show that the waveform of the source current has the same shape as the system voltage, therefore, a unity power factor is achieved in this case.

4.3.1.4 Three-Phase Harmonic Load and Sinusoidal Reference Voltage

If a fundamental sinusoidal source current is preferred, another reference voltage should be used other than the system voltage when it is distorted, which is usually the fundamental component of the system voltage $\boldsymbol{v}_s(t)$. The source current will be sinusoidal and in phase with the reference voltage $\boldsymbol{v}_p(t)$. The simulation parameters are listed in

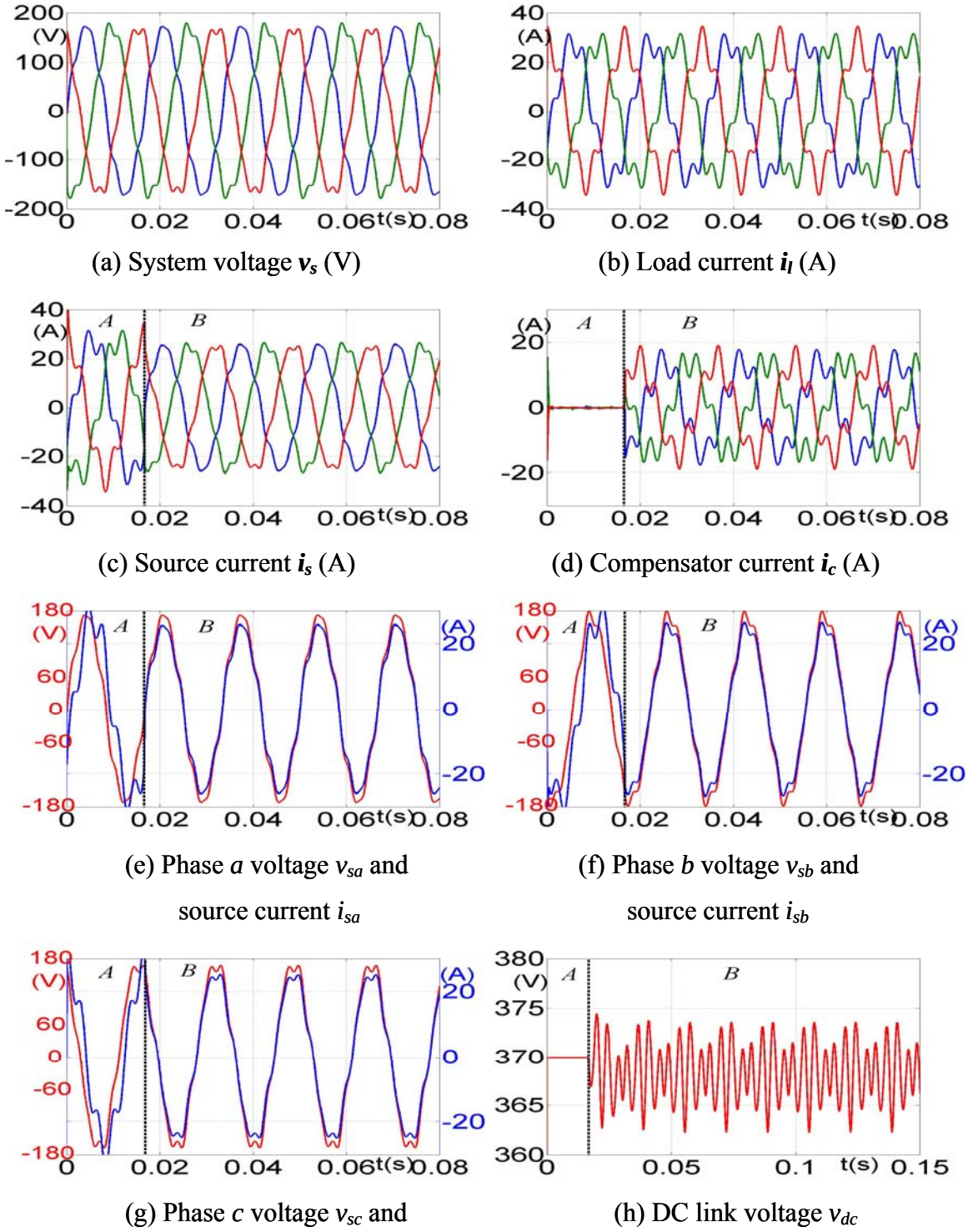

(a) System voltage $\boldsymbol{v_s}$ (V)

(b) Load current $\boldsymbol{i_l}$ (A)

(c) Source current $\boldsymbol{i_s}$ (A)

(d) Compensator current $\boldsymbol{i_c}$ (A)

(e) Phase *a* voltage v_{sa} and source current i_{sa}

(f) Phase *b* voltage v_{sb} and source current i_{sb}

(g) Phase *c* voltage v_{sc} and source current i_{sc}

(h) DC link voltage v_{dc}

Figure 4.8. Three-phase harmonic load compensation with distorted $\boldsymbol{v_s}$.

Table 4.4. Parameters of the three-phase harmonics compensation with sinusoidal $\boldsymbol{v_p}$.

rms of the system voltage $\boldsymbol{v_s}$ (line-to-neutral) (V)	120
rms of the fundamental load current $\boldsymbol{i_l}$ (A)	20
Fundamental frequency (Hz)	60
DC link capacitance C (μF)	500
DC link voltage v_{dc} (V)	400
Coupling inductance L_c (mH)	1
Averaging interval T_c	$T/2$
Switching frequency (kHz)	20

Table 4.4 and the results are illustrated in Figure 4.9. The DC link voltage is higher than the previous case, because all the nonactive components in the load current are provided by the compensator this time. The system voltage and the load current are shown in Figures 4.9a and 4.9b. The reference voltage, which is the fundamental component of the system voltage, is shown in Figure 4.9c. The phase *a* source current and reference voltage are compared in Figure 4.9d, which shows that the source current is fundamental sinusoidal and in phase with the reference voltage.

4.3.1.5 Three-Phase Diode Rectifier Load

A three-phase diode rectifier is a common nonlinear load. The current of a diode rectifier is shown in Figure 4.10a (phase *a*). It is a periodic waveform with the same period as the fundamental period of the system voltage, thus the current can be decomposed into a fundamental component and harmonics. However, different from the harmonics load discussed in the previous subsection, the current drawn by a diode-based rectifier is not continuous, and the variation of the current with time di/dt is very large

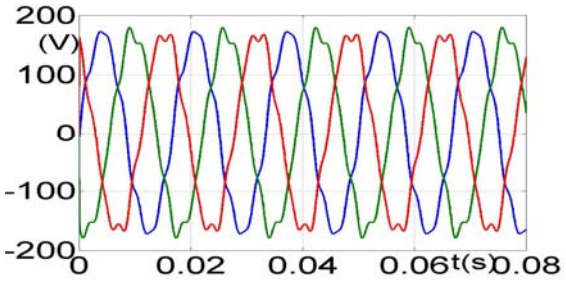

(a) System voltage $\boldsymbol{v_s}$ (V)

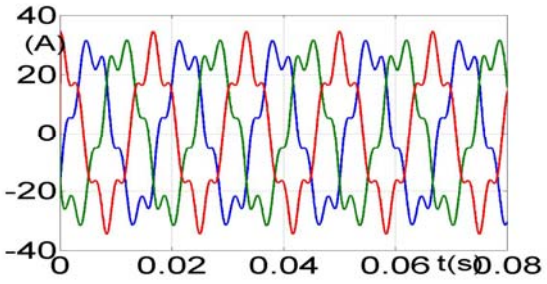

(b) Load current $\boldsymbol{i_l}$ (A)

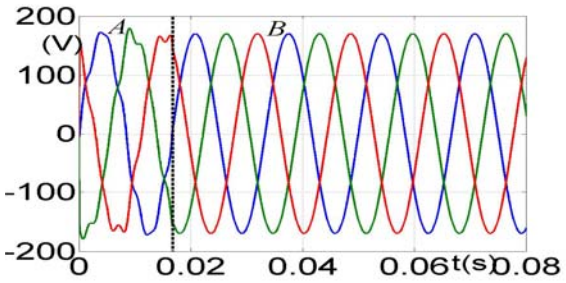

(c) Reference voltage $\boldsymbol{v_p}$ (V)

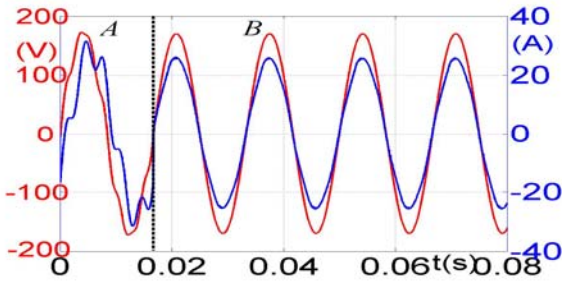

(d) Phase a reference voltage v_{pa} and source current i_{sa}

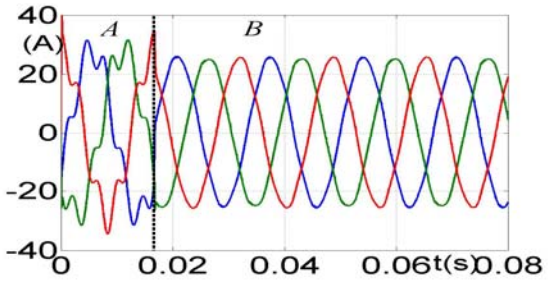

(e) Source current $\boldsymbol{i_s}(t)$ (A)

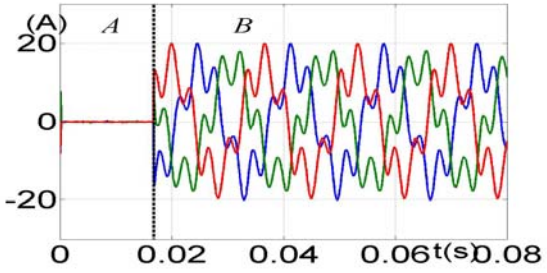

(f) Compensator current $\boldsymbol{i_c}$ (A)

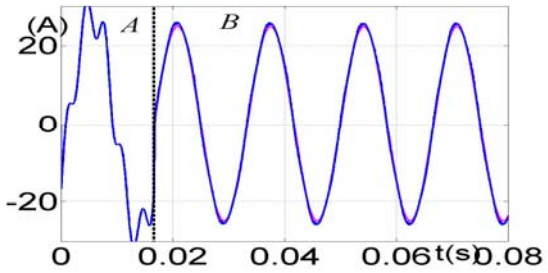

(g) Phase a calculated source current and real source current

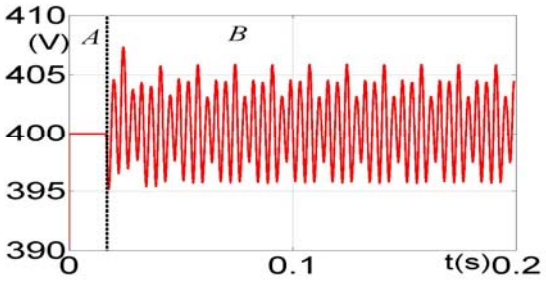

(h) DC link voltage v_{dc} (V)

Figure 4.9. Three-phase harmonic load compensation with sinusoidal $\boldsymbol{v_p}$.

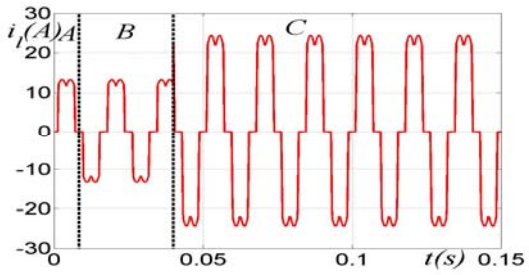

(a) Load current of phase a, i_{la}

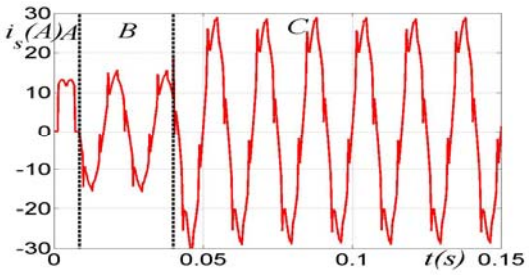

(b) Source current of phase a, i_{sa}, $V_{dc} = 2.6V_s$

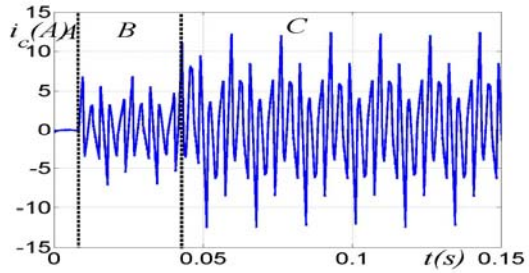

(c) Compensator current of phase a, i_{ca}, $V_{dc} = 2.6V_s$

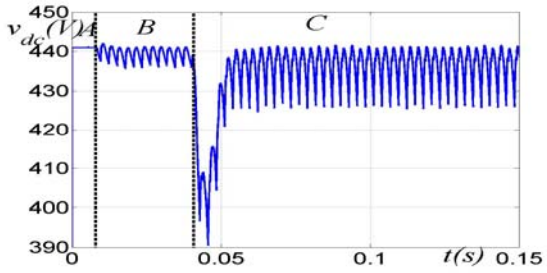

(d) DC link voltage v_{dc}, $V_{dc} = 2.6V_s$

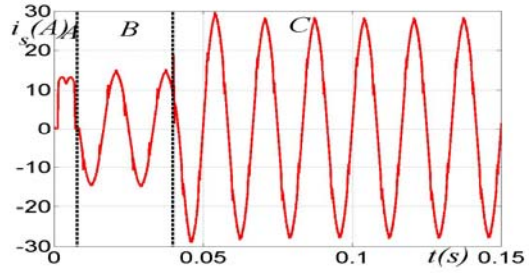

(e) Source current of phase a, i_{sa}, $V_{dc} = 5.2V_s$

Figure 4.10. Simulation of rectifier load compensation.

(di/dt = 5.8×10^4 A/s in this example). Therefore, there are special issues in the compensation of a rectifier load.

At t = 0.04 s, there is a sudden load change which causes the load current to increase (the second dash line in Figure 4.10a). In Figure 4.10b, during the time interval A, $\boldsymbol{i}_s(t)$ is supplying the full load current while the compensator is off. The compensator is on during the time interval B and $\boldsymbol{i}_s(t)$ is close to a sinusoid, and in the time interval C, $\boldsymbol{i}_s(t)$ is shown after the sudden load change. Figure 4.10c shows the nonactive current which is provided by the compensator, which is highly distorted. The load change has an impact on the DC link voltage, which drops about 50 volts when the load changes. To regulate v_{dc}, some active current is drawn. The sudden load change requires a larger capacitance than a steady load.

The source current $i_{sa}(t)$ in Figure 4.10b has some spikes, which is caused by the large variation of the current with time. According to (4.3), the compensator output voltage $\boldsymbol{v}_c$ is given by

$$\boldsymbol{v}_c = \boldsymbol{v}_s + L_c \frac{d\boldsymbol{i}_c}{dt}.$$

A large di_c/dt requires a large v_c; however, if the DC link voltage does not meet this requirement, the compensator is unable to provide the nonactive current as required by the nonactive power theory, and spikes occur in the source current accordingly. Figure 4.10b and Figure 4.10e show the source current when the DC link voltage V_{dc} is $2.6V_s$ and $5.2V_s$, respectively, where V_s is the amplitude of the system line-to-neutral voltage. The spikes in Figure 4.10e are smaller than those in Figure 4.10b, which shows that a source current with less spikes can be achieved by increasing the DC link voltage.

However, a higher DC link voltage requires a higher voltage rating of the compensator and results in higher compensator losses. In practice, the DC link voltage can be chosen between $2V_s$ to $3V_s$.

4.3.1.6 Three-Phase Load with Sub-Harmonics

The frequencies of sub-harmonics are not a multiple integer of the fundamental frequency. In this simulation, the voltage is fundamental pure sine wave, and the load current has a sub-harmonic component with frequency $f_s = 2f/3$, where f is the fundamental frequency. The nonactive current is completely compensated if the averaging interval T_c is a multiple integer of the common multiple of the fundamental component and the sub-harmonic component, which is $3T$ in this case.

The simulation results are shown in Figure 4.11. The system voltage $\boldsymbol{v}_s(t)$ and load current $\boldsymbol{i}_l(t)$ are shown in Figures 4.11a and 4.11b respectively. Figures 4.11c and 4.11d are the source current and the compensator current when $T_c = T/2$. Figures 4.11e and 4.11f are the source current and the compensator current when $T_c = T$. The fundamental nonactive component is completely compensated, but the sub-harmonics component is not completely eliminated. As illustrated, there are still sub-harmonics in the source current. The sub-harmonics are completely compensated if $T_c = 3T$, as shown in Figures 4.11g and 4.11h.

4.3.2 Three-Phase Unbalanced *RL* Load

In a three-phase four-wire system, i.e., a neutral line is present, and the load or the source voltage is unbalanced, there will be a neutral current flowing in the neutral line. A

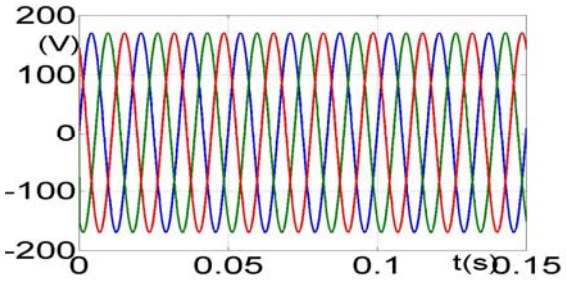

(a) Source voltage $\boldsymbol{v_s}$ (V)

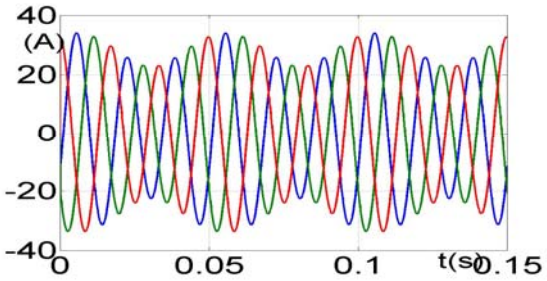

(b) Load current $\boldsymbol{i_l}$ (A)

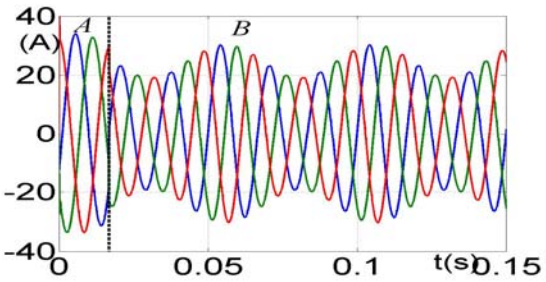

(c) Source current $\boldsymbol{i_s}$, $T_c = T/2$

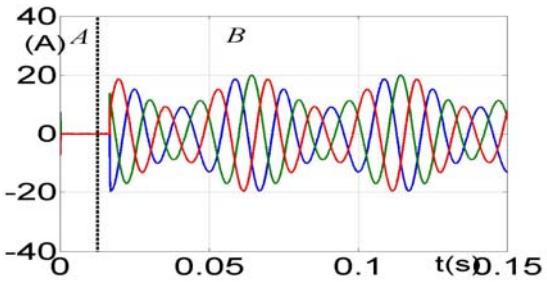

(d) Compensator current $\boldsymbol{i_c}$, $T_c = T/2$

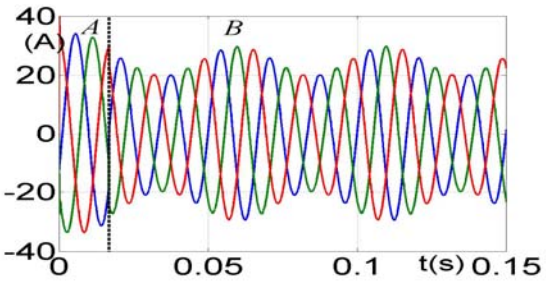

(e) Source current $\boldsymbol{i_s}$, $T_c = T$

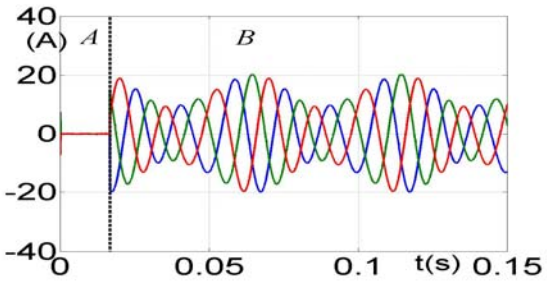

(f) Compensator current $\boldsymbol{i_c}$, $T_c = T$

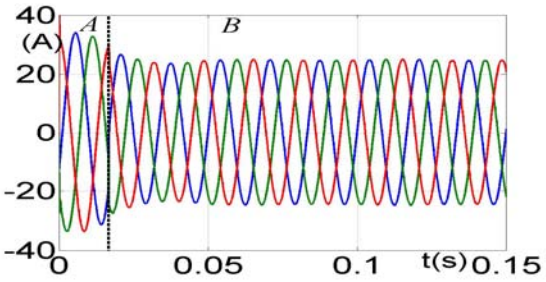

(g) Source current $\boldsymbol{i_s}$, $T_c = 3T$

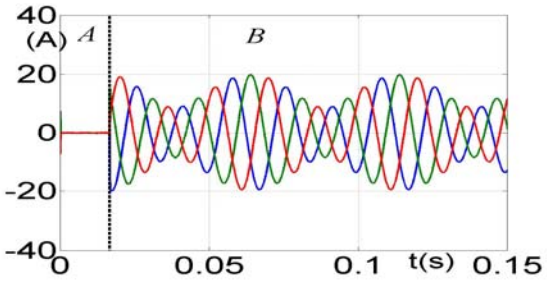

(h) Compensator current $\boldsymbol{i_c}$, $T_c = 3T$

Figure 4.11. Simulation of sub-harmonics load compensation.

three-phase four-wire system is balanced if the phase angle between each two phases is 120°, and all the phases have the same magnitude; otherwise it is unbalanced.

An unbalanced load current with both unequal amplitudes and unbalanced phase-angles is first simulated. In this case, the voltage is balanced. The rms values of the three-phase currents are 16A (20% lower), 20A, and 18A (10% lower), and the phase angles are 30°, 27°, and 33° lagging to the voltage, respectively (Figure 4.12b). The voltage is fundamental pure sine wave and balanced as shown in Figure 4.12a.

The phase *a* source current before compensation (time interval A) and after compensation (time interval B) is shown in Figure 4.12d (red waveform). After compensation, the source current is in phase with the phase *a* voltage (blue waveform). Figure 4.12e shows the three-phase source current before and after compensation. The three-phase currents are now balanced, i.e., equal amplitude and equal phase angle between each other. Figure 4.12f shows the neutral current of the utility before and after compensation. After compensation, the source neutral current is near zero (theoretically it is zero, but it is near zero because of the control tracking error), and the load neutral current now is provided by the compensator.

4.3.3 Single-Phase Load

4.3.3.1 Single-Phase *RL* Load

Based on the equivalent circuit of the nonactive power compensation system in Figure 4.3a, the compensator current $i_c(t)$, the compensator output voltage $v_c(t)$, and the system voltage $v_s(t)$ satisfy

$$L_c \frac{di_c(t)}{dt} = v_c(t) - v_s(t) . \tag{4.29}$$

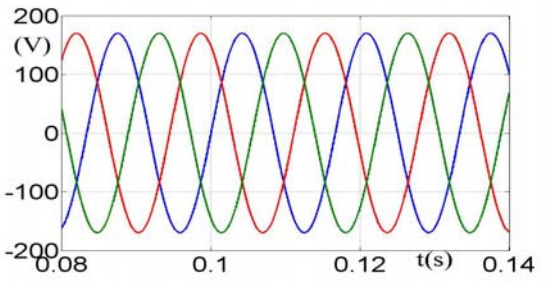

(a) System voltage $\boldsymbol{v_s}$ (V)

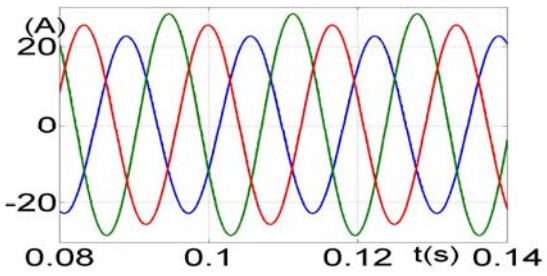

(b) Load current $\boldsymbol{i_l}(t)$

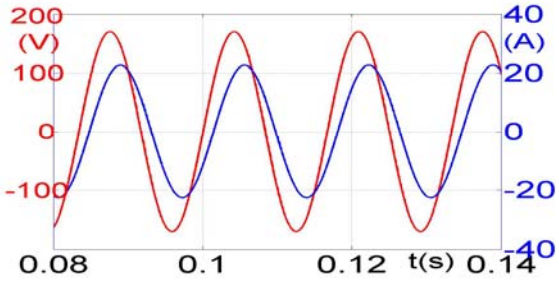

(c) Phase *a* voltage v_{sa} and load current i_{la}

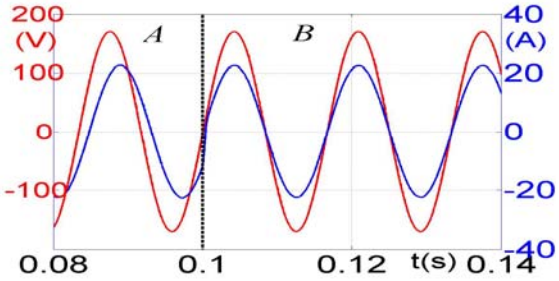

(d) Phase a voltage v_{sa} and source current i_{sa}

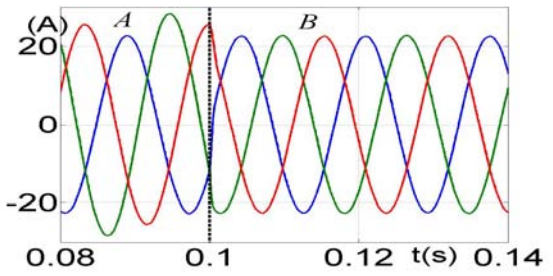

(e) Source current $\boldsymbol{i_s}$ (A)

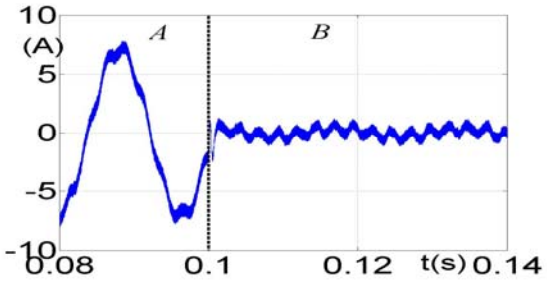

(f) Source neutral current i_{sn} (A)

Figure 4.12. Three-phase unbalanced *RL* load.

In the fundamental nonactive power compensation case, let

$$v_s(t) = \sqrt{2}V_s \cos(\omega t) . \tag{4.30}$$

The fundamental component of the $v_c(t)$ is in phase with $v_s(t)$, and the amplitude is larger than $v_s(t)$ when the compensator is providing inductive power to the system. If the high frequency components in $v_c(t)$ are neglected, $v_c(t)$ can be written as

$$v_c(t) = \sqrt{2}V_c \cos(\omega t) . \tag{4.31}$$

Apply the Laplace transformation to (4.29),

$$I_c(s) = \sqrt{2}\frac{V_c - V_s}{L_c}\frac{1}{s^2 + \omega^2} . \tag{4.32}$$

Therefore, the nonactive current in the time domain is

$$i_c(t) = \sqrt{2}\frac{V_c - V_s}{\omega L_c}\sin(\omega t) . \tag{4.33}$$

The amplitude of the nonactive current is calculated according to the generalized nonactive power theory presented in Chapter 3, and denoted as $\sqrt{2}I_c$. The rms value of the compensator output voltage V_c is then

$$V_c = \omega L_c I_c + V_s . \tag{4.34}$$

This is the rms value of the compensator output voltage for fundamental nonactive current compensation, which is also valid in three-phase systems. A smaller coupling inductor is preferred so that the compensator output voltage is lower; however, a certain amount of inductance is needed to filter the ripples in the nonactive compensator current $i_c(t)$. The DC link voltage V_{dc} is equal to the peak value of V_c.

The energy stored in the DC link capacitor $E_{dc}(t)$ is

$$E_{dc}(t) = \frac{1}{2} C v_{dc}^2(t) \ . \tag{4.35}$$

The maximum energy variation in C is

$$\Delta E_{dc} = \frac{1}{2} C (v_{dc}^2(t_{\max}) - v_{dc}^2(t_{\min})) , \tag{4.36}$$

where $v_{dc}(t_{max})$ is the maximum value of the DC link voltage and $v_{dc}(t_{min})$ is the minimum value. The energy variation ΔE_{dc} can also be written as

$$\Delta E_{dc} = \int_{t_{\min}}^{t_{\max}} v_{dc}(t) i_{dc}(t) dt , \tag{4.37}$$

where $v_{dc}(t)$ and $i_{dc}(t)$ are the voltage and current of the DC link capacitor, respectively. Usually the DC link current $i_{dc}(t)$ is not measured, therefore, the energy variation on the DC link capacitor ΔE_{dc} is approximately equal to the energy variation of the nonactive compensator, i.e.,

$$\Delta E_{dc} = \int_{t_{\min}}^{t_{\max}} v_s(t) i_c(t) dt = V_s I_c \frac{T}{4} . \tag{4.38}$$

Combine (4.36) and (4.38), and it is assumed that the DC link voltage varies around V_{dc}, i.e.,

$$\frac{1}{2} C ((V_{dc} + \Delta V_{dc})^2 - (V_{dc} - \Delta V_{dc})^2) = V_s I_c \frac{T}{4} . \tag{4.39}$$

Therefore, the DC link capacitance C is

$$C = \frac{V_s I_c T}{2 V_{dc} \Delta V_{dc}} . \tag{4.40}$$

The DC link voltage variation ΔV_{dc} is inversely proportional to the capacitance, therefore for a nonactive power compensator, the capacitance requirement can be

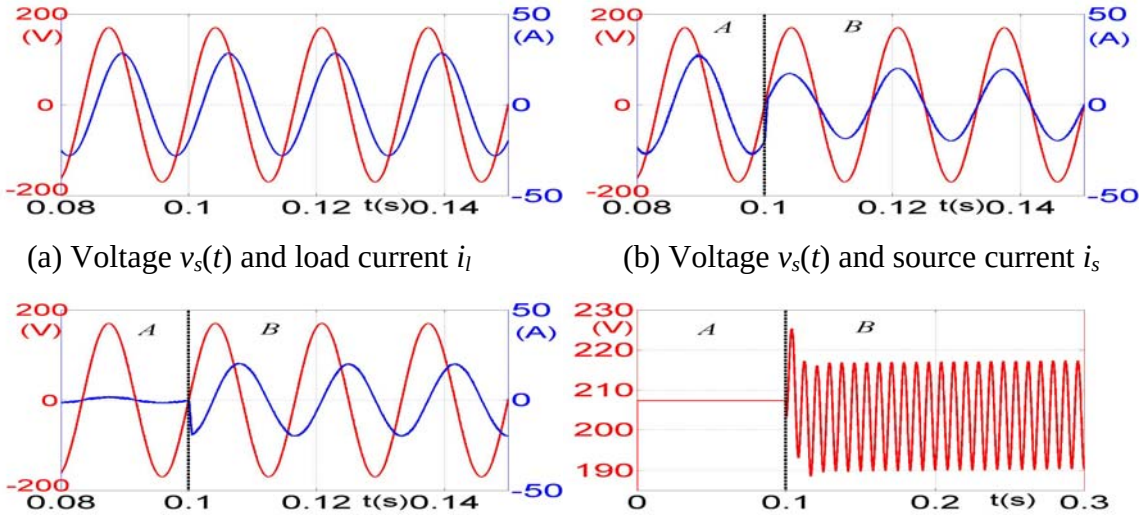

(a) Voltage $v_s(t)$ and load current i_l (b) Voltage $v_s(t)$ and source current i_s

(c) Voltage $v_s(t)$ and compensator current i_c (d) DC link voltage v_{dc}

Figure 4.13. Simulation of single-phase load in a single-phase system.

determined if the DC link voltage variation is specified. The capacitance requirement in a three-phase fundamental nonactive power system is much smaller than in a single-phase system with the same amount of nonactive current, because the instantaneous nonactive power is zero in a three-phase system and not zero in a single-phase system, which requires more DC link energy storage, i.e. higher DC link capacitance for a given system.

A single-phase *RL* load is simulated and the simulations results are shown in Figure 4.13. Figure 4.13a shows the system voltage $v_s(t)$ (red waveform) and the load current $i_l(t)$ (blue waveform), which is lagging. Figure 4.13b shows the source current before (time interval *A*) and after compensation (time interval *B*). After compensation, the source current is in phase with the voltage. Figure 4.13c shows the compensator current and the system voltage. The compensator current is 90° out of phase with the voltage. Figure 4.13d shows the DC link voltage $v_{dc}(t)$, which has a ripple, but the average value is

kept constant by drawing a certain amount of active current to make up for compensator losses.

4.3.3.2 Single-Phase Pulse Load

Some loads draw a large magnitude current for a short period (from half of a cycle to a few cycles), which may cause voltage sag in a weak power system. Single-phase loads in three-phase power systems can cause the system to become unbalanced (either unbalanced magnitude or unbalanced phase angle). This may result in a high neutral current, or a distortion in voltage. Single-phase loads also result in harmonics at all odd multiples of the fundamental, but the most substantial of them are typically the triplen harmonics. Triplens add together in the neutral line and result in a high neutral current. A single-phase pulse load is studied in this section.

A pulse current is represented by a triangle waveform. The duration of this current may be a fraction of the line frequency cycle, or up to several cycles. The current may be zero or a sine wave of a much smaller magnitude compared to the irregular pulse current; therefore, it is simplified to zero at all the times other than the pulse current interval (i_l is shown in Figure 4.14a). Figures 4.14 and 4.15 show the simulation results for $T_c = T/2$ (Figure 4.14) and $T_c = 2T$ (Figure 4.15) with $v_p = v_f$ for both cases. To simplify the simulation, the voltage waveform is assumed to be a sine wave. However, note that the results also apply to the case of a source voltage that contains harmonics or is non-sinusoidal. Figure 4.16 shows the peak source current normalized with respect to load current for various compensation intervals and phase angles between the current pulse and source voltage for a pulse waveform such as those shown in Figure 4.14 and Figure 4.15. With the averaging interval T_c changing from $T/2$ to $2T$, i_s decreases from 0.6 p.u.

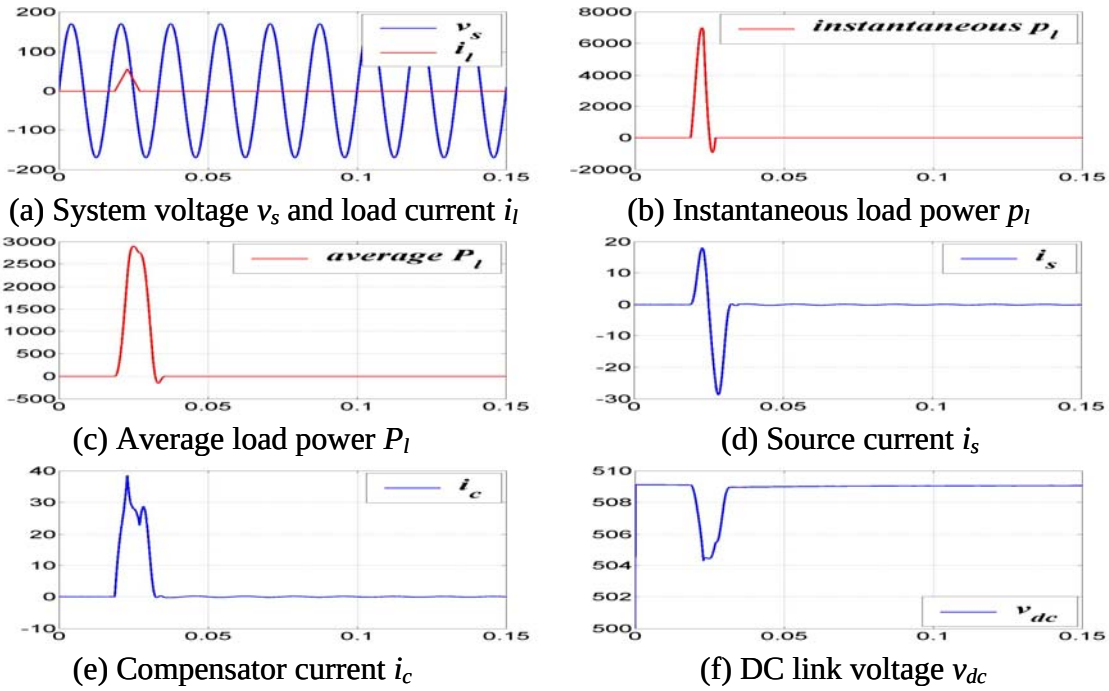

(a) System voltage v_s and load current i_l (b) Instantaneous load power p_l

(c) Average load power P_l (d) Source current i_s

(e) Compensator current i_c (f) DC link voltage v_{dc}

Figure 4.14. Simulation of single-phase pulse load, $T_c = T/2$.

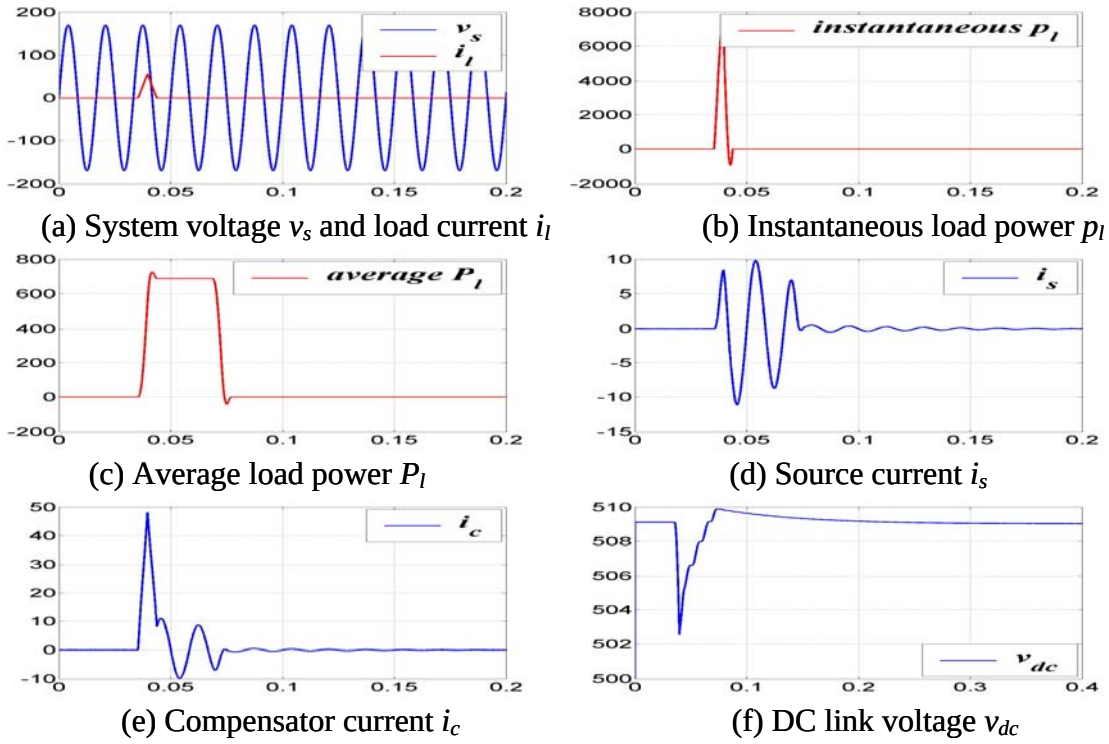

(a) System voltage v_s and load current i_l (b) Instantaneous load power p_l

(c) Average load power P_l (d) Source current i_s

(e) Compensator current i_c (f) DC link voltage v_{dc}

Figure 4.15. Simulation of single-phase pulse load, $T_c = 2T$.

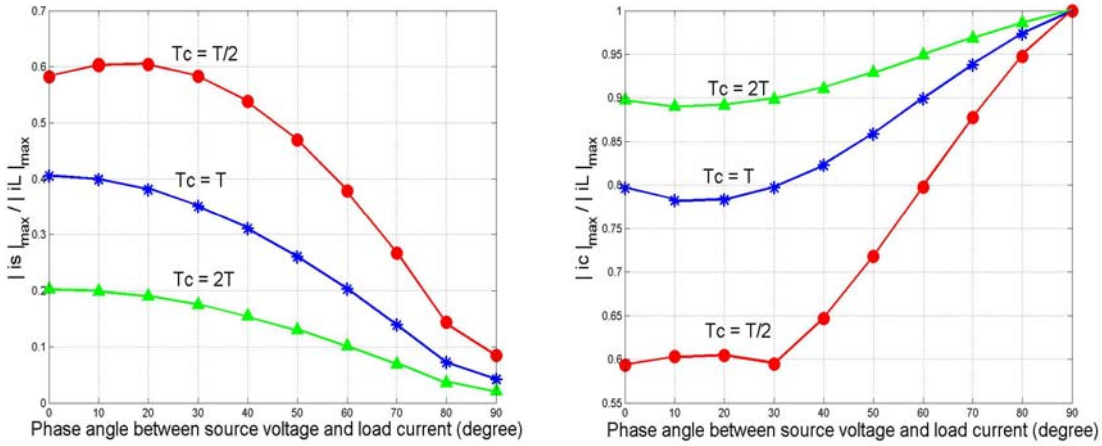

(a) Peak source current (b) Peak compensator current

Figure 4.16. Compensator current normalized with respect to load current for different compensation times and load current phase angles.

to 0.2 p.u. of the load current while i_c increases modestly from 0.6 to 0.9 p.u. of the load current.

If the phase angle between the source voltage and pulse current is small, which is common for many systems, a small increase in energy storage capacity will result in a much better compensation (i.e., much smaller source current). In the case of a large phase angle difference with a compensation period of $2T$, i_c increases 10% (from 0.9 to 1.0 p.u. of the load current); while in the case of a compensation period of $T/2$, i_c increases approximately 70% (from 0.6 to 1.0 p.u.). This is because if the compensator uses $T_c = 2T$, it must have a larger energy storage capacity (relative to choosing $T_c = T/2$) to accommodate not only a longer compensation interval, but also a larger instantaneous reactive component. Thus, a compensator with larger energy storage can provide better compensation and support a load that has a large reactive component.

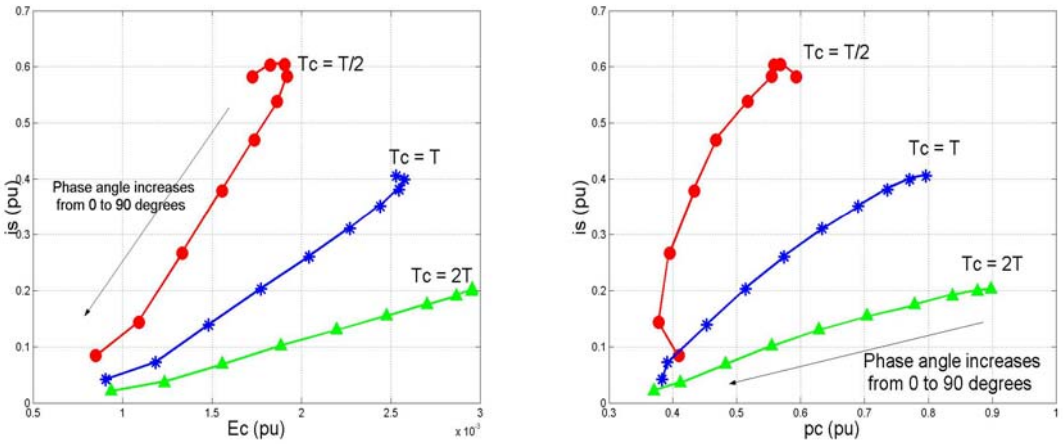

(a) Peak source current plotted as a function of the compensator's energy storage requirement

(b) Power requirement for different T_c and load current phase angles

Figure 4.17. Compensator energy storage requirement and power rating requirement.

Figure 4.17 shows the peak source current plotted as a function of the compensator's energy storage requirement and the instantaneous power requirement for various compensation times and load current phase angles. At longer averaging intervals, the power drawn from the source is distributed during T_c so that it has a smaller peak value instead of a short duration, high power pulse. The compensator's instantaneous power requirement is more concentrated so that a higher energy rating is required for short time durations. Over the complete compensation period, the compensator provides only reactive power and does not consume or generate any active power because the load energy is provided by the source. Thus, a trade-off between a smoother source current waveform with lower amplitude and the size of the compensator components must be considered when choosing the value of T_c.

4.3.4 Non-Periodic Load

Theoretically, the period T of a non-periodic load is infinite (a period much larger than the fundamental period of the utility). The nonactive components in a load cannot be completely compensated by choosing T_c as $T/2$ or T, or even several multiples of T. Figure 4.18a shows a three-phase non-periodic load current waveforms (red waveform) and the system voltage waveforms (blue waveform). Figure 4.18b shows the source currents after compensation, with $T_c = T/2$, $2T$, and $10T$, respectively. With $T_c = T/2$, there is still significant nonactive component in i_s with variable peak values and a non-sinusoidal waveform. With $T_c = 2T$, the variation of the amplitude of i_s is smaller, and with $T_c = 10T$, i_s is close to a sine wave with less nonactive component. A longer T_c "smoothes" the source current waveforms. Theoretically, i_s could be a pure sine wave if T_c goes to infinity, but in practice, such a T_c cannot be implemented nor is it necessary. If T_c is large enough, increasing T_c further will not typically improve the compensation results significantly. For example, in the case shown in Figure 4.18, the total harmonic distortion (THD) of i_s is 6% with $T_c = 2T$, and with $T_c = 10T$, the THD is only slightly smaller (4%). Typically, there is no need to increase T_c to a larger value as the small decrease in THD is often not worth the larger capital costs (higher ratings of the compensator components and therefore higher capital expenses).

4.4 Discussion

In nonactive power compensation, there are several factors which have significant influence on the choice of compensator type, the power rating of the compensator, the energy storage requirement of the compensator, and the compensation results. Some of

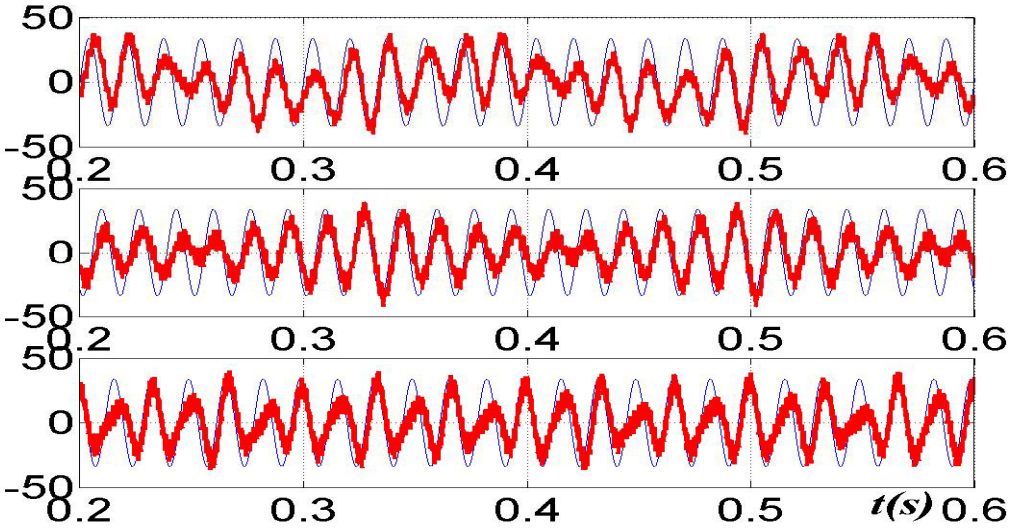

(a) Load current i_l and system voltage v_s

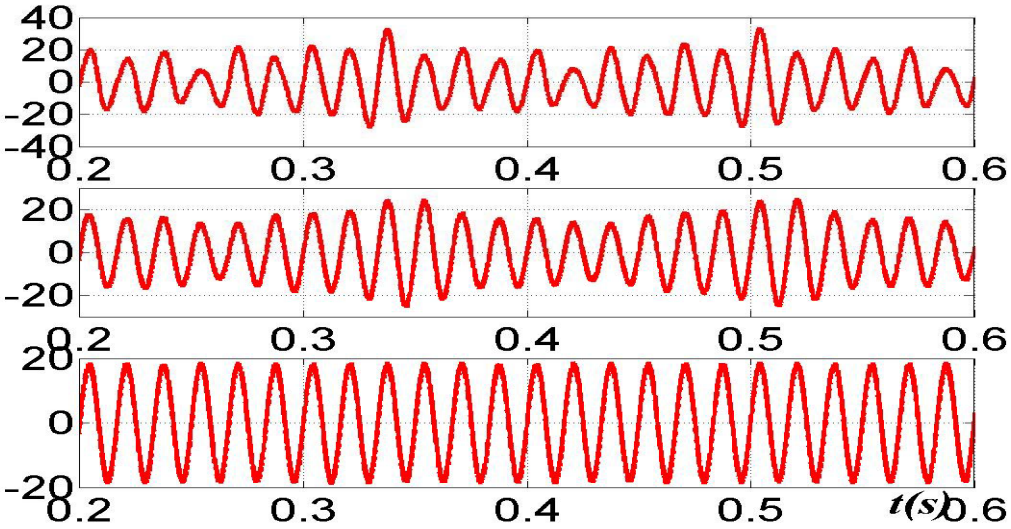

(b) Phase a of source current i_{sa} after compensation

$T_c = T/2$, $2T$, and $10T$

Figure 4.18. Simulation of non-periodic load compensation.

these factors are related to the nonactive power theory itself, which include the averaging interval T_c, and the reference voltage v_p, while others are practical issues related to the implementation of the compensation system. In this dissertation, the coupling inductance L_c, the power rating of the compensator, and the capacitance of the DC link have been taken into consideration.

4.4.1 Averaging Interval, T_c

If there are only harmonics in the load current, as in subsections 4.3.1.1 – 4.3.1.5, T_c does not change the compensation results as long as it is an integral multiple of $T/2$, where T is the fundamental period of the system. Here, the nonactive current is completely compensated, and a purely sinusoidal source current with a unity power factor is achieved.

However, in other cases, such as a three-phase load with sub-harmonics (see subsection 4.3.1.6), a single-phase pulse load (see subsection 4.3.3.2), or a non-periodic load (see subsection 4.3.4), T_c has significant influence on the compensation results, and the power and energy storage rating of the compensator's components. With longer T_c, a better source current will result, but at the cost of higher power rating for the switches and capacitance. There is a tradeoff between better compensation and higher system ratings (i.e., costs). On the other hand, a longer T_c does not necessarily yield a significantly better source current waveform. For a specific system, there is an appropriate T_c with which the compensation can be achieved. For example, in subsection 4.3.1.6, T_c depends on the frequency of the sub-harmonics.

4.4.2 DC Link Voltage v_{dc}

Generally, the compensator output voltage v_c is the sum of the system voltage and the voltage drop on the coupling inductor. The rms value of the required compensator output voltage V_c at the worst situation, i.e., all the nonactive components reach the peak value at the same time is

$$V_c = X_c I_c + V_s . \tag{4.41}$$

The compensator current I_c includes all the nonactive current components that are compensated, therefore, the reactance X_c has different values for nonactive components of different frequencies. The higher order harmonics will have larger voltage drop on the inductance. The required DC link voltage V_{dc} for a three-phase system is

$$V_{dc} = 2\sqrt{2}V_c . \tag{4.42}$$

The required DC link voltage V_{dc} for a single-phase system is

$$V_{dc} = \sqrt{2}V_c . \tag{4.43}$$

4.4.3 Coupling Inductance, L_c

The coupling inductance L_c between the power system and the compensator could be the inductance of a step-up transformer or a coupling reactor. It acts as the filter of the compensation current i_c, which has high ripple content due to the compensator's PWM control of the switches.

Generally a smaller L_c is preferred, because a large L_c requires a higher compensator output voltage, i.e., a higher DC link voltage. In practice, L_c is chosen so that the fundamental voltage drop on this inductor is 3% - 9% of the system voltage V_s. The inductance L_c is

$$L_c = (3\% - 9\%)\frac{V_s}{\omega I_c}. \tag{4.44}$$

4.4.4 DC Link Capacitance Rating, *C*

The DC link capacitance rating *C* is proportional to the maximum energy storage variation of the capacitor. According to the discussion in Section 3.1, the average power of the compensator $P_c(t)$ over T_c is zero. Energy is neither generated nor consumed by the compensator, therefore, the energy stored in the capacitor is a constant at rated DC link voltage V_{dc} given by

$$E_c = \frac{1}{2}CV_{dc}^{\ 2}. \tag{4.45}$$

However, the instantaneous power is not necessarily zero. The compensator generally has a capacitor for energy storage, and this capacitor operates in two modes, i.e., charge and discharge. Different capacitance values are required to fulfill different compensation tasks. The maximum energy variation in the capacitor is the integral of $v_s(t)i_c(t)$ between time t_{max} when the capacitor goes from discharge to charge, and t_{min} when the capacitor goes from charge to discharge, or vice versa.

$$\Delta E_c = \int_{t_{\min}}^{t_{\max}} \boldsymbol{v}_s^{\boldsymbol{T}}(t)\boldsymbol{i}_c(t)dt\ . \tag{4.46}$$

The energy variation on the DC link capacitor causes the voltage variation, that is

$$\Delta E_c = E_c(t_{\max}) - E_c(t_{\min}) = \frac{1}{2}C(V_{dc}^2(t_{\max}) - V_{dc}^2(t_{\min}))\,. \tag{4.47}$$

The required DC link capacitance *C* is

$$C = \frac{2\Delta E_c}{V_{dc}^2(t_{\max}) - V_{dc}^2(t_{\min})} = \frac{2\int_{t_{\min}}^{t_{\max}} \boldsymbol{v}_s^T(t)\boldsymbol{i}_c(t)dt}{V_{dc}^2(t_{\max}) - V_{dc}^2(t_{\min})}. \quad (4.48)$$

For different applications, the energy variation ΔE_c is different, which determines the capacitance rating, for a given DC link voltage variation. In a three-phase *RL* load case, because the instantaneous nonactive power is zero at all times, the current flowing into or out of the DC link capacitor is zero. Therefore, a small capacitor can meet the requirement of this case. A large energy storage variation happens when the load is unbalanced, or there is a sudden load change, or a single-phase system, and a large capacitance is required.

4.5 Summary

The generalized nonactive power theory was implemented in a shunt compensation system, which was configured to perform the nonactive power compensation for a three-phase four-wire system. The current that the compensator was required to provide was calculated based on the generalized nonactive power theory presented in Chapter 3. A control scheme was developed to regulate the DC link voltage of the inverter, and to generate the switching signals for the inverter based on the required nonactive current.

The compensation system was simulated, and different cases were studied. The simulation results showed that the generalized nonactive power theory proposed in this dissertation was applicable to the nonactive power compensation in three-phase four-wire systems, single-phase systems, load currents with harmonics, and non-periodic load currents. This theory was adapted to different compensation objectives by changing the

reference voltage $\boldsymbol{v_p}(t)$ and the averaging interval T_c. The practical issues such as the DC capacitance rating, the DC link voltage, and the coupling inductance were also discussed.

CHAPTER 5

Experimental Verification

In the previous chapter, the generalized nonactive power theory was implemented in a parallel nonactive power compensator, and different cases were simulated. A compensator experimental setup was built, which is described in this chapter. Four different types of load, a three-phase balanced *RL* load, a three-phase diode rectifier load, a three-phase unbalanced *RL* load, and a single-phase load are tested. The experimental results are analyzed, and the generalized instantaneous nonactive power theory is verified.

The experimental system configuration and the equipment will be shown in subsection 5.1, and the experimental results are elaborated and analyzed in subsection 5.2. Subsection 5.3 contains conclusions and summary of this chapter.

5.1 System Configuration

The system configuration simulated in Chapter 4 is adopted in the experimental system, as shown in Figure 5.1. The actual power components are used in the experiments, while the calculation and control is performed in Simulink.

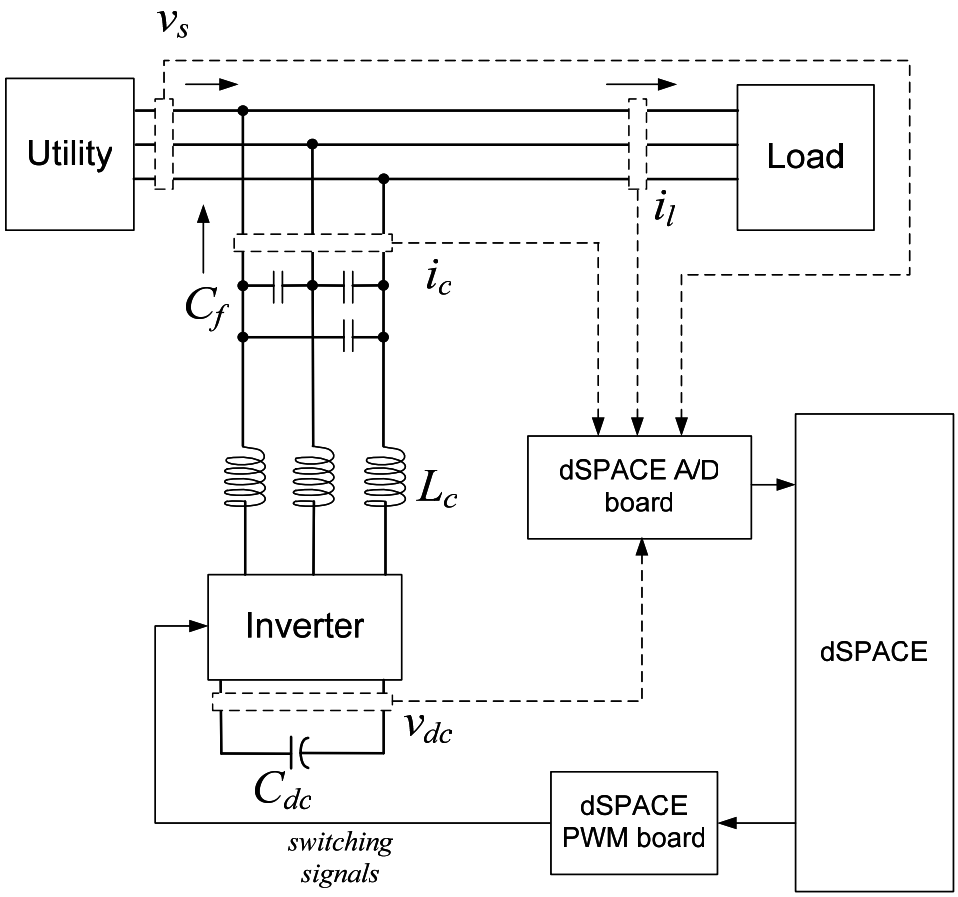

Figure 5.1. Experimental configuration of the nonactive power compensator.

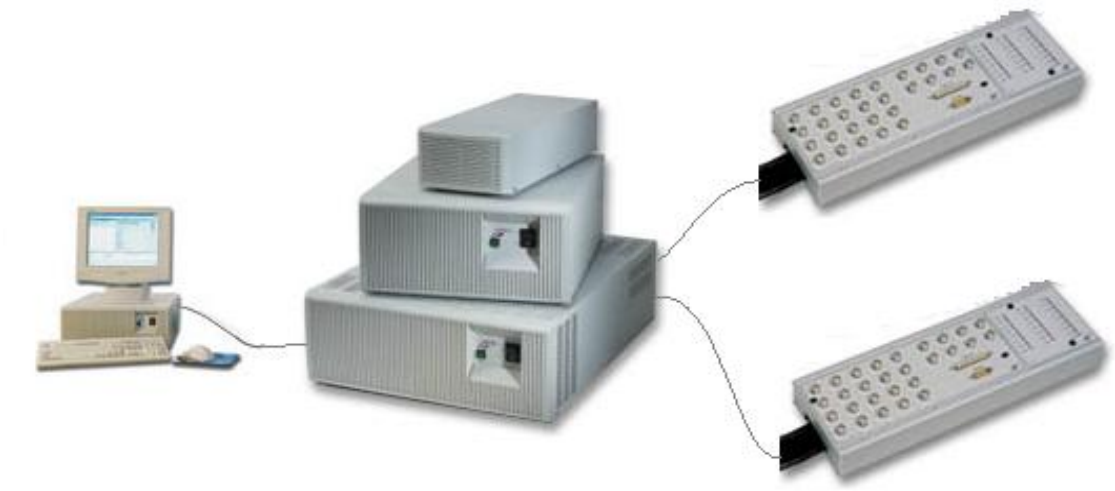

Host PC Expansion box panels

Figure 5.2. dSPACE system configuration.

5.1.1 dSPACE System

dSPACE, a real-time control platform, is used to implement the Simulink controller on hardware to perform the real-time control of the nonactive power compensator. In this experiment, as shown in Figure 5.2, the dSPACE system uses a personal computer (PC) as the host computer. An expansion box is connected to the host computer via an optical fiber. Two panels are connected to the expansion box, one is an analog-to-digital board, and the other is a PWM signal output board. The voltages and currents are measured by voltage potential transducers (PTs) and current transducers (CTs), and the measurement signals are input to the analog-to-digital board, where these analog signals are converted to digital signals for calculation and control purposes. The PWM gate signals used to control the inverter switches are generated and output from the dSPACE PWM output board.

The control system of the parallel nonactive power compensator consists of two parts, i.e., MATLAB/Simulink and dSPACE. MATLAB is a platform for numeric calculations, analysis, and visualization. Simulink is an interactive environment for modeling and offline simulation with block diagrams. The state diagrams in Simulink can be integrated with Stateflow and Real-Time Workshop to automatically generate C code from Simulink block diagrams and Stateflow systems. Together with dSPACE's Real-Time Interface, these tools provide a seamless transition from a block diagram to dSPACE's real-time hardware.

The compensation is operating in a high EMI environment mainly because of the inverter switching on and off high voltage and/or high current. The measurement devices and the control system are vulnerable to the high EMI, and errors are introduced to the system. The inverter was put into a metal box to isolate the strong EMI source from other equipment. Some filtering capacitors are used in the compensation system to mitigate the ripple in the compensator current.

A picture of the experiment setup is shown in Figure 5.3. The components of the setup will be presented in the following subsections.

5.1.2 The Utility

The utility is a three-phase, four-wire power system. In the simulations presented in Section 4.3.1, the system voltage is highly distorted, which will not be the case in the experiments, since the voltage distortion in the real power system is fairly small.

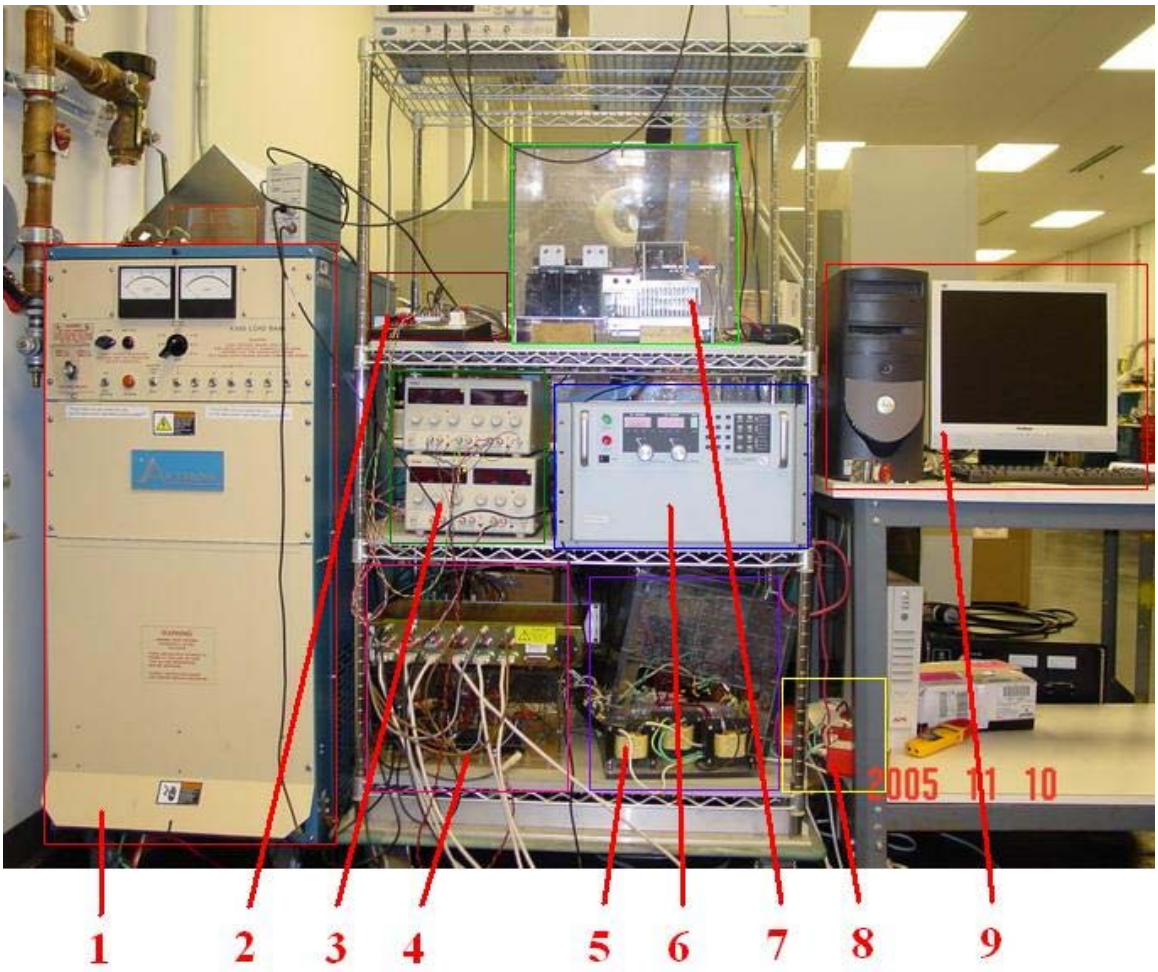

1. Resistor load bank
2. Interface of dSPACE and the inverter
3. Power supplies for the interface and the inverter drive board
4. Voltage transducers
5. Coupling inductors and load inductors
6. DC power supply
7. Inverter
8. Current transducers
9. dSPACE host PC

Figure 5.3. Experiment setup of the nonactive power compensation system.

Table 5.1. Ratings of the commercial inverter.

DC link voltage	800 V
DC link capacitance	3300 μF
IGBT current	75 A
Switching frequency	20 kHz

5.1.3 Loads

A three-phase balanced *RL* load, a three-phase diode rectifier load, a three-phase unbalanced *RL* load, and a single-phase load will be tested to verify the validity of the nonactive power theory. A three-phase diode rectifier is a typical nonlinear load which draws a highly-distorted current consisting of a fundamental component and high-order harmonics.

5.1.4 Inverter

A Powerex POW-R-PAK^{TM} configurable IGBT based 3-phase inverter is used in the experiment. The topology of the inverter is the same as shown in Figure 2.2. The ratings of this inverter are shown in Table 5.1.

In Figure 5.3, the DC power supply is used to charge the DC link capacitor to the rating value. When the compensator is operating, the DC power supply is switched off. The compensator does not use a power source and the DC link voltage is self-regulated by obtaining active power from the utility source.

An interface is needed to convert the PWM output signals from the dSPACE, which are 5V; to 15V PWM signals to drive the switch gate drives on the inverter. An interface was built, and its schematic is shown in Figure 5.4.

Three capacitors C_f are connected between phases between the coupling inductors and the PCC, as shown in Figure 5.1. These capacitors filter the ripple in the compensator current. Table 5.2 is a list of the components in the experimental setup, and their ratings are also shown.

5.2 Experimental Results

In the chosen set of experiments, the nonactive current required by the load is provided by the compensator so that the source only needs to provide active power.

In the experiments, as explained in Chapter 4 (see Figure 4.4), the three-phase current produced by the compensator is given by

$$\boldsymbol{i}_{\boldsymbol{c}}^{*}(t) = \boldsymbol{i}_{\boldsymbol{cn}}^{*}(t) + \boldsymbol{i}_{\boldsymbol{ca}}^{*}(t)\,. \tag{5.1}$$

Recall that

$$\boldsymbol{i}_{\boldsymbol{ca}}^{*}(t) = \boldsymbol{v}_{\boldsymbol{s}}(t)[K_{P1}(V_{\boldsymbol{dc}}^{*} - v_{dc}) + K_{I1}\int_{0}^{t}(V_{\boldsymbol{dc}}^{*} - v_{dc})dt]\,, \tag{5.2}$$

where $\boldsymbol{v}_{\boldsymbol{s}}(t) = [v_{sa}(t),\ v_{sb}(t),\ v_{sc}(t)]^T$ is the three-phase system voltage. This is the current required to keep the compensator capacitor charged against losses in the compensator.

Also, recall that $\boldsymbol{i}_{\boldsymbol{cn}}^{*}$ is specified as

$$\boldsymbol{i}_{\boldsymbol{cn}}^{*}(t) = \boldsymbol{i}_{\boldsymbol{l}}(t) - \boldsymbol{i}_{\boldsymbol{s}}(t)\,, \tag{5.3}$$

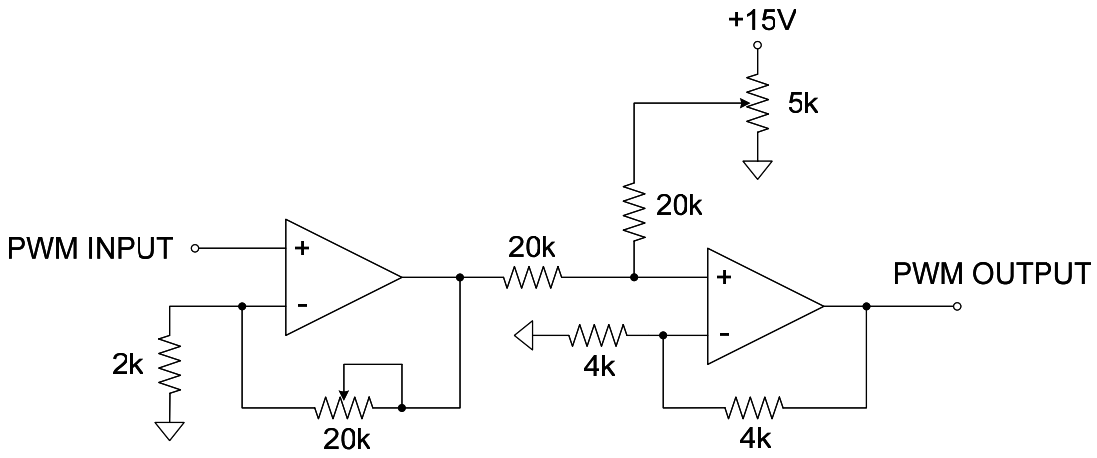

Figure 5.4. Schematic of the interface between dSPACE and the inverter.

Table 5.2. Components of the nonactive power compensation system.

Device	**Manufacturer /model**	**Ratings**	
Inverter	Powerex POW-R-PAK™ PP75T120	Current (A)	DC voltage (V)
		75	800
Three-phase resistor bank	Avtron K595	Power (kW)	Line-to-line voltage (V)
		55.5	250/500
Load inductor	Triad-Utrad C-59U	Inductance (mH)	Current (A)
		10	12.5 DC
Coupling inductor	Amveco L1510	Inductance (mH)	Current (A)
		10	15 DC
Voltage transducer	LEM CV 3-500	Primary voltage (V)	Bandwidth
		500	DC to 300 kHz
Current transducer	Danfysik ULTRASTAB® 866	Primary current (A)	Bandwidth
		600	DC to 100 kHz
DC power supply	Magna-power	Current (A)	DC voltage (V)
		10	800

$$\boldsymbol{i}_s(t) = \begin{bmatrix} i_{sa}(t) \\ i_{sb}(t) \\ i_{sc}(t) \end{bmatrix} = \frac{P(t)}{V_p^2(t)} \begin{bmatrix} v_{pa}(t) \\ v_{pb}(t) \\ v_{pc}(t) \end{bmatrix}, \tag{5.4}$$

$$P(t) = \frac{1}{T_c} \int_{t-T_c}^{t} p(\tau) d\tau \,, \tag{5.5}$$

$$p(t) = v_{sa}(t) i_{la}(t) + v_{sb}(t) i_{lb}(t) + v_{sc}(t) i_{lc}(t) \,, \tag{5.6}$$

and

$$V_p(t) = \sqrt{\frac{1}{T_c} \int_{t-T_c}^{t} \boldsymbol{v}_p^T(\tau) \boldsymbol{v}_p(\tau) d\tau} \,. \tag{5.7}$$

where, in all the experiments, $\boldsymbol{v}_p(t) = \boldsymbol{v}_s(t)$.

The control diagram of the experimental setup is shown in Figure 5.5. Table 5.3 lists the parameters that do not change throughout the experiments. Other parameters that do change with the experiments will be listed in each experiment.

5.2.1 Three-Phase Balanced *RL* Load

A three-phase balanced *RL* load compensation is performed under the conditions listed in Table 5.4. The three phase system voltage waveforms $[v_{sa}(t), v_{sb}(t), v_{sc}(t)]^T$ are shown in Figure 5.6a. The load current waveforms $[i_{la}(t), i_{lb}(t), i_{lc}(t)]^T$ are plotted in Figure 5.6b, together with the phase *a* system voltage $v_{sa}(t)$, to show the phase angle between the system voltage and the load current. The load current lags the system voltage in a *RL* load.

Figure 5.6c shows the source current $\boldsymbol{i}_s(t)$ after compensation, together with phase *a* voltage. The amplitude of the source current is smaller than the load current, and the

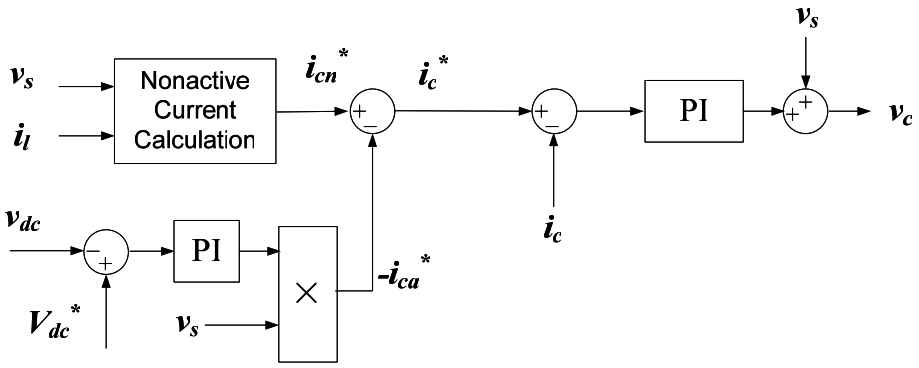

Figure 5.5. Control diagram of the experimental setup.

Table 5.3. Parameters of the experiments.

System voltage (line-to-neutral rms)	120 V
System frequency $f = 1/T$	60 Hz
Coupling inductance	10 mH
DC link capacitance	3300 μF
Control stepsize	80 μs
Switching frequency	12.5 kHz
DC link voltage PI controller	KP = 0.2, KI = 0

Table 5.4. Parameters of the three-phase balanced *RL* load compensation.

Load resistance	10.8 Ω
Load inductance	20 mH
DC link voltage	400 V
Averaging interval T_c	$T/2$
Nonactive current PI controller	KP = 40, KI = 0

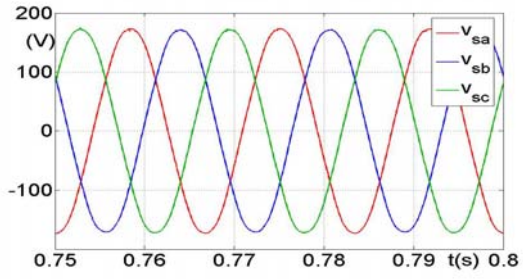

(a) System voltage $\boldsymbol{v_s}(t)$

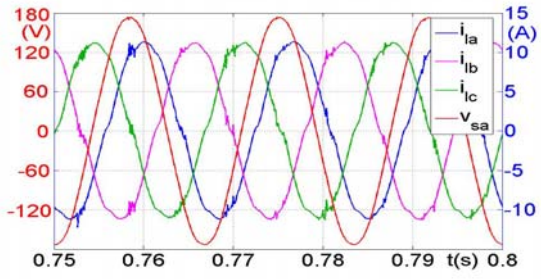

(b) Load current $\boldsymbol{i_l}(t)$

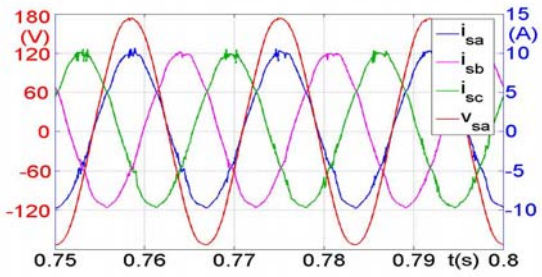

(c) Source current $\boldsymbol{i_s}(t)$

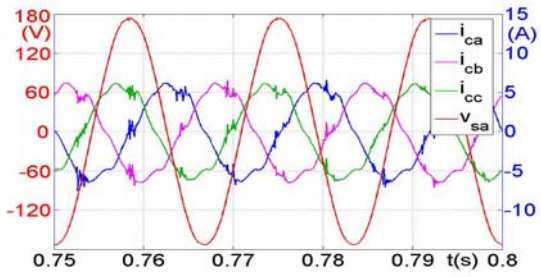

(d) Compensator current $\boldsymbol{i_c}(t)$

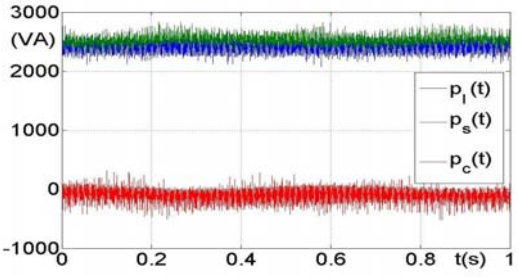

(e) Instantaneous powers

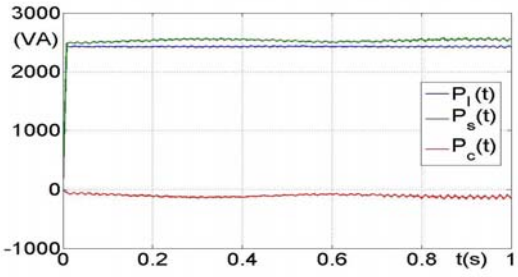

(f) Average powers

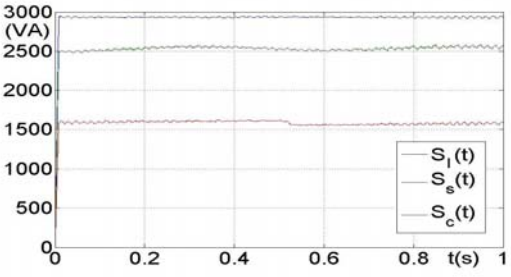

(g) Apparent powers

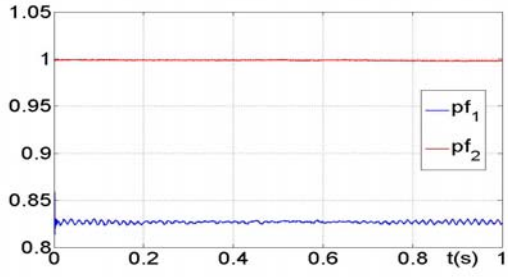

(h) power factors

Figure 5.6. Three-phase balanced *RL* load compensation.

Table 5.5. Powers of the three-phase balanced *RL* load compensation.

Theoretical powers (VA)		Experimental powers (VA)	
Average power $P(t)$	2426	Average load power $P_l(t)$	2426
Average active power $P_a(t)$	2426	Average source power $P_s(t)$	2533
Average nonactive power $P_n(t)$	0	Average compensator power $P_c(t)$	-107
Apparent power $S(t)$	2933	Apparent load power $S_l(t)$	2934
Apparent active power $P_p(t)$	2426	Apparent source power $S_s(t)$	2537
Apparent nonactive power $Q(t)$	1649	Apparent compensator power $S_c(t)$	1584

source current is in phase with the system voltage. The compensator current $\boldsymbol{i}_c(t)$ is illustrated in Figure 5.6d. This current, which is about 90º out of phase with the system voltage, contains mostly nonactive current.

To further analyze the compensation results, the instantaneous powers (instantaneous power $p(t)$, instantaneous active power $p_a(t)$, and instantaneous nonactive power $p_n(t)$), the average powers (average power $P(t)$, average active power $P_a(t)$, and average nonactive power $P_n(t)$), and the apparent powers (apparent power $S(t)$, apparent active power $P_p(t)$, and apparent nonactive $Q(t)$) are calculated based on the system voltage and the load current. The average powers and apparent powers are shown in the second column in Table 5.5. $P(t) = P_a(t) = P_p(t)$, $P_n(t) = 0$, and $S^2(t) = P_p^2(t) + Q^2(t)$. They are consistent with the discussion in Chapter 3.

The powers of the experimental results are listed in the fourth column of Table 5.5. The instantaneous load power is

$$p_l(t) = \boldsymbol{v}_s^T(t)\boldsymbol{i}_l(t)\,. \tag{5.7}$$

The instantaneous source power is

$$p_s(t) = \boldsymbol{v}_s^T(t)\boldsymbol{i}_s(t)\,. \tag{5.8}$$

The instantaneous compensator power is

$$p_c(t) = \boldsymbol{v}_s^T(t)\boldsymbol{i}_c(t)\,. \tag{5.9}$$

The average load power is

$$P_l(t) = \frac{1}{T_c}\int_{t-T_c}^{t} \boldsymbol{v}_s^T(\tau)\boldsymbol{i}_l(\tau)d\tau\,. \tag{5.10}$$

The average source power is

$$P_s(t) = \frac{1}{T_c}\int_{t-T_c}^{t} \boldsymbol{v}_s^T(\tau)\boldsymbol{i}_s(\tau)d\tau\,. \tag{5.11}$$

The average compensator power is

$$P_c(t) = \frac{1}{T_c}\int_{t-T_c}^{t} \boldsymbol{v}_s^T(\tau)\boldsymbol{i}_c(\tau)d\tau\,. \tag{5.12}$$

The apparent load power is

$$S_l(t) = V_s(t)I_l(t)\,. \tag{5.13}$$

The apparent source power is

$$S_s(t) = V_s(t)I_s(t)\,. \tag{5.14}$$

And the apparent compensator power is

$$S_c(t) = V_s(t)I_c(t)\,. \tag{5.15}$$

The instantaneous load power $p_l(t)$, instantaneous source power $p_s(t)$, and the instantaneous compensator power $p_c(t)$ are shown in Figure 5.6e. According to the

analysis in Chapter 3 (Table 3.2), the instantaneous active power is equal to the instantaneous power, and the instantaneous nonactive power is zero (see the instantaneous powers in the first and second columns of Table 5.5). In Figure 5.6e, the instantaneous source power is slightly larger than the instantaneous load power, and the instantaneous compensator power is negative. This is because the compensator draws a small amount of active current from the utility to meet the losses. Therefore, the compensator current contains a small amount of active current, and the instantaneous compensator power contains a small amount of active power component. The average load power $P_l(t)$, average source power $P_s(t)$, and the average compensator power $P_c(t)$ are shown in Figure 5.6f. They have similar characteristics as the instantaneous powers except that these waveforms are smoother.

The apparent load power $S_l(t)$, apparent source power $S_s(t)$, and the apparent compensator power $S_c(t)$ are shown in Figure 5.6g. Theoretically, these nine powers are all constant (Table 3.2). The average values of the waveforms in Figures 5.6f and 5.5g are calculated and listed in the fourth column of Table 5.5. The difference between the second column and the fourth column of Table 5.5 is mainly because of the DC link voltage regulation which is not considered in the generalized nonactive power theory. In the experiment, instead of zero, the compensator power has some active power component drawn from the utility.

Figure 5.6h shows the power factors before and after compensation. pf_1 is the power factor before the compensation, which is $P(t)/S(t) = 0.8269$; after compensation, the power factor of the source current (pf_2) is $P_a(t)/P_p(t) = 0.9984$. Therefore, the nonactive power compensator can improve the load power factor to nearly unity power factor.

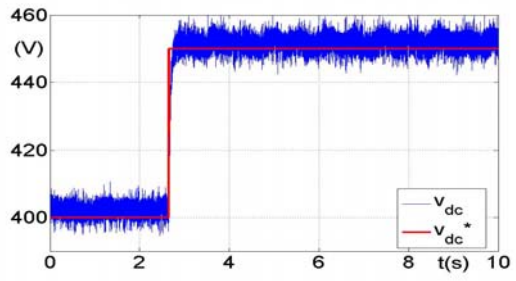

(a) DC link voltage change

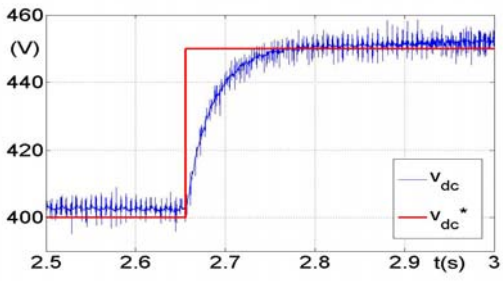

(b) DC link voltage change (short period)

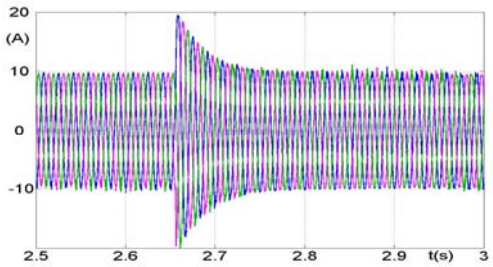

(c) Source current $\boldsymbol{i}_s(t)$

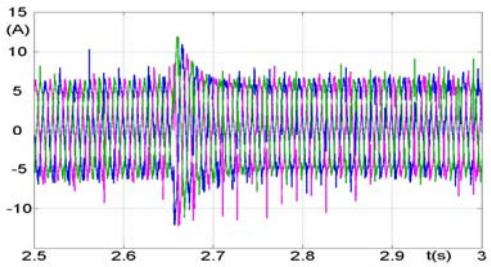

(d) Compensator current $\boldsymbol{i}_c(t)$

Figure 5.7. Regulation of DC link voltage in three-phase balanced *RL* load compensation.

Figure 5.7 shows the DC link voltage control. In Figure 5.7a, the red waveform is the reference DC voltage, which is 400V at the beginning, and a step change is made to the reference to 450V at t = 2.66s. The blue waveform is the actual DC link voltage measured by the PT. Figure 5.7b is a short period around the step change. To regulate the DC voltage from 400V to 450V, the compensator draws a larger amount of active current than usual to charge the capacitor. This is controlled by the DC link voltage PI controller. The dynamic process of the source current and the compensator current are shown in Figures 5.7c and 5.7d. Because of the constraints of the system, for instance, the current and/or power ratings of the components in the compensator, only a limited current can be drawn from the utility, which causes the actual DC link voltage to reach the new

reference value in about 0.1s. A higher current rating would allow a faster dynamic response.

5.2.2 Three-Phase Unbalanced *RL* Load

For this test, the inductors of the *RL* load are not equal in each phase, therefore, the three phase load currents are not balanced any more, as shown in Figure 5.8b. The load inductors are 30mH, 10mH, and 10mH, respectively. The DC link voltage is 450V. Other parameters are listed in Table 5.6. The three phase system voltages are balanced, which is shown in Figure 5.8a. The rms values of the three phase load current is shown in the second column of Table 5.7. Figure 5.8c shows the source currents after compensation, which are nearly balanced compared to the load current. The compensation current is shown in Figure 5.8d. The three phase source current rms values are listed in the third column of Table 5.7. The unbalance of the three-phase currents is calculated as

$$I_{unbalance} = \frac{\max\{|I_a - I_b|, |I_b - I_c|, |I_c - I_a|\}}{Avg(I_a, I_b, I_c)}, \tag{5.16}$$

where

$$Avg(I_a, I_b, I_c) = (I_a + I_b + I_c)/3. \tag{5.17}$$

The unbalance of the load current is 38.97%, and the unbalance of the source current is improved to 4.92% after compensation.

5.2.3 Sudden Load Change and Dynamic Response

In this case, a sudden change is applied to the three-phase *RL* load to test the dynamic response of the nonactive power compensator. The parameters are listed in Table 5.8. The waveforms in Figure 5.9a are the three phase system voltage. In Figure 5.9b, the load

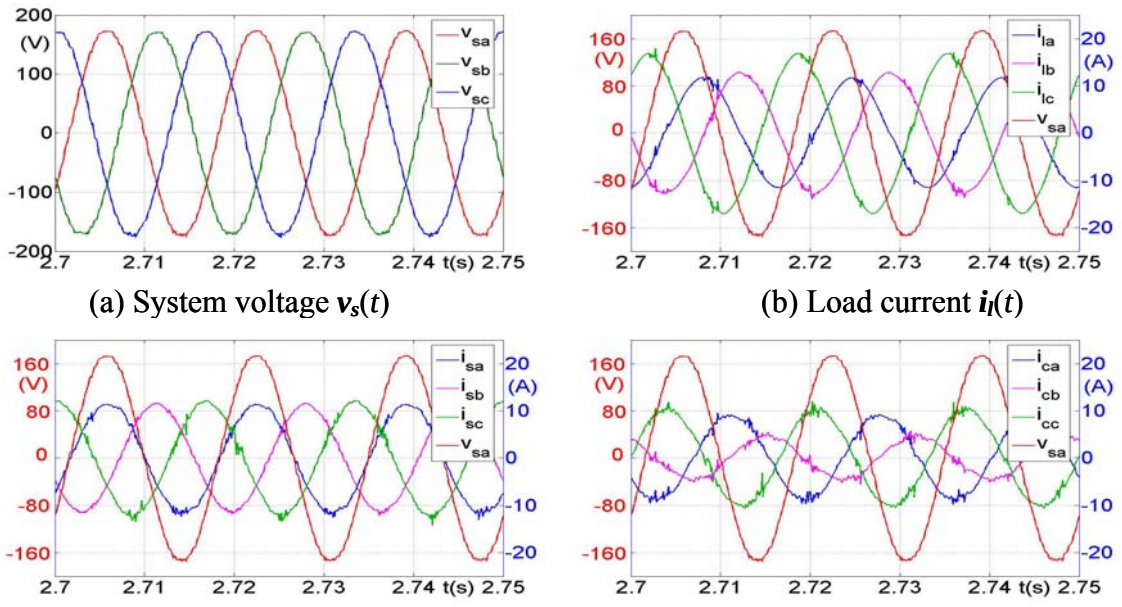

(a) System voltage $\boldsymbol{v_s}(t)$ (b) Load current $\boldsymbol{i_l}(t)$

(c) Source current $\boldsymbol{i_s}(t)$ (d) Compensation current $\boldsymbol{i_c}(t)$

Figure 5.8. Three-phase unbalanced *RL* load compensation.

Table 5.6. Parameters of the three-phase unbalanced *RL* load compensation.

Load resistance	10.8 Ω
Load inductance	30, 10, 10 mH
DC link voltage	450 V
Averaging interval T_c	$T/2$
Nonactive current PI controller	KP = 40, KI = 0

Table 5.7. RMS current values of the unbalanced load compensation.

	I_l (A)	I_s (A)
Phase *a*	8.06	8.11
Phase *b*	9.00	7.95
Phase *c*	11.81	8.35
$I_{unbalance}$	38.97%	4.92%

Table 5.8. Parameters of the three-phase sudden load change compensation.

Load resistance	10.8 Ω
Load inductance	20 mH
DC link voltage	400 V
Averaging interval T_c	$5T$
Nonactive current PI controller	KP = 40, KI = 0

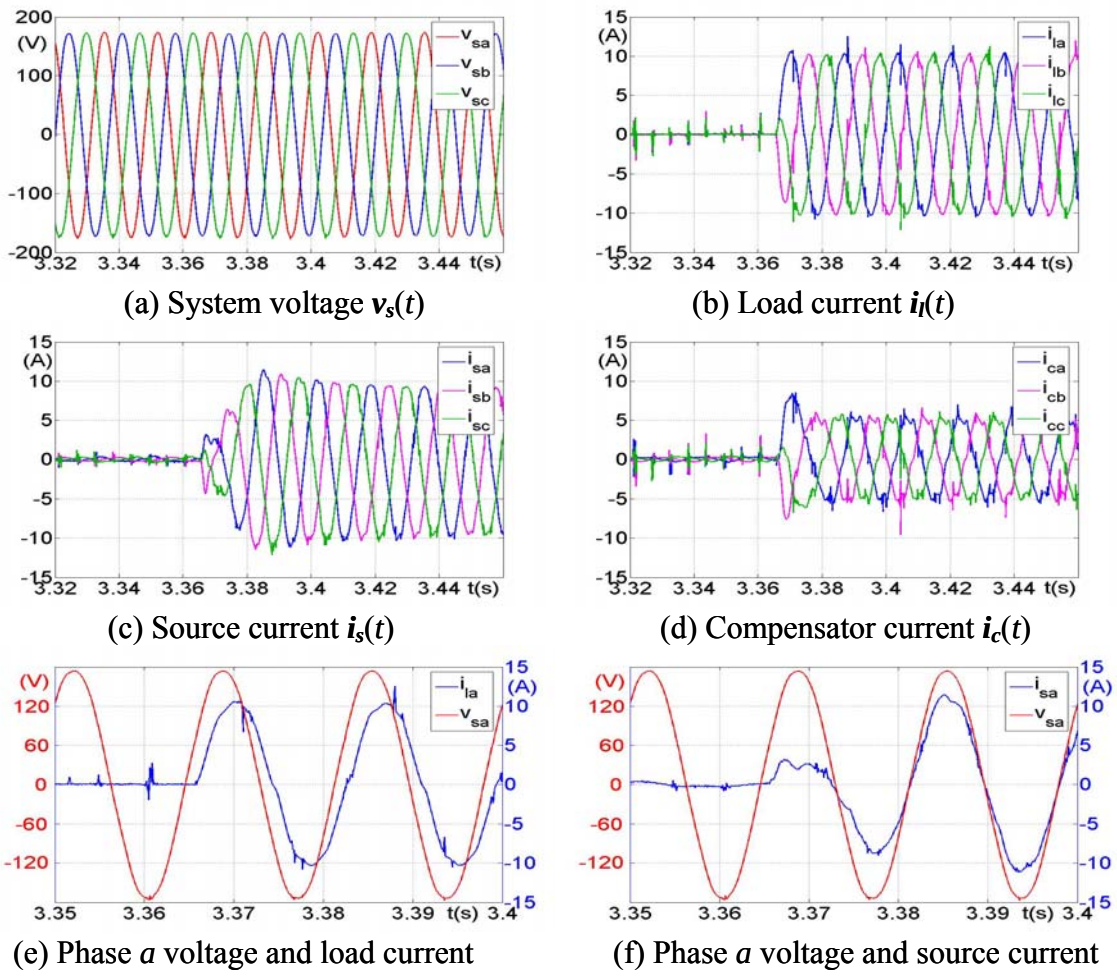

(a) System voltage $\boldsymbol{v_s}(t)$ (b) Load current $\boldsymbol{i_l}(t)$

(c) Source current $\boldsymbol{i_s}(t)$ (d) Compensator current $\boldsymbol{i_c}(t)$

(e) Phase *a* voltage and load current (f) Phase *a* voltage and source current

Figure 5.9. Dynamic response of three-phase *RL* load compensation.

current is zero at the beginning, and it is changed to 10A (peak value) at t = 3.366s. The source current and compensator current are shown in Figures 5.9c and 5.9d, respectively. There is a transient in both the source current and the compensator current. There are two factors that influence the dynamic response of the nonactive compensation, one is the averaging interval T_c, and the other one is the DC link voltage regulation. In this case, T_c = 5T, therefore, the source current slowly increases from zero to the steady-state value. Before the source current reaches the steady state, it increases to a maximum value and then decreases to the steady state value, this is because of the DC link voltage regulation, which draws some active current to regulate the DC link voltage. For a faster dynamic response, a shorter T_c is preferred. Figures 5.9e and 5.9f are the phase *a* load current and source current with the system voltage, to show the phase angle between the voltage and the current. The load current lags the voltage, while the source current is in phase with the voltage; therefore, a unity power factor is achieved.

5.2.4 Three-Phase Diode Rectifier Load

A three-phase diode rectifier load is a typical nonlinear load in the power system. The topology of a three-phase diode rectifier is shown in Figure 5.10a, and the typical load currents are shown in Figure 5.10b. A resistive load is used on the DC side of the rectifier. The parameters are shown in Table 5.9. The DC link voltage is set to 500V. The measured load current is shown in Figure 5.11b, which is highly distorted. Figures 5.11c and 5.11d show the source current and compensator current when the DC link voltage is 500V. The source current is still distorted, which is mainly because of the large *di/dt* in the load current. As discussed in Chapter 4, a large *di/dt* requires a large DC link voltage for full compensation, i.e., a large inverter output voltage, so that the compensator can

Table 5.9. Parameters of the three-phase rectifier compensation.

DC link voltage	500, 600, 700 V
Averaging interval T_c	$T/2$
Nonactive current PI controller	KP = 60, 100, 120, KI = 0

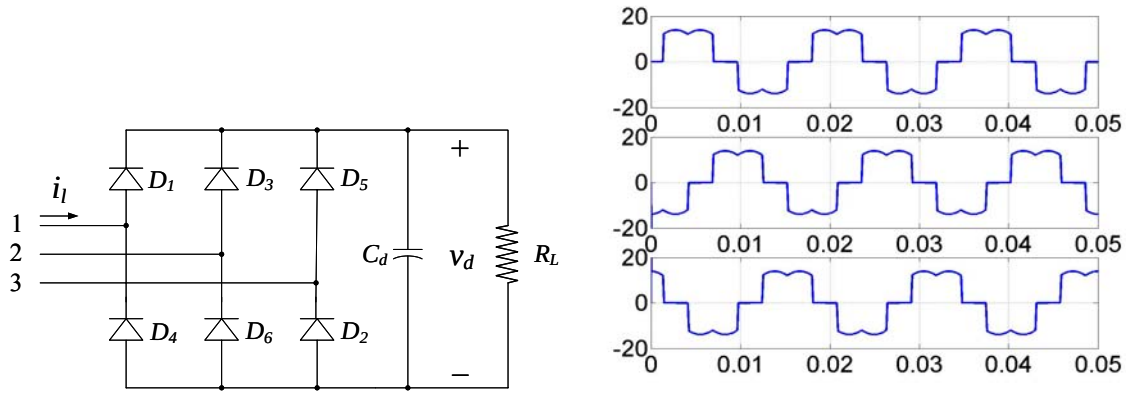

(a) Three-phase diode rectifier (b) Current waveforms of a diode rectifier

Figure 5.10. A three-phase diode rectifier load.

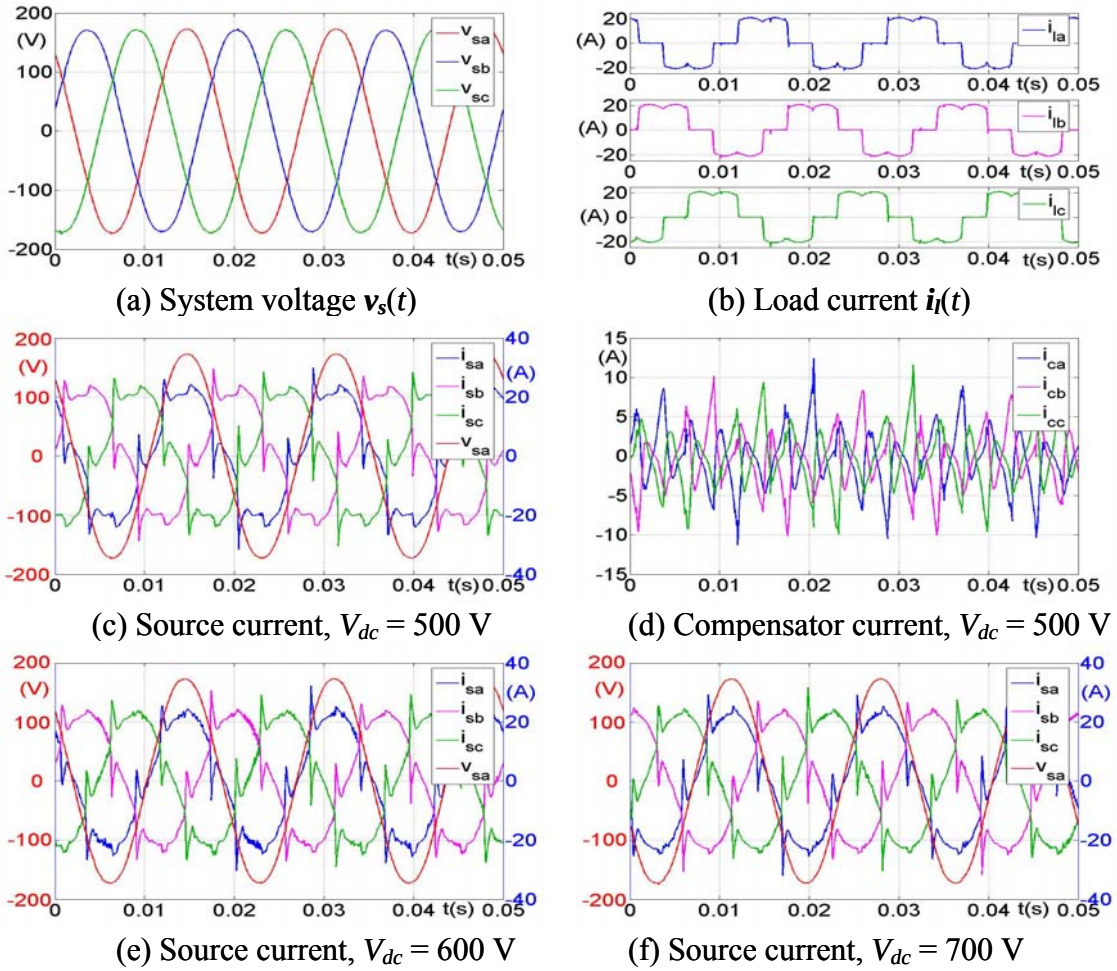

(a) System voltage $\boldsymbol{v}_s(t)$ (b) Load current $\boldsymbol{i}_l(t)$

(c) Source current, V_{dc} = 500 V (d) Compensator current, V_{dc} = 500 V

(e) Source current, V_{dc} = 600 V (f) Source current, V_{dc} = 700 V

Figure 5.11. Diode rectifier load compensation.

Table 5.10. THD of the currents in the rectifier load compensation.

	V_{dc} = 500V		V_{dc} = 600V		V_{dc} = 700V	
	THD of i_l (%)	THD of i_s (%)	THD of i_l (%)	THD of i_s (%)	THD of i_l (%)	THD of i_s (%)
phase *a*	29.90	25.40	30.19	21.55	30.07	18.51
phase *b*	29.96	25.40	30.09	21.28	30.76	19.29
phase *c*	29.96	25.17	30.38	20.90	30.02	18.73
average	29.94	25.32	30.22	21.24	30.28	18.84

inject a large amount of current in a very short period. However, it is often not practical to have very high DC link voltage. Increasing the DC link voltage to 600V and 700V, the resulting source currents are shown in Figures 5.11e and 5.11f, respectively. The red sinusoidal waveforms in these figures are the phase *a* voltage, to show that the currents are in phase with the voltage. By increasing the DC link voltage from 500V to 600V and then 700V, the waveforms of the source current are improving, i.e., closer to a sinusoid.

Table 5.10 lists the THD of the load currents and source currents in the three cases. The THD of the load current is about 30%. The THD of the source current is 25.32% (average value of the three phases) when the DC link voltage is 500V, and it decreases to 21.24% and 18.84% when the DC link voltage is 600V and 700V, respectively.

5.2.5 Single-Phase Load

An *RL* load is connected between phase *a* and phase *b* in the three-phase system while phase *c* is left open (unloaded). The resistor is 29.2Ω, and the inductor is 10mH. The DC link voltage is 500V. Other parameters are shown in Table 5.11. The voltage and

Table 5.11. Parameters of the single-phase *RL* load compensation.

Load resistance	29.2 Ω
Load inductance	10 mH
DC link voltage	500 V
Averaging interval T_c	$T/2$
Nonactive current PI controller	KP = 40, KI = 0

the load current are shown in Figures 5.12a and 5.12b, respectively. The load current in phase *a* and phase *b* are equal in magnitude and opposite in phase, and the current in phase *c* is zero. The rms values of the three phase load currents are listed in the second column of Table 5.12. The rms value of the phase *c* load current is slightly more than zero because of the measurement error as a result of IGBT switching. The source current and the compensator current are shown in Figures 5.12c and 5.12d, respectively. The magnitudes of phase *a* and phase *b* source currents are reduced and there is a current in phase *c*. The rms values of the three phase source currents are shown in the third column of Table 5.12. The values of phase *a* and phase *b* are reduced and the three phases are more balanced after compensation.

5.3 Conclusions and Summary

The generalized nonactive power theory proposed in this dissertation is implemented in a parallel nonactive power compensation system. A three-phase balanced *RL* load, a three-phase unbalanced *RL* load, a three-phase diode rectifier load, and a single-phase *RL* load are tested. The experimental results verify that the generalized nonactive power theory is suitable for parallel nonactive compensation. The experimental results are

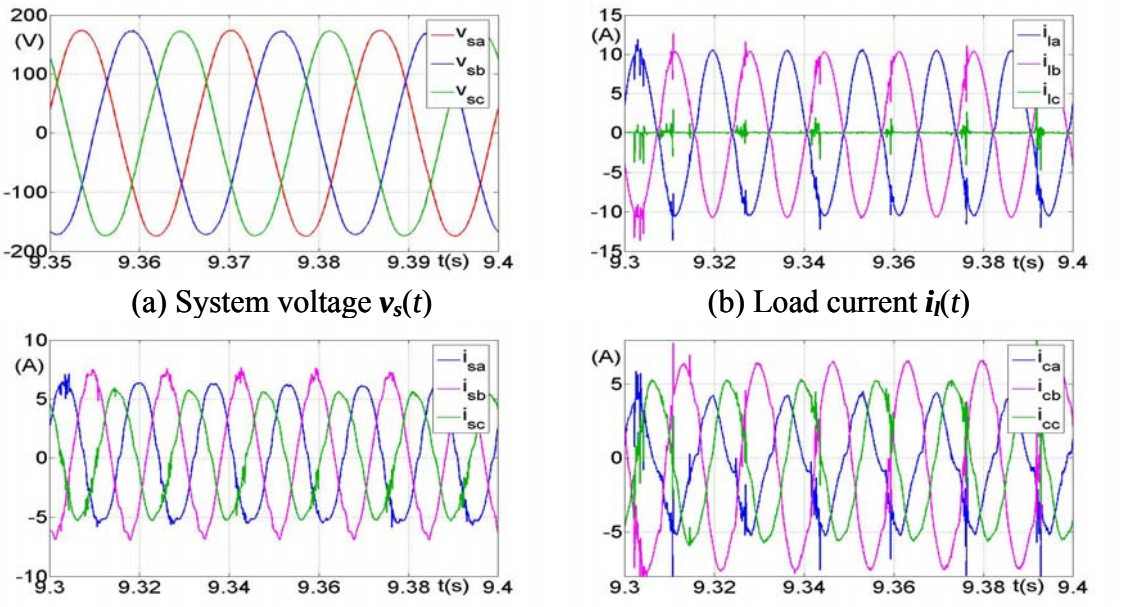

(a) System voltage $\boldsymbol{v_s}(t)$ (b) Load current $\boldsymbol{i_l}(t)$

(c) Source current $\boldsymbol{i_s}(t)$ (d) Compensator current $\boldsymbol{i_c}(t)$

Figure 5.12. Single-phase load compensation.

Table 5.12. RMS current values of the single-phase load compensation.

	I_l (A)	I_s (A)
Phase *a*	7.20	4.44
Phase *b*	7.22	4.97
Phase *c*	0.43	3.97
$I_{\text{unbalance}}$	137.17%	22.42%

consistent with the theoretical analysis in Chapter 3 as well as the simulation results in Chapter 4.

1. The experimental results show that this theory is valid in three-phase and single phase systems. The single-phase load is connected between two phases in a three-phase system. After compensation, the source current has a unity power factor and is nearly balanced.
2. The theory is applicable to both sinusoidal and non-sinusoidal systems. An *RL* load (fundamental nonactive power compensation) and a diode rectifier load (harmonics load) are tested. In the case of fundamental nonactive power compensation, the fundamental nonactive current component is provided by the compensator, and nearly unity power factor is achieved. In the diode rectifier case, a reduction in the harmonics content of the source current is achieved.
3. The theory is applicable to both balanced and unbalanced systems. In the experiments, there is no connection between the inverter's DC link middle point and the power system's neutral point. The compensator topology and control scheme are simpler than for a three-phase four-wire system. The results show that the three-phase unbalanced load currents are balanced and the power factor is unity after compensation.
4. The experimental results are consistent with the discussion in Chapter 4 on the DC link voltage requirement and the DC link capacitance.
5. The definitions of active and nonactive currents/powers are instantaneous, which allows a fast dynamic response by the compensator. The dynamic

response is related to the averaging interval, the power rating and/or current rating of the compensator, and the control system speed.

CHAPTER 6

Conclusions and Future Work

The dissertation is summarized in subsection 6.1, and the future work is proposed in subsection 6.2.

6.1 Conclusions

Despite that mature power systems have adopted the form of three-phase ac power for over 100 years, modern power systems have been complicated by a variety of nonlinear loads. With the existence of harmonics, sub-harmonics, non-periodic waveforms, etc., the standard definitions of average active power and reactive power of three-phase, sinusoidal ac power systems are no longer able to express these physical phenomena. Definitions of nonactive current and the instantaneous nonactive power are required to describe, measure, and compensate the nonactive current and power in power systems. Several theories have been proposed since the 1920s; however, none of them provide an explicit definition of instantaneous nonactive power/current which is applicable to all of the different cases. Their disadvantages include

1. No generalized theory. They are valid only in some specific situations. Some are valid only in three-phase, three-wire systems, some are valid only in periodic systems, and some are valid only in steady-state systems.

2. Not strictly instantaneous definition. At lease one cycle of the fundamental period is required to calculate the harmonic components.

In addition, some definitions do not have any physical meanings, and some definitions cannot be used in a nonactive power compensation application.

A generalized nonactive power theory was presented in this dissertation for nonactive power compensation. The instantaneous active current, the instantaneous nonactive current, the instantaneous active power, and the instantaneous nonactive power were defined in a system which did not have any limitations such as the number of the phases, the voltage and the current were sinusoidal or non-sinusoidal, periodic or non-periodic. By changing the reference voltage and the averaging interval, this theory had the flexibility to define nonactive current and nonactive power in different cases. It was shown that other nonactive power theories discussed in Chapter 2 could be derived from this more general theory by changing the reference voltage and the averaging interval. The flexibility was illustrated by applying the theory to different cases such as a sinusoidal system, a periodic system with harmonics, a periodic system with sub-harmonics, and a system with non-periodic currents.

This theory was implemented using a shunt compensator. The current that the compensator was required to provide was calculated based on the generalized nonactive power theory. A control scheme was developed to regulate the DC link voltage of the inverter, and to generate the switching signals for the inverter based on the required nonactive current. The compensation system for different cases was studied. The simulation and experimental results showed that the theory proposed in this dissertation was applicable to nonactive power compensation in three-phase four-wire systems,

single-phase systems, load currents with harmonics, and non-periodic load currents. The DC link capacitance rating, the DC link voltage requirement, and the coupling inductance rating are determined in a three-phase *RL* load case, and these requirements for other cases are also discussed.

6.2 Future Work

The generalized nonactive power theory was presented, and its application in a shunt nonactive power compensation system was simulated and implemented in experiments.

1. *More research on the economic analysis*. The generalized nonactive power theory was used in different systems, and the averaging interval, the reference voltage, the DC link capacitance, the DC link voltage, and the coupling inductance were discussed and the requirements were determined based on the compensation objectives. More research needs to be done on the analysis of the capital cost by choosing different ratings and the system and/or customer benefit by installing a nonactive power compensator.
2. *The implementation of the generalized nonactive power theory in other flexible ac transmission systems (FACTS) applications*. The theory is applicable for nonactive power compensators with various configurations, such as a hybrid nonactive compensator, a multilevel-inverter-based nonactive compensator, an interline power flow controller, or a unified power flow controller. These FACTS devices control both the active and the nonactive power flow between the source and the load and between different transmission lines. They provide nonactive power compensation, as

well as ancillary services such as voltage stability, transient stability, and power oscillation damping.

3. *The utilization of the nonactive power theory in distributed energy resources*. The power electronic interfaces of the distributed energy resources provide the connection to the power system, by converting dc power to ac power, and/or adjusting the power level, and/or synchronizing with the power system. The interfaces can also be used to control both the instantaneous active power and the nonactive power of the distributed energy resources themselves and the power systems as well. Therefore, the distributed energy resources can simultaneously be active power sources and nonactive power compensation systems that can perform multi-purpose tasks.
4. *System-wide active and/or nonactive power control and operation*. System-wide, or at least the nearby distribution system is taken into consideration by the nonactive power compensation system, instead of only the system/load operation information at the local site. Network communication technology will be needed to perform the system-wide monitoring, analysis, and control. The individual nonactive power compensation system and other FACTs will have "brains" to exchange information with the central control and other intelligent devices, receive remote commands from the central control, and perform local active and/or nonactive power flow control tasks based on the local situation and the system-wide operation requirements.

References

[1] *IEEE Standard Dictionary of Electrical and Electronics Terms*, 1993, pp. 988 – 989.

[2] S. Fryze, "Active, Reactive, and Apparent Power in Non-Sinusoidal Systems," Przeglad Elektrot., no. 7, 1931, pp. 193 – 203. (In Polish)

[3] C. I. Budeanu, "Reactive and Fictitious Powers," Inst. Romain de I'Energie, Bucharest, Rumania, 1927. (In Romanian)

[4] L. M. Tolbert, T. G. Habetler, "Comparison of Time-Based Non-Active Power Definitions for Active Filtering," *IEEE International Power Electronics Congress*, October 15-19, 2000, Acapulco, Mexico, pp. 73 – 79.

[5] N. L. Kusters, W. J. M. Moore, "On the Definition of Reactive Power under Non-Sinusoidal Conditions," *IEEE Transactions on Power Apparatus and Systems*, Vol. PAS-00, Sept. 1980.

[6] C. H. Page, "Reactive Power in Nonsinusoidal Situations," *IEEE Transactions on Instrumentation and Measurement,* Vol. IM-29, Dec. 1980, pp. 420 – 423.

[7] J. L. Willems, "A New Interpretation of the Akagi-Nabae Power Components for Non-Sinusoidal Three-Phase Situations," *IEEE Transactions on Instrumentation and Measurement*, Vol. 41, Aug. 1992, pp. 523 – 527.

[8] L. Rossetto, P. Tenti, "Evaluation of Instantaneous Power Terms in Multi-Phase System: Techniques and Applications to Power-Conditioning Equipment," *ETEP*, Vol. 4, Nov. 1994, pp. 469 – 475.

[9] F. Z. Peng, J. S. Lai, "Generalized Instantaneous Reactive Power Theory for Three-Phase Power Systems," *IEEE Transactions on Instrumentation and Measurement*, Vol. 45, Feb. 1996, pp. 293 – 297.

[10] X. Dai, G. Liu, R. Gretsch, "Generalized Theory of Instantaneous Reactive Quantity for Multiphase Power System," *IEEE Transactions on Power Delivery*, Vol. 19, July 2004, pp. 965 – 972.

[11] H. Akagi, Y. Kanazawa, A. Nabae, "Instantaneous Reactive Power Compensators Comprising Switching Devices without Energy Storage Components," *IEEE Transactions on Industry Applications*, Vol. IA-20, May 1984, pp. 625 – 631.

[12] H. Akagi, A. Nabae, "The *p-q* Theory in Three-Phase System under Non-Sinusoidal Conditions," *ETEP*, Vol. 3, 1993, pp. 27 – 31.

[13] L. S. Czarnecki, "On Some Misinterpretations of the Instantaneous Reactive Power *p-q* Theory," *IEEE Transactions on Power Electronics*, Vol. 19, May 2004, pp. 828 – 836.

[14] H. Kim, F. Blaabjerg, B. Bak-Jensen, J. Choi, "Instantaneous Power Compensation in Three-Phase Systems by Using p-q-r Theory," *IEEE Transactions on Power Electronics*, Vol. 17, Sept. 2002, pp. 701 – 710.

[15] H. Kim, F. Blaabjerg, B. Bak-Jensen, "Spectral Analysis of Instantaneous Powers in Single-Phase and Three-Phase Systems With Use of p-q-r Theory," *IEEE Transactions on Power Electronics*, Vol. 17, Sept. 2002, pp. 711 – 720.

[16] M. Depenbrock, "The FBD Method, a Generally Applicable Tool for Analyzing Power Relations," *IEEE Transactions on Power Systems*, Vol. 8, May 1993, pp. 381 – 387.

[17] J. H. R. Enslin, J. D. Van Wyk, "Measurement and Compensation of Fictitious Power Under Nonsinusoidal Voltage and Current Conditions," *IEEE Transactions on Instrumentation and Measurement*, Vol. 37, Sept. 1988, pp. 403 – 408.

[18] J. H. R. Enslin, J. D. Van Wyk, "A New Control Philosophy for Power Electronic Converters as Fictitious Power Compensators," *IEEE Transactions on Power Electronics,* Vol. 5, Jan. 1990, pp. 88 – 97. Discussion, Vol. 5, Oct. 1990, pp. 503 – 504.

[19] J. H. R. Enslin, J. D. Van Wyk, M. Naude, "Adaptive, Closed-Loop Control of Dynamic Power Filters as Fictitious Power Compensators," *IEEE Transactions on Industrial Electronics*, Vol. 37, June 1990, pp. 203 – 211.

[20] D. A. Marshall, J. D. Van Wyk, "An Evaluation of the Real-Time Compensation of Fictitious Power in Electric Energy Networks," *IEEE Transactions on Power Delivery*, Vol. 6, Oct. 1991, pp. 1774 – 1780.

[21] A. Ferrero, G. Superti-Furga, "A New Approach to the Definition of Power Components in Three-Phase Systems under Non-Sinusoidal Conditions," *IEEE Transactions on Instrumentation and Measurement*, Vol. 40, June 1991, pp. 568 – 577.

[22] A. Ferrero, A. P. Morando, R. Ottoboni, G. Superti-Furga, "On the Meaning of the Park Power Components in Three-Phase Systems under Non-Sinusoidal Conditions," *ETEP*, Vol. 3, Jan. 1993, pp. 33 – 43.

[23] A. Nabae, T. Tanaka, "A New Definition of Instantaneous Active-Reactive Current and Power Based on Instantaneous Space Vectors on Polar Coordinates in Three-Phase Circuits," *IEEE/PES 1996 Winter Meeting*, Baltimore, MD.

[24] L. S. Czarnecki, "What Is Wrong with the Budeanu Concept of Reactive and Distortion Power and Why it Should Be Abandoned," *IEEE Transactions on Instrumentation and Measurement*, Vol. 36, Sept. 1987, pp. 834 – 837.

[25] H. Lev-Ari, A. M. Stankovic, "Hilbert Space Techniques for Modeling and Compensation of Reactive Power in Energy Processing Systems," *IEEE Transactions on Circuits and Systems*, Vol. 50, April 2003, pp. 540 – 556.

[26] W. Shepherd, P. Zakikhani, "Suggested Definition of Reactive Power for Nonsinusoidal Systems," *Proceedings IEE*, Vol. 119, Sept. 1972, pp. 1361 – 1362. Discussion, Vol. 120, no. 1, p. 108. Discussion, Vol. 120, no. 7, pp. 796 – 798. Discussion, Vol. 121, no. 5, pp. 389 – 390. Discussion, Vol. 121, no. 7, pp. 705 – 706.

[27] D. Sharon, "Reactive Power Definition and Power-Factor Improvement in Nonlinear Systems," *Proceedings IEE*, Vol. 120, no. 6, June 1973, pp. 704 – 706. Discussion, Vol. 121, no. 5, pp. 390 – 391. Discussion, Vol. 121, no. 7, pp. 705 – 706.

[28] E. B. Makram, R. B. Haines, A. A. Girgis, "Effect of Harmonic Distortion in Reactive Power Measurement," *IEEE Transactions on Industry Applications*, Vol. 28, July 1992, pp. 782 – 787.

[29] M. A. Slonim, J. D. Van Wyk, "Power Components in a System with Sinusoidal and Nonsinusoidal Voltages and/or Currents," *IEE Proceedings-B*, Vol. 135, March 1988, pp. 76 – 84.

[30] M. A. Slonim, "Distortion Power in Linear and Nonlinear Systems," *International Journal of Electronics*, Vol. 68, no. 5, May 1990, pp. 769 – 778.

[31] A. M. Stankovic, H. Lev-Ari, "Frequency-domain observations on definitions of Reactive Power," *IEEE Power Engineering Review*, Vol. 20, June 2000, pp. 46 – 48.

[32] L. S. Czarnecki, "Current and Power Equations at Bidirectional Flow of Harmonic Active Power in Circuits with Rotating Machines," *ETEP*, Vol. 3, Jan. 1993, pp. 45 – 52. Discussion, Vol. 4, Nov. 1994, pp. 509 – 512.

[33] S. Sun, S. Huang, "On the Meaning of Nonsinusoidal Active Currents," *IEEE Transactions on Instrumentation and Measurement*, Vol. 40, Feb. 1991, pp. 36 – 38.

[34] A. Marganitz, "Power Measurement of Periodic Current and Voltages by Digital Signal Processing," *ETEP*, Vol. 2, March 1992, pp. 117 – 123.

[35] L. Cristaldi, A. Ferrero, G. Superti-Furga, "Current Decomposition in Asymmetrical Unbalanced Three-Phase Systems under Nonsinusoidal Conditions," *IEEE Transactions on Instrumentation and Measurement*, Vol. 43, Feb. 1994, pp. 63 – 68.

[36] L. Cristaldi, A. Ferrero, G. Superti-Furga, "Power and Current Decomposition into Time- and Frequency-Domain Components: Analysis and Comparison," *ETEP*, Vol. 4, Sept. 1994, pp. 359 – 369.

[37] A. Wolf, M. Thamodharan, "Reactive Power Reduction in Three-Phase Electric Arc Furnace," *IEEE Transactions on Industrial Electronics*, Vol. 47, Aug. 2000, pp. 729 – 733.

[38] B. Singh, K. Al-Haddad, A. Chandra, "A Review of Active Filters for Power Quality Improvement," *IEEE Transactions on Industrial Electronics*, Vol. 46, Oct. 1999, pp. 960 – 971.

[39] F. Z. Peng, "Harmonic Sources and Filtering Approaches," *Industry Applications Magazine*, Vol. 7, July-Aug. 2001, pp. 18 – 25.

[40] M. El-Habrouk, M. K. Darwish, P. Mehta, "A Survey of Active Filters and Reactive Power Compensation Techniques," *Power Electronics and Variable Speed Drives,* Sept. 2000, Conference Publication No. 475, pp. 7 – 12.

[41] A. M. Massoud, S. J. Finney, B. W. Williams, "Practical Issues of Three-Phase, Three-Wire, Voltage Source Inerter-Based Shunt Active Power Filters," *IEEE International Conference on Harmonics and Quality of Power,* September 12 - 15, 2004, Lake Placid, New York.

[42] S. K. Jain, P. Agarwal, H. O. Gupta, "A Control Algorithm for Compensation of Customer-Generated Harmonics and Reactive Power," *IEEE Transactions on Power Delivery*, Vol. 19, No. 1, Jan. 2004, pp. 357 – 361.

[43] G. E. Valderrama, P. Mattavelli, A. M. Stankovic, "Reactive Power and Unbalance Compensation Using STATCOM with Dissipativity-Based Control," *IEEE Transactions on Control Systems Technology*, Vol. 9, Sept. 2001 pp. 718 – 727.

[44] B. M. Han, S. I. Moon**,** "Static Reactive-Power Compensator Using Soft-Switching Current-Source Inverter," *IEEE Transactions on Industrial Electronics*, Vol. 48, Dec. 2001, pp. 1158 – 1165.

[45] M. K. Mishra, A. Joshi, A. Ghosh, "A New Algorithm for Active Shunt Filters Using Instantaneous Reactive Power Theory," *IEEE Power Engineering Review*, Vol. 20, Dec. 2000, pp. 56 – 58.

[46] Y. Zhong, "Three-Phase Reactive Power Compensation Using a Single-Phase AC/AC Converter, " *IEEE Transactions on Power Electronics*, Vol. 14, Sept. 1999, pp. 816 – 822.

[47] F. Z. Peng, L. M. Tolbert, "Compensation of Non-Active Current in Power Systems - Definitions from Compensation Standpoint," *IEEE Power Engineering Society Summer Meeting*, July 15-20, 2000, Seattle, Washington, pp. 983 – 987.

[48] M. D. Manjrekar, P. Steimer, T. A. Lipo, "Hybrid Multilevel Power Conversion System: a Competitive Solution for High Power Applications," *IEEE Transactions on Industry Applications*, Vol. 36, May-June 2000, pp. 834 – 841.

[49] N. Mohan, T. M. Undeland, W. P. Robbins, "Power Electronics: Converters, Applications, and Design," *John Wiley and Sons*, Second Edition, 1995.

[50] N. G. Hingorani, L. Gyugi, "Understanding FACTS: Concepts and Technology of Flexible AC Transmission Systems," *IEEE Press*, 1999.

[51] A. Ghosh, G. Ledwich, "Power Quality Enhancement Using Custom Power Device," *Kluwer Academic Publishers*, 2002.

[52] Y. Xu, J. N. Chiasson, L. M. Tolbert, "Nonactive Current Definition and Compensation Using a Shunt Active Filter," *IEEE International Conference on Harmonics and Quality of Power,* September 12 - 15, 2004, Lake Placid, New York.

[53] Y. Xu, L. M. Tolbert, F. Z. Peng, J. N. Chiasson, J. Chen, "Compensation-Based Nonactive Power Definition," *IEEE Power Electronics Letters*, vol. 1, no. 2, June 2003, pp. 45 – 50.

Vita

Yan Xu received her B.S. in July 1995 from Shanghai Jiaotong University, China majoring in Electric Power Engineering. She received her M.S. in April 2001 from North China Electric Power University, China majoring in Electric Power Engineering. She worked at Anhui Province Electric Power Company, Maanshan Branch from August 1995 to August 1998 as an electrical engineer. She also worked at Beijing Pengfa Xingguang Power Electronics Co. Ltd. from August 2001 to December 2001 as a research and development engineer.

Yan Xu started her Ph.D. program at the Department of Electrical and Computer Engineering, The University of Tennessee in January 2002. At the same time, she joined the Power Electronics Laboratory at The University of Tennessee as a graduate research assistant, working on reactive power theory and STATCOM control issues. She has worked at Oak Ridge National Laboratory since 2005 by helping to install and setup a STATCOM in the Reactive Power Laboratory. She graduated with a Doctor of Philosophy degree in Electrical Engineering from The University of Tennessee in May 2006.